UNIVERSITÀ DI PARMA

UNIVERSITÀ DEGLI STUDI DI PARMA

DOTTORATO DI RICERCA IN

BIOTECNOLOGIE E BIOSCIENZE

CICLO XXXIV

THE YEAST *Saccharomyces cerevisiae*: A HELPFUL TOOL TO STUDY MUTATIONS IN GENES ASSOCIATED WITH HEREDITARY OPTIC NEUROPATHIES (HON)

Coordinator:

Prof. Marco Ventura

Tutor:

Prof. Enrico Baruffini

Dottorando: Andrea Degiorgi

ANNI ACCADEMICI 2018/2019-2020/2021

ABSTRACT

The hereditary optic neuropathies (HON) comprise a group of disorders that are characterized by selective loss of retinal ganglion cells (RGCs), leading to optic nerve atrophy and different degrees of visual impairment and blindness. Clinical variability often makes recognition and classification difficult. Traditionally, classification has relied on the recognition of similar characteristics and similar patterns of transmission, but genetic analysis now permits the specific diagnosis. Thanks to next generation sequencing thirteen mutations were identified. The yeast *Saccharomyces cerevisiae* is extensively used as a genetic system to study mitochondrial diseases, giving the possibility to prove with high confidence the link between novel mutations and mitochondrial pathologies, since yeast can survive without mitochondrial DNA and by fermenting. Once the mutant strains were constructed, the pathogenicity of these variants were demonstrated exploiting the analysis of the OXPHOS metabolism. In particular, it was shown that all the variants identified in patients led to a reduction in both oxidative growth and respiration, allowing to connect the pathological patients' phenotype with the presence of the substitutions. Mild and severe phenotypes were observed, and to better understand the mechanisms underlying the disease, a series of molecular analyzes have been performed. Investigation on the enzymatic activity, in the *SDHA* and *ACO2* mutant strains, highlighted a positive correlation with the results obtained in the OXPHOS metabolism analysis with that of the enzymatic capacity, suggesting that the expression of the pathological phenotype could be due to an enzymatic deficiency. For the other mutants, containing *MTFMT* and *MECR,* a series of analysis were performed. In *MECR* strains, a deficiency in lipoic acid was observed, since the mitochondrial fatty acids biosynthesis pathway is blocked. Lipoic acid is an essential cofactor for some of the enzymes important for the Krebs cycle, therefore a reduction in lipoic acid content was compatible with the oxidative defects observed. On the other hand, *MTFMT,* responsible for the formylation of the met-tRNA^{met} led to defects in mitochondrial protein synthesis which could explaining the pathological phenotype in patients. Furthermore, since *ACO2* and *SDHA* mutations were in heterozygous condition, inheritance studies have been performed and, the diploid condition recreated in yeast, allowed to detect the pathological defect. In almost all the mutants, the dominance was confirmed, explaining that with haploinsufficiency or negative dominance. The results showed that yeast is an excellent tool for validation but also for extrapolating information on the inheritance of mutations.

CHAPTER 1: INTRODUCTION

1.1 THE MITOCHONDRIA

Mitochondria are cytoplasmic organelles of the eukaryotic cells and are considered their "power station". Energy is obtained from the oxidation of sugars, fatty acids, organic acids and other compounds such as ethanol and glycerol to produce ATP (adenosine triphosphate), the fuel that drives most of the life reactions. The origin of the mitochondria is dated 1.5 billion years ago, when an aerobic bacterium, through a phagocytosis event, was engulfed by a eukaryotic progenitor and maintained during evolution (Lane and Martin 2010; Schwartz 1973; Herst et al. 2017). The 'mitochondrial unit' length ranges from 1 µm to 5 µm with an average diameter of about 0.5 µm. These organelles are surrounded by two membranes with different characteristics, allowing them to establish a close connection between their structure and function (Figure 1.1). The main difference between the two membranes lies in the different degrees of permeability. The outer mitochondrial membrane (OMM) separates the cytosol from the mitochondrion and is mainly composed of porin, a transmembrane channel that confers high permeability to ions and small molecules with a molecular weight lower than 5000 Da, making the intermembrane space similar to the cytosol. On the other hand, the internal mitochondrial membrane (IMM), composed of 20% cardiolipin (Horvath and Daum 2013), makes the membrane poorly permeable to charged molecules, allowing the formation of electro-chemical gradients that drives the ATP production.

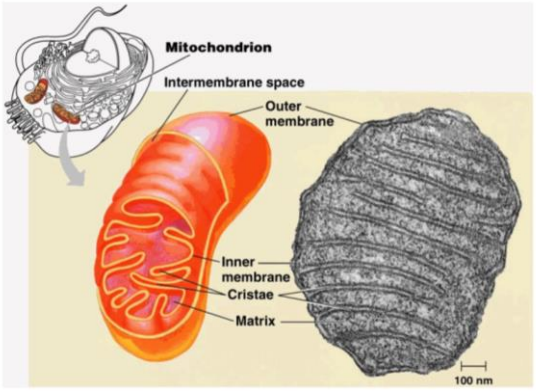

Figure1.1: Mitochondrion representation

The IMM forms a series of invaginations towards the matrix, called *cristae*, where the respiratory enzymes are concentrated. The *cristae* organization has the effect to increase the inner membrane surface, optimizing energy production processes (Joubert and Puff 2021; Ikon and Ryan 2017).

These organelles are important not only for energy production but play pivotal roles in many other cellular processes, such as apoptosis, thermogenesis, calcium homeostasis and reactive species of oxygen (ROS) production. Another peculiar feature of mitochondria concerns their incredibly dynamic ability (Dimmer et al. 2002); in fact, their morphology and distribution can change depending on the cell energy demand (Bereiter-Hahn and Vöth 1994; Warren and Wickner 1996; Hermann and Shaw 1998; Yaffe 1999; Yu and Pekkurnaz 2018). The number is highly variable, from a single mitochondrion in some unicellular algae to tens of thousands in oocytes, but in most cases, there are on average 500-1000. However, the count of mitochondria numbers has been overcome and replaced by the concept of mitochondrial mass, maintained through mitochondrial fusion and fission processes. The fission and fusion processes, continuously remodel the mitochondria organization and allow rapid responses to the outside stimuli.

1.2 mtDNA: STRUCTURE AND FUNCTIONS

During evolution, mitochondria have maintained their own genome, even if many massive events of genes migration in the nucleus have occurred. Human mitochondrial DNA (h-mtDNA), the first genome to be sequenced (Anderson et al. 1981; Basu et al. 2020), is a 16.5-kb circular double-stranded molecule with a high degree of compaction due to the absence of intronic sequences. The length and the sequence of the mtDNA are species dependent. Unlike humans, in fact, the yeast *S. cerevisiae* has mtDNA of variable lengths ranging from ∼68 (short strain) to 86 kb (long strain), mainly in a linear form (Foury et al. 1998). The h-mtDNA encodes for 22 tRNAs, which are specific to the mitochondrial translational machinery, 2 rRNAs, and 13 proteins that take part in oxidative phosphorylation processes (Figure 1.2).

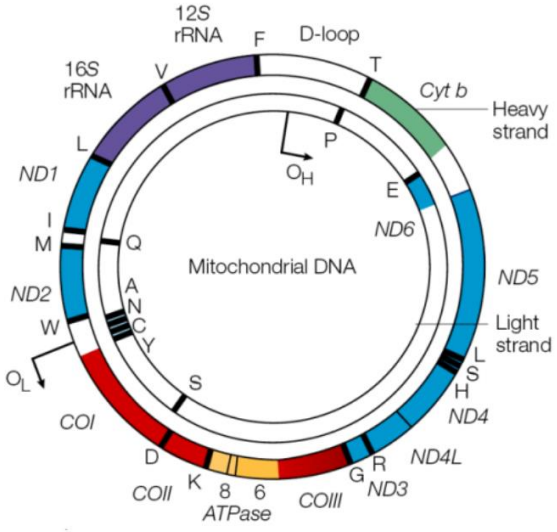

Figure 1.2: h-mtDNA map. Genes encoding subunits of complex I are in blue; genes encoding cytochrome b of Complex III are in green; genes encoding subunits of Complex IV are in red; genes encoding for subunits of ATP synthase are in yellow. (Taylor and Turnbull 2005)

All the other proteins (~1300) involved in the respiratory chain and mitochondrial pathways are nuclear-encoded, synthesized in the cytosol, and imported into mitochondria through the TOM/TIM super-complex (Neupert and Herrmann 2007; Ryan and Hoogenraad 2007; Gomkale et al. 2021). To maintain mitochondrial functionality, a finely regulated recognition of mitochondrial import signal and the subsequent transfer of these proteins are requested (Harbauer et al. 2014). Mitochondrial DNA, unlike human nuclear DNA, which is always present in two copies, has a variable copy number mainly dependent on both cell type or particular stimuli and conditions. Cells of tissues with a high energy requirement, such as skeletal and cardiac muscles, have up to 5000-10000 copies of mtDNA (D'Erchia et al. 2015). Moreover, even pathological conditions such as cancer and diabetes (Reznik et al. 2016; Chien et al. 2012) or aging (He et al. 2014) can lead to a variation in the mtDNA content. Despite the absence of histone-like mitochondrial proteins, mtDNA cannot be considered "naked" because takes part in protein-DNA complexes called nucleoids, which are autonomous replicative units anchored to the IMM (Holt et al. 2007; Kukat et al. 2011; Bonekamp and Larsson 2018). Proteomics analyses of native cross-linked nucleoids have determined the major components of these structures. It is possible to distinguish two different classes: proteins involved in replication and proteins involved in transcription processes. The most abundant proteins connected to

mitochondrial replication are POLG, Twinkle and mtSSB, while those involved in transcription are POLRMT, TFAM, TFB2M and TEFM (Rubio-Cosials and Solà 2013; Garrido et al. 2003). TFAM protein belongs to the high-mobility proteins group, promotes the initiation of transcription by recruiting the RNA polymerase POLRMT, playing an important role in this process by binding, folding and unfolding the mtDNA. TFAM can compact the mtDNA inducing a 180° U-turn when bound to the DNA (Bonekamp and Larsson 2018), and the degree of compaction of mtDNA is closely linked to its presence; a ratio of 1 molecule of TFAM every 16 Bp of DNA, in basal conditions, has been estimated. TFB2M and TEFM are specific transcription factors: the former induces structural changes in the RNA polymerase enzyme promoting the recognition and capture of the non-template DNA strand, the latter is a transcription elongation factor that increases mitochondrial RNA polymerase processivity (Hillen et al. 2017; Minczuk et al. 2011). In mammals and fungi, all processes in which the synthesis of new mtDNA occurs, such as replication, repair and recombination are accomplished by the unique mitochondrial replicase, the DNA polymerase gamma (POLG o POLγ) (Ropp and Copeland 1996; Pinz and Bogenhagen 2006; Longley et al. 1998). POLG is a heterotrimer protein composed of one catalytic and two accessory subunits which increase both catalytic activity and processivity (Yakubovskaya et al. 2006; Euro et al. 2011). In humans the catalytic subunit, POLG(A), encoded by *POLG* gene located on chromosome 15q25, consists of 1239 amino acids subdivided into three domains:

- N-terminal domain with 3'→5' exonuclease activity (residues 170-440), involved in the proofreading activity

- C-terminal domain characterized by polymerase activity (residues 440–475 and 785–1239), involved in the synthesis of new mtDNA

- Spacer region that connects the two domains (residues 475–785)(T A Kunkel and Soni 1988; Thomas A. Kunkel and Mosbaugh 1989; Graziewicz, Longley, and Copeland 2006; Gilea et al. 2021) and which contains two subdomains. The former is implicated in intrinsic processivity and the latter is involved in processivity mediated by the interaction with the accessory subunits, encoded by the *POLG2* gene (Lee, Kennedy, and Yin 2009)

The replication of mammalian mtDNA, in which POLG is the key player, is continuous and asymmetrical, both in space and time. Based on the nucleotide composition, it is possible to identify an H (heavy) and an L (light) strand on mtDNA (Berk and Clayton 1974; Falkenberg 2018). Unlike the replication of the nuclear DNA, every single strand (H and L) is synthesized continuously, without the presence of Okazaki fragments. Moreover, the synthesis of the two strands begins from different origins, called O_H and O_L (spatial asymmetry) and at different times (temporal asymmetry). In 1972, Vinograd and co-workers proposed the strand displacement model to explain this process (Robberson, Kasamatsu, and Vinograd 1972). The mtDNA contains two regions that act as transcription initiation sites called HSP (Heavy Strand Promoter) and LSP (Light Strand Promoter). According to this theory, the mtDNA synthesis, starts from O_H, using a short primer inserted by POLRMT in the LSP region to produce the new H-strand. The replication process is facilitated by TWINKLE, a protein with 5'→3' helicase activity, which helps the opening of the double helix. In this initial step, there is no contemporaneous L-strand synthesis and the parental H-strand is bound by the mitochondrial single-strand binding protein (mtSSB) to prevent random RNA synthesis on the displaced strand from the mitochondrial RNA polymerase (POLRMT) (Miralles Fusté et al. 2014). When the replicative machinery replicates two-thirds of the genome, reaches the other origin of replication (O_L), and the displaced parental H-strand folds into a stem–loop structure (Falkenberg 2018). This particular conformation blocks mtSSB from binding mtDNA, and a small fragment of single-stranded DNA in the loop region remains accessible to the POLRMT which initiates RNA synthesis (Fusté et al. 2010). The processivity of POLRMT on single-stranded DNA is low, and after 25 nucleotides is switched with POLγ, allowing the L-strand DNA synthesis (Wanrooij et al. 2008; Wong and Clayton 1985). After this polymerase substitution, H- and L-strand synthesis proceeds until the two strands complete the entire circle. (Figure 1.3)

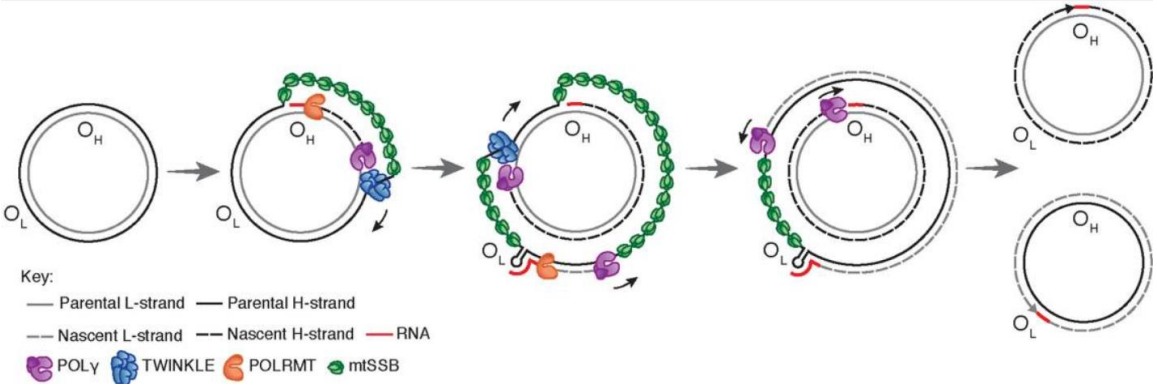

Figure 1.3: Strand displacement model (Falkenberg 2018)

1.3 THE TWO MAIN MITOCHONDRIAL PROCESSES: KREBS CYCLE AND OXIDATIVE PHOSPHORYLATION

1.3.1 Krebs cycle

Sugars and fatty acids are the main energy sources of the cells, which, through oxidation processes, are converted into carbon dioxide, releasing energy used for ATP synthesis. Enzymes which catalyze the oxidative degradation of these compounds are in the mitochondrial matrix. Glucose and other sugars are oxidized in the cytoplasm, via glycolysis, into pyruvate. Pyruvate is then imported in mitochondrion, where it undergoes oxidative decarboxylation reaction, producing acetyl-coenzyme A (Acetyl-CoA) (Ochoa 2006; Perham 2000; McCommis and Finck 2015). Fatty acids, mainly deriving from the mobilization process of triglycerides in eukaryotes, are imported into the mitochondrial matrix through the acylcarnitine transport system. In the mitochondrial matrix, the fatty acids are converted into acyl-coenzyme A, template of the β-oxidation process, consisting of four reactions. Each β-oxidation cycle produces one acetyl-CoA and one acyl-coenzyme A (two carbon atoms shorter) molecules. In higher eukaryotes, β-oxidation occurs mainly in the mitochondria and, for very long-chain fatty acids, in peroxisomes, while in yeast this catabolic process occurs primarily in peroxisomes and subsequently the acetyl groups are transported into the mitochondria, through the acetyl-carnitine system. Acetyl-CoA, resulting from these degradative processes, is oxidized to carbon dioxide through the Krebs cycle (tricarboxylic acids cycle or TCAs) (figure 1.4).

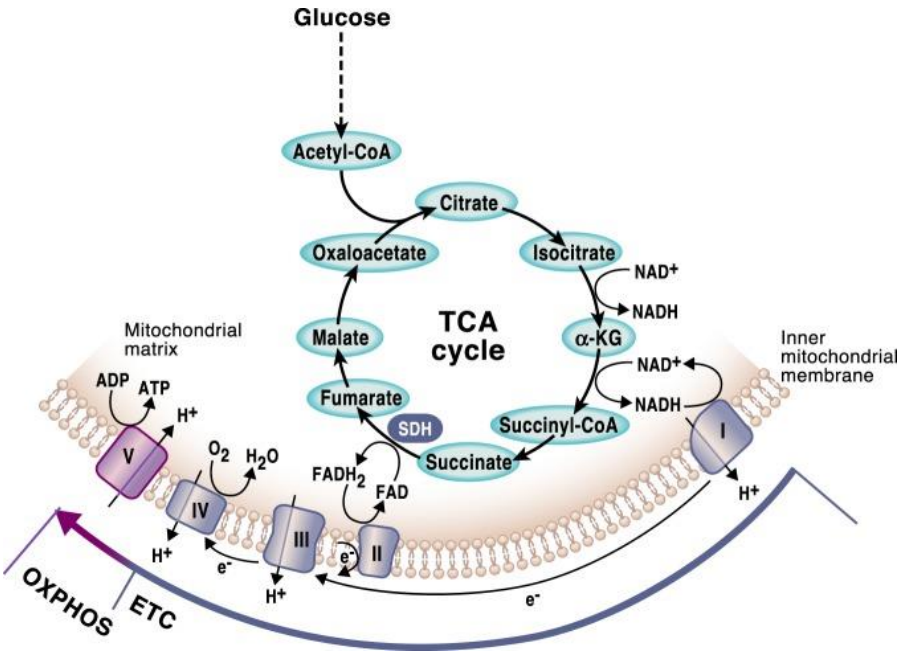

Figure 1.4: Krebs cycle schematic representation (Martínez-Reyes and Chandel 2020)

The tricarboxylic acid cycle is the principal oxidative process of respiration, through which all metabolic "fuels" (carbohydrates, lipids, proteins and other compounds) are catabolized in aerobic tissues. The Krebs cycle is composed of eight reactions, that convert one molecule of acetyl-CoA into two molecules of carbon dioxide, one molecule of ATP, three molecules of NADH and one molecule of $FADH_2$. The cycle starts with a condensation reaction, catalyzed by citrate synthase enzyme, which combines a molecule of oxaloacetate (4 carbon atoms) and a molecule of acetyl-CoA (2 carbon atoms) to form oxaloacetate (6 carbon atoms). The second step involves the isomerization of citrate to isocitrate, catalyzed by aconitase, more detailed below. In the third step, isocitrate is converted into alpha-ketoglutarate by isocitrate dehydrogenase. In this phase, a dehydrogenation reaction to form oxalosuccinate occurs: being this molecule highly unstable, it is immediately converted to alpha-ketoglutarate with the release of carbon dioxide and reduction of nicotinamide adenine dinucleotide (NADH) cofactor. The fourth step of the Krebs cycle involves a subsequent decarboxylation reaction catalyzed by a multi-protein complex called alpha-ketoglutarate dehydrogenase, in which the product of the previous step is converted into succinyl-CoA, releasing carbon dioxide. Succinyl-CoA synthase, the fifth enzyme in the cycle, couples the cleavage of succinyl-CoA to the synthesis of a nucleotide triphosphate (GTP), which can be rapidly interconverted into ATP by the action of a nucleoside diphosphate kinase:

$$GDP + ADP \rightleftarrows GDP + ATP \qquad \Delta G^{\circ\prime} = 0$$

Succinate dehydrogenase, detailed later, subsequently catalyzes the stereoscopic dehydrogenation of succinate to fumarate. Fumarate hydratase (fumarase) catalyzes the seventh reaction of the cycle, in which the fumarate double bond is reduced to form malate. The reaction proceeds thanks to the formation of an unstable carbanion transition state. The final reaction leads to the regeneration of oxaloacetate, catalyzed by malate dehydrogenase. In this NAD^+ dependent step, the hydroxyl group of the malate is oxidized, with simultaneous transfer of a proton and two electrons to NAD^+, forming NADH. Most of the energy released is therefore stored in the form of reducing power. In fact, at the end of each cycle, the net balance provides the production of 3 NADH, 1 $FADH_2$ and 1 GTP (or ATP) molecules. It is important to emphasize that the Krebs cycle is not fundamental only for oxidative metabolism but provides intermediates, such as oxaloacetate and α-ketoglutarate, essential for the synthesis of amino acids. Another example is the succinyl-CoA, used for the synthesis of heme and other porphyrins. Oxaloacetate and α-ketoglutarate are the ketoacids used to form aspartate and glutamate, respectively, through transamination reaction. Since these and other reactions tend to deplete the intermediates of the citric acid cycle, the progress of the cycle could fail if processes able to restore the stocks of these intermediates did not exist. These processes constitute the anaplerotic pathways. Although they are not usually classified as anaplerotic, transamination reactions can also be considered a source of these molecules, since they are reversible reactions that can produce intermediates of the Krebs cycle. Consequently, cells that have an abundance of amino acids can convert them into intermediates of the citric acid cycle by transamination generating α-ketoglutarate and oxaloacetate from glutamate and aspartate. Another enzyme, glutamic dehydrogenase, constitutes another possibility for the synthesis of α-ketoglutarate from glutamate. In addition, many plants and some microorganisms, including the yeast *Saccharomyces cerevisiae*, can convert two-carbon compounds to four-carbon intermediates of TCA through the glyoxylate cycle.

1.3.2 Oxidative phosphorylation

NADH and $FADH_2$, derived from β-oxidation and the Krebs cycle, are molecules with a high energy level in the form of reducing power. They contain electrons with high transfer potential and when these electrons are used to reduce molecular oxygen (a very potential harmful

molecule) to water, a large amount of free energy is released. In aerobic organisms, oxidative phosphorylation is the main mechanism used to synthetize ATP, thanks to the conversion of the energy resulting from the oxidative degradation of organic substances into ATP. The progressive passage of the electrons through carrier proteins with increased affinity is associated with the pumping of protons into the intermembrane space, generating an electrochemical gradient based on the different H^+ concentrations between the intermembrane space (IMS) and the matrix, through the inner membrane. This gradient is dissipated at the level of ATP synthase, the fifth complex of the electron transport chain, that couples the re-entry of protons into the matrix with the ATP synthesis, starting from ADP and inorganic phosphate. Electrons are transported through carriers with lower reduction potential to those with higher reduction potential, which cyclically accept and donate electrons. The classes of transporters present in the mitochondrial transport chain are:

Iron-sulfur centers (Fe-S), which represent the prosthetic groups of iron-sulfur proteins, in which one or more iron atoms are linked via coordination bonds to inorganic sulfur atoms or sulfur atoms of cysteines. In the Fe-S centers, the effective electron carriers are the iron atoms which, cyclically, accept (reducing themselves into a ferrous ion Fe^{2+}) and release the electron (re-oxidizing to ferric ion Fe^{3+})

Respiratory cytochromes are proteins complexed whit a heme-type molecule, which confers the ability to absorb visible light, with a characteristic spectrum. Respiratory cytochromes are divided into three classes according to the peak of absorption in the visible light: cytochrome a, with an absorption peak at 602 nm; cytochrome b, with an absorption peak at 560 nm; cytochrome c, with an absorption peak at 550 nm. In cytochromes, the electron carriers are the heme groups, mainly formed by Fe^{2+} ion (Cu^+ in the case of cytochromes a)

Ubiquinone, or coenzyme Q, presents a quinone structure that, unlike the other transporters, is not complexed to proteins. The quinone scaffold is composed of a specific number of isoprenoid units (10 in mammalian cells), which allow it to diffuse freely in the mitochondrial membrane. Ubiquinone can accept two electrons, passing from the oxidized form (ubiquinone)

to the partially reduced form (semiquinone), and then to the totally reduced form (ubiquinol) after the bond of the second electron.

The oxidative phosphorylation system (OXPHOS) comprises five multiprotein complexes (complexes I to V) and two mobile electron carriers (Ubiquinone and Cytochrome c) incorporated into the IMM phospholipid bilayer (Figure 1.5).

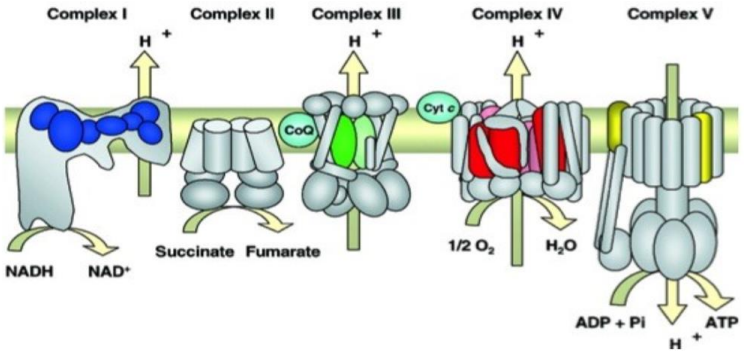

Figure 1.5: Electron transport chain representation (M. Zeviani 2004)

Complex I (or NADH-coenzyme Q reductase, or NADH dehydrogenase) contains 30 different polypeptides and transfers two electrons from NADH to coenzyme Q. The prosthetic group of one of these subunits, the flavine mononucleotide (FMN), cyclically accepts electrons and protons from NADH, transferring them to the iron-sulfur centers.

Complex II (or succinate-coenzyme Q reductase or succinate dehydrogenase) catalyzes the transfer of two electrons from succinate to coenzyme Q. It is the only complex that also acts as enzyme in Krebs cycle, catalyzing the oxidation of Succinate to Fumarate. Coenzyme Q diffuses freely across the inner mitochondrial membrane and transfers electrons to complex III.

Complex III (or cytochrome c-coenzyme Q oxidoreductase) contains 10 polypeptides, heme groups and iron-sulfur center; it is involved in the transfer of electrons from coenzyme Q to cytochrome c. The transfer takes place in the following order: cytochromes b (b_{562} and b_{566}),

iron-sulfur centers and cytochrome c. Cytochrome c differs from other cytochromes since it behaves as a protein weakly anchored to the inner membrane, able to spreads along it.

Complex IV (or cytochrome c oxidase) contains 13 polypeptides and catalyzes the transfer of electrons from cytochrome c to the final acceptor, oxygen. It consists of cytochromes a, a_3 and copper atoms (Cu_B and Cu_A center);

Complex V (or ATP synthase) is a complex with enzymatic activity that synthesizes ATP using the electrochemical gradient generated during the transport of electrons from the reduced molecules to oxygen. The transport of electrons is concomitant to the pumping of protons through the inner membrane, from the matrix to the IMS, through the respiratory complexes: this pumping creates a gradient of protons across the membrane, which provides the energy for the synthesis of ATP. The dissipation of this gradient through complex V allows the synthesis of ATP starting from ADP and inorganic phosphate.

The mitochondrial respiratory chain is a conserved system among eukaryotic organisms. Unlike humans, complex I is absent in *Saccharomyces cerevisiae.* Yeast contains three NADH dehydrogenases distributed on both external (Nde1 and Nde2) and internal (Ndi1) surfaces of the inner mitochondrial membrane. During respiratory glucose dissimilation, eukaryotes produce cytosolic NADH via glycolysis. This NADH must be reoxidized outside the mitochondria, because the mitochondrial inner membrane is impermeable to NADH. In *Saccharomyces cerevisiae* this process is accomplished by external NADH dehydrogenases Nde1p or Nde2p, while the internal Ndi1p oxidizes the NADH generated in the mitochondria (Matus-Ortega et al. 2015). For the assembly and maintenance of active respiratory complexes, a series of accessory factors are required. The assembly of complexes I, III, IV and V must bypass some aspects. The subunits are encoded by two different genomes (nuclear and mitochondrial), so that coordination is required between synthesis and assembly. Consequently, there are many dedicated proteins involved in the assembly of these complexes. Genetic analysis of yeast-deficient respiratory mutants led to the identification of several assembly factors or

chaperones, necessary for the biogenesis of respiratory complexes. Several *helper* proteins, involved in post-translational assembly of respiratory chain complexes, have been identified. Among these factors, the most abundant are involved in the synthesis of the prosthetics groups, or mediates insertion of respiratory subunits within the membrane or facilitates the assembly of the complexes (Barrientos et al. 2009; Lenaz and Genova 2010). Recently, two important complex II assembly factors were discovered in humans, fundamental for the oxidative phosphorylation (OXPHOS) activity (Ghezzi et al. 2009; Hao et al. 2009). Although there is a plethora of proteins involved in these mechanisms, oxidative phosphorylation is not a perfect process since, even in normal conditions, a fraction (0,2-2%) of the electrons transported through the respiratory complexes leads to the formation of reactive oxygen species (ROS) (Green and Reed 1998). The ROS mitochondrial origin was identified in complex I and complex III of the respiratory chain during the normal transfer of electrons from the NADH to molecular oxygen, forming superoxide anion (Lenaz 1998; Forkink et al. 2015). For this reason, it is necessary to defuse these potentially harmful agents by exploiting antioxidant systems, which help to maintain these substances at physiological levels as they have an important role in cell signaling and homeostasis. Generally, the production of superoxide anion is controlled by superoxide dismutase (SOD) present in cytosol, mitochondria and in the extracellular space, which converts the superoxide anion into hydrogen peroxide (H_2O_2). H_2O_2 is then converted into molecular oxygen (O_2) and water (H_2O) through glutathione peroxidase or catalase. (Wallace et al. 1988; Y. Wang et al. 2018). When the electron transport is damaged, superoxide anion production reaches high levels and the cell protection enzymes fail to control it. In these cases, oxidative stress, resulting from the presence of ROS, can damage both mitochondrial and nuclear DNAs leading to the onset of degenerative disorders, cancer and aging (Schieber and Chandel 2014).

1.4 MITOCHONDRIAL DISEASES

The energy deficit of mitochondrial metabolism in humans leads to a heterogeneous group of clinical syndromes called mitochondrial diseases (MDs) (Massimo Zeviani and Carelli 2007). Currently, MDs are altogether the most common pathologies among the genetic ones, affecting 1 in 5000 people (Ng and Turnbull 2016). Although the mitochondrion is the site of various fundamental metabolic pathways, mitochondrial diseases refer to a large group of clinical

phenotypes characterized by OXPHOS deficiency. MDs have typically a progressive course and include a broad spectrum of clinical phenotypes associated with oxidative phosphorylation insufficiency, which makes diagnosis difficult and complex. The most affected tissues are those with higher energy demand and therefore more dependent on oxidative metabolism, such as nervous tissue, skeletal and cardiac muscle, but also kidneys, liver, the endocrine system and retina (Land et al. 2004; Frazier, Thorburn, and Compton 2019) (Figure 1.6). Consequently, patients may present, in various combinations and different degrees of impairment, muscle degeneration, heart disease, movement disorders, diabetes mellitus, renal failure, dementia and various ophthalmological symptoms (McKenzie, Liolitsa, and Hanna 2004). Based on this knowledge, mitochondrial pathologies can be defined mostly multisystemic and determine symptoms associated with multiple tissues and organs. Recognition of these pathologies is often difficult due to common symptoms in multiple pathologies, while others are specific to some diseases (Schon, Bonilla, and DiMauro 1997)

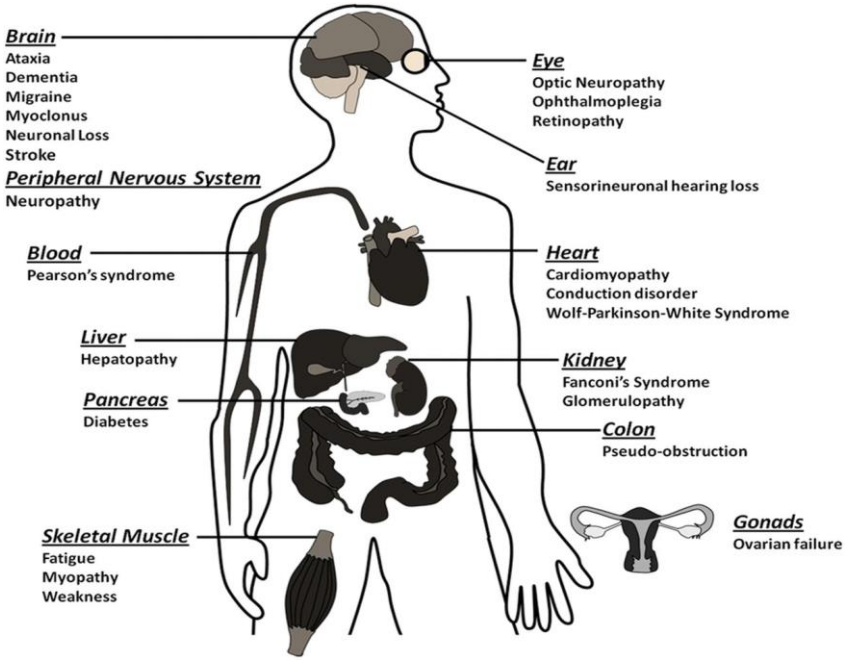

Figure 1.6: Clinical spectrum of mitochondrial diseases

(P. F. Chinnery and Hudson 2013).

A genetic-clinical classification for mitochondrial pathologies has been proposed (Leonard and Schapira 2000; M. Zeviani 2004). It is possible to distinguish five classes of genes involved in mitochondrial diseases:

- genes that encode structural components of the respiratory chain
- genes encoding for assembly factors of OXPHOS complexes
- genes that encode proteins involved in the synthesis of non-protein components of the respiratory chain
- genes that encode proteins indirectly related to OXPHOS
- genes involved in the mtDNA stability

Another important clustering of mitochondrial diseases is mainly based on the type of inheritance: genetic defects can involve mitochondrial DNA (mtDNA) or nuclear DNA (nDNA). As previously mentioned, mtDNA in the cells is present in a variable number of copies and based on this, it is possible to distinguish two different situations: mutations in mitochondrial genes that affect all mtDNA copies (homoplasmy) or only a percentage of them (heteroplasmy). In the latter case, there is a threshold level of mutated mtDNA required for the expression of the biochemical defect. Since mtDNA is maternally transmitted, these pathologies are subjected to maternal inheritance. The genetic defect, besides being inherited from mother to child, can arise spontaneously as *de novo* sporadic mutations. Point mutations or mtDNA rearrangements (mtDNA deletions) are the most common cause of mtDNA-related diseases. Approximately 1 in 200 individuals is affected by mtDNA point mutations and in most cases in heteroplasmic condition, but in only few people the mutant mtDNA molecules exceed the threshold (Elliott et al. 2008). This means that the ratio of normal/mutated mtDNA is the main factor that determines the onset of the disease. MERRF (myoclonic epilepsy with ragged red fibers), MELAS (mitochondrial encephalomyopathy with lactic acidosis and stroke-like episodes) NARP (neurogenic weakness, ataxia and retinitis pigmentosa) are some representative disorders caused by heteroplasmic mutations (Nils-Gran Larsson et al. 1995; Vergani et al. 1999; Nissanka and Moraes 2020). Otherwise, sporadic mtDNA mutations arising during embryonic development, lead to the onset of different types of diseases, such as Kearns–Sayre syndrome (KSS), progressive external ophthalmoplegia (PEO) and Pearson syndrome. Mutations in mtDNA have been considered for a long time the predominant cause of mitochondrial disease.

However, today it is known that the diseases are caused by mutations in the nuclear genes in more than 50% of adult cases and more than 80% of cases with onset during infancy or childhood. Since oxidative phosphorylation and other mitochondrial processes are extremely complex, the number of genes potentially involved is very high and could coincide with the entire mitochondrial proteome (Calvo and Mootha 2010).

1.5 HEREDITARY OPTIC NEUROPATHIES

The optic nerve is highly dependent on mitochondria. A broad category of optic neuropathies, with both genetic and environmental origin, are caused by mitochondrial dysfunctions (Sadun 2002). Mitochondrial hereditary optic neuropathies (HON) are disorders characterized by dysfunction and loss of retinal ganglion cell (RGC), with consequent loss of central vision. For this reason, they represent an important cause of chronic visual dysfunction (Yu-Wai-Man, Griffiths, and Chinnery 2011). The two most common forms of HON are Dominant Optic Atrophy (DOA) and Leber's hereditary optic neuropathy (LHON). It was established that 60-70% of DOA cases are caused by mutations in the nuclear gene *OPA1,* encoding for a protein involved in the mitochondrial dynamics, in particular in fusion pathway. LHON is a maternally transmitted disease that predominantly affects young males. It was discovered as a clinical entity in 1871 by the ophthalmologist Theodore Leber, and in 1988 it was reported as the first hereditary mitochondrial disease (Wallace et al. 1988). LHON is mainly due (95% of the subjects studied) to three mtDNA points mutations (m.3460G>A / *MTND1*, m.11778G>A / *MTND4*, and m.14484T>C / *MTND6*) in genes encoding for complex I subunits of the mitochondrial respiratory chain (Carelli, Ross-Cisneros, and Sadun 2004).The symptoms in HON patients are characterized by rapid loss of central vision in one eye. This manifestation is generally painless and is associated with abnormalities in the perception of the colors. Often the second eye can be affected after a few days or months, rarely after years. Vision loss is usually permanent, although a mild spontaneous recovery may occur. Blindness is generally the only clinical manifestation of HON, but in some patients, cardiac, skeletal or neurological dysfunctions have been reported (Carelli, Ross-Cisneros, and Sadun 2004; Yu-Wai-Man, Griffiths, and Chinnery 2011). The disease penetrance, calculated as the affects numbers on the total of carriers, is very high in males compared to females (Alfredo A Sadun et al. 2003). Penetrance is heterogeneous, can vary between families and within the same pedigree. Factors that can influence the disease

include heteroplasmy, environmental factors (such as the use of alcohol and tobacco), mtDNA haplotype and modifications in the nuclear genes (epigenetics modification). Although in many families the mitochondrial pathogenic mutations are present in homoplasmic conditions, not all the individuals of the maternal line develop the illness, hypothesizing the existence of additional genetic determinants, such as modifications of nuclear genes(Carelli, Ross-Cisneros, and Sadun 2004; Hudson et al. 2007; Shankar et al. 2008; Castellani et al. 2020). Thanks to the advent of new highly processive sequencing techniques (next generation sequencing, or NGS) it has been possible to implement the ability to link the specific genetic defect with the patient's pathological phenotype (optic atrophy). (Achilli et al. 2012). Mutations in other genes were associated with HON (e.g. *TMEM126A*, *ACO2*, *AFG3L2*, *MFN2*, *SPG7*, *WFS1*, *C12orf65*, *OPA3*), even if in some cases the diagnosis is not certain (Barbet et al. 2003; Hanein et al. 2009; Metodiev et al. 2014; Tucci et al. 2014; Reynier et al. 2004; Charif et al. 2015). Therefore, in many subjects affected by HON, the gene causing the dysfunction is unknown and the identification of new pathological genes, represents the goal for a better and faster diagnosis. For this purpose, a powerful and easy tool is the patients' exome sequencing through NGS, followed by bioinformatic analysis aimed at identifying the allegedly pathological mutation(s). Once the mutation is identified as potentially pathogenic, however, rigorous validation is required to associate the genetic defect to the pathology. Such validation can be performed through phenotypic and biochemical *in vitro* tests, in patients' cells and in suitable model organisms (Claypool 2013).

1.6 *S. cerevisiae* AS A MODEL FOR MITOCHONDRIAL DISEASES

Several of the scientific knowledge concerning the principal properties of human mitochondria derives from studies performed in model systems including the yeast *S. cerevisiae*. Yeast shares many cell characteristics with higher eukaryotes and for this reason, it has been defined as a "honorary mammal" (Resnick and Cox 2000). All the intracellular structures present in mammalian cells, including mitochondria (Botstein 1991) and the principal metabolic processes, are conserved in yeast. The use of *S. cerevisiae* as a model organism has several advantages: it grows quickly in different cultural conditions and can exist both in the haploid and diploid state, making possible to study the effect of both dominant and recessive mutations. A broad range of genetic engineering tools is available, including high-efficiency

transformation with single or multi-copy plasmids. The possibility to perform gene knockouts in yeast is facilitated by two important characteristics: the high degree of genome compaction and the high efficiency of homologous recombination, which allow the insertion of deletion-cassette in a specific locus. These features have been exploited extensively for the selection, screening, and identification of mutant phenotypes, as well as for the creation of new mutant strains. *S. cerevisiae* was the first eukaryotic organism whose genome has been completely sequenced; the entire nucleotide sequence (12.8 Mb), about 250 times shorter than the human genome, was published in 1996 (Goffeau et al. 1996). Genome analysis identified more than 6300 genes (Goffeau et al. 1996; Johnston 2000; Sáez-Vásquez and Gadal 2010), about 5 times less than those of humans but 1.5 times greater than the *Escherichia coli* genes (Blattner et al. 1997; Venter et al. 2001). Hence, the yeast expresses a minimal set of genes needed to support the survival of eukaryotic organisms. 15% of the open reading frames (ORFs) of the yeast genome remain without an assigned function (Costanzo et al. 2001; Sickmann et al. 2003; Yang et al. 2017). Despite this limitation, *S. cerevisiae* is currently one of the few eukaryotic organisms in which both genomic and proteomic analyzes are performed efficiently (Kumar and Snyder 2001; Hughes et al. 2000; Uetz and Hughes 2000; Martzen et al. 1999; Zhu et al. 2001). Thanks to the high homologous recombination efficiency and using a high-throughput strategy, haploid and diploid yeast strains collection were generated: a total of 5943 *Saccharomyces cerevisiae* strains were constructed, each with a precise deletion in non-essential genes (Winzeler et al. 1999). Interestingly, 46% of known human proteins possess homologs in yeast and 31% of the proteins encoded by yeast genome have a human ortholog (Venter et al. 2001; Laurent et al. 2020). The conserved proteins between yeast and humans are involved in the essential mechanisms of cellular life, such as DNA replication, recombination and repair, RNA transcription and translation, communication between subcellular compartments, general metabolism and mitochondrial biogenesis. However, human proteins have often more complex structures and different domains architecture. Despite this, several studies have shown that yeast genes share a significant identity sequence with 30-40% of the human genes associated with diseases (Yang et al. 2017; Bassett et al. 1996). Another extremely important and peculiar characteristic of *S. cerevisiae* is that, unlike most eukaryotic organisms, it can survive even in the absence of respiratory function and in the presence of mitochondrial DNA deletions or lack of it, providing a fermentable carbon source in the medium (Tzagoloff and Dieckmann 1990). This characteristic makes yeast particularly useful to study molecular basis in human

pathologies due to mitochondrial metabolism dysfunctions. Yeast mutants with altered respiratory chain are called respiratory deficient (RD) mutants, unable to grow on non-fermentable carbon sources such as ethanol, glycerol, acetate and lactate, but only on fermentable substrates. RD mutants form small colonies on glucose and, based on this characteristic, are called "*petite*" colonies. The morphology of the mutated strains is a consequence of the inability to metabolize ethanol, produced during the glucose fermentation, or other non-fermentable carbon sources. While in high eukaryotic cells, most of the ATP derives from the metabolic pathways present in the mitochondria or lactic fermentation, in yeast cells ATP is produced through two ways:

- glycolysis and fermentation, when glucose or other sugars are used as carbon source
- respiration and oxidative phosphorylation, when a non-fermentable carbon source is added to the medium

Petite mutants can result from both mutations in nuclear genes (*pet* mutants) and from mitochondrial genome mutations (cytoplasmic *petite* or simply *petite*). While *pet* mutants arise spontaneously at low frequency, cytoplasmic *petites* are spontaneously generated with a very high frequency (1-10%), because the mtDNA has a greater predisposition to the mutations onset. (Nagai, Yanagishima, and Nagai 1961; Contamine and Picard 2000; Lodi et al. 2015). The *petite* colonies frequency is variable and closely related to the strain background, ploidy and growing conditions. Thanks to the ability to remain viable despite mtDNA alterations, *S. cerevisiae* is defined *petite* positive, unlike organisms (called *petite* negative) which cannot grow on fermentable carbon sources (e.g. glucose) in the absence of an intact mitochondrial genome. In yeast, some phenotypes related to the mitochondrial metabolism dysfunctions are easily observable; in fact, mutations that inhibit mitochondrial functionality can determine growth reduction or inhibition on non-fermentable carbon sources, alteration of respiratory activity and absorption or levels of the respiratory cytochromes. Several studies have shown that yeast is a suitable model system to demonstrate the pathogenicity of mutated genes involved in mitochondrial diseases (Fontanesi 2004; Palmieri et al. 2005; Schwimmer et al. 2005; Spinazzola et al. 2009; Rinaldi et al. 2010; Baruffini et al. 2011; Ceccatelli Berti et al. 2021). As already

discussed, the diagnosis of mitochondrial pathologies is often complex, especially for the ones involving mutations in nuclear genes where it is difficult to relate the clinical phenotype to the genetic defect. In fact, mutations in the same gene can generate different symptoms and mutations in different genes can lead to the same pathological phenotype. Consequently, even when it is possible to find several families with components that exhibit the same symptoms, there is no guarantee that they harbor the same genetic defect (Patrick F. Chinnery 2003). Therefore, to identify allegedly pathological mutations, classical genetic techniques followed by sequencing analysis are performed. The identification of pathological mutations is difficult because, among the different individuals, many polymorphisms are present. Discerning between pathological mutations and polymorphism is a delicate process, which cannot be based only on predictive bioinformatic programs but requires a validation system. Hence, the validation process is defined as the study in a model system of the mutation effects on several phenotypes. Validation is obviously more important in sporadic cases when the patient's family history is not available. The workflow to create a yeast model is schematized in figure 1.7.

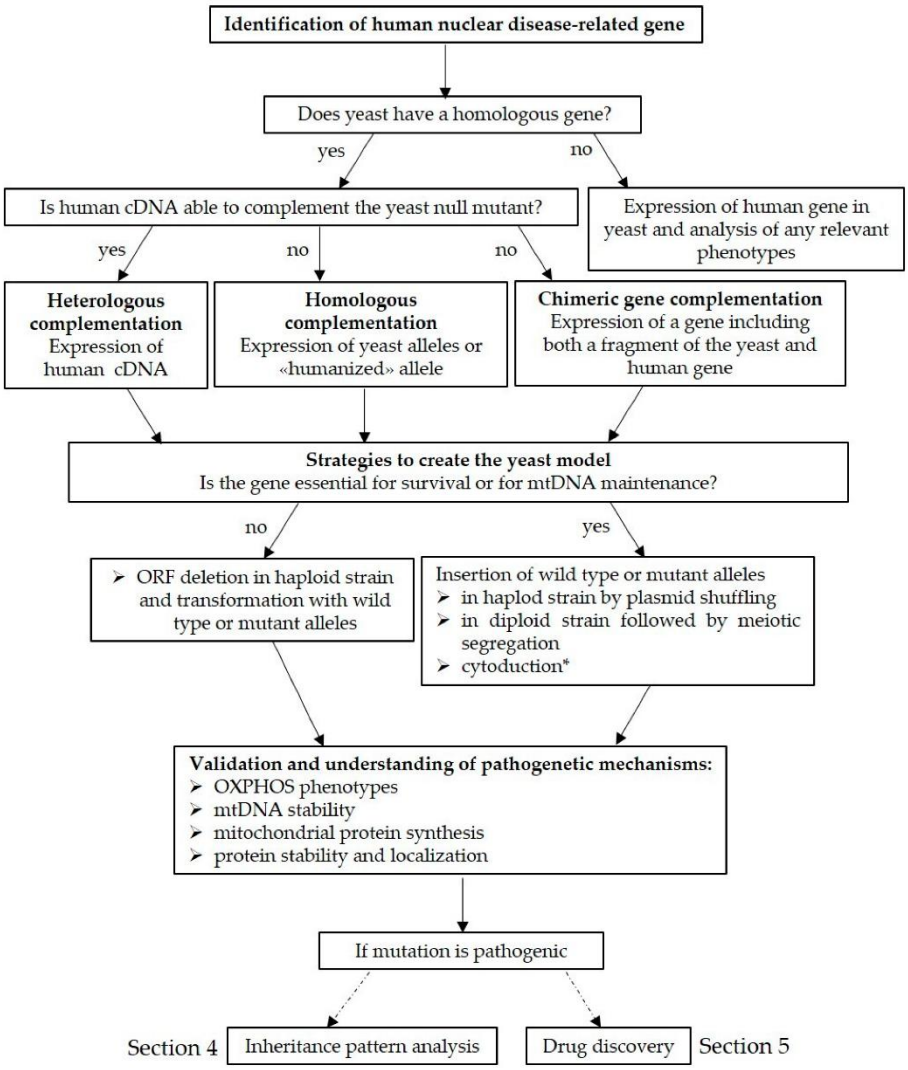

Figure 1.7: Schematic representation of the workflow to create a mitochondrial disease yeast mode (image taken from the review "The Power of Yeast in Modelling Human Nuclear Mutations Associated with Mitochondrial Diseases" (Ceccatelli Berti et al. 2021)

To build a yeast model, the first step to do is to understand whether the gene implicated in human pathology has an ortholog in the yeast genome. If the gene in analysis is absent in yeast, it can be cloned into an expression vector under the control of an appropriate promoter to regulate the expression of the putative pathological gene. Some examples of this type of model concern neurodegenerative diseases, associated with protein misfolding and the consequent formation of inclusion bodies. The "humanized" yeast model has been used in the recent past to understand the pathogenetic mechanisms of degenerative diseases such as Parkinson's, Huntington's and polyglutamine (poly(Q)) (Khurana and Lindquist 2010). When the gene

identified in patients as a possible cause of the disease has an ortholog in yeast, homologous, heterologous or chimeric complementation can be used. If the human cDNA complements the deletion of the yeast orthologous gene, a heterologous complementation approach can be performed, in which the cDNA of interest is inserted into a yeast expression vector, optimizing its expression levels by selecting an appropriate promoter, and subsequently introduced in the corresponding yeast null mutant strain. For example, this type of approach has been used for the construction of models related to GRACILE syndrome-related gene *BCS1L*, encoding a mitochondrial chaperone involved in the correct assembly of complex III (Fernandez-Vizarra et al. 2007; Tuppen et al. 2010; de Lonlay et al. 2001; Cruciat et al. 1999). Another example of heterologous complementation regard *COASY* (Dusi et al. 2014; Ceccatelli Berti et al. 2015), a mitochondrial gene encoding for the coenzyme A synthase (Aghajanian and Worrall 2002), whose mutations are associated with CoPAN (COASY protein-associated neurodegeneration), a neurogenerative disorder characterized by damage of the mitochondrial processes and brain iron accumulation (Dusi et al. 2014; Di Meo et al. 2020). This type of approach allows having a direct confirmation of the pathological role of the gene identified in patients, but on the other hand, it is not always practicable as it is strictly dependent on both the ability to complement the deletion of the yeast gene and the optimization of the protein expression level. When these situations occur, it is possible to follow a different strategy, performing the homologous complementation. The key point of this approach is based on the fact that if an amino acid residue is totally or partially conserved during evolution, it is possible to hypothesize that has the same function in both human and yeast protein. When this condition occurs, the effects of the mutation inserted in the yeast gene will replicate the pathological role of the substitution in the human gene involved in the disease. If by aligning the *S. cerevisiae* and human protein sequences the amino acid is conserved, it is possible to directly insert the mutation into the corresponding yeast amino acid. On the other hand, when the mutation lies into a non-conserved residue but within a stretch conserved during evolution, assuming that the function of this portion exactly replicates what happens in the human protein, an alternative strategy may be followed. In fact, it is possible to build both a humanized control allele, in which the original yeast amino acid is replaced with the human wild-type residue (humanized allele), and also the mutated allele bearing the mutation under investigation. Both alleles, under the control of their physiological promoter, are inserted into a vector used to transform the null yeast strain. First of all, the ability of the humanized allele to complement the deletion of the wild-

type gene is analyzed; then the effect of the mutation on several phenotypes related to mitochondrial processes in yeast is evaluated. An example of validations using the homologous complementation strategy concerns *ISCU*. This gene encodes a protein involved in the genesis and assembly of Fe-S clusters, and mutations in this gene are related to skeletal and cardiac myopathy (Olsson et al. 2008; Kollberg et al. 2009). In this case the variants, which are in heterozygosis in patients, were modeled in the orthologous yeast gene (*ISU1*), demonstrating both the pathogenicity and the dominance of such mutations (Legati et al. 2017). When the previous strategies are not feasible, because the cDNA doesn't complement or the mutation falls into a poorly conserved region, the construction of a "chimeric" gene harboring a region of the human gene and a region of the yeast gene can be used. One of the main reasons for which the heterologous complementation fails is due to a partially different mitochondrial import system of the proteins encoded in the nucleus between human and yeast. In fact, the mitochondrial targeting sequence (MTS) of human proteins maybe not recognized in yeast, preventing the translocation. To overcome this problem, it is possible to generate a fusion gene (chimera) in which the human MTS signal has been replaced with that of yeast, allowing the correct localization of the protein. This approach has been used for the construction of various disease models, such as *POLG*, and *SPG7* and *AFG3L2*, two subunits of the m-AAA complex, an ATP-dependent metalloprotease located in the inner mitochondrial membrane (Magri et al. 2018; Atorino et al. 2003). Sometimes, to enhance the complementation, it is necessary to replace not only the MTS but also a portion of the human protein by replacing it with that of yeast. For example, to study the potentially pathological mutations in *OPA1*, a gene involved in mitochondrial dynamics, and *ANT1*, which encodes for a mitochondrial ADP/ATP carrier, "true" fusion proteins were constructed (Nolli et al. 2015; Nasca et al. 2017; Lodi et al. 2006; Hatanaka et al. 2001). Once the best strategy to build a yeast disease model has been identified, a series of phenotypes related to mitochondrial activity can be analyzed to highlight the mutation pathogenicity, including oxidative growth, respiratory activity, protein and mRNA stability, mitochondrial protein synthesis and enzymatic assays (better discussed in the "Material and Methods" and in the "Results" sections).

1.7 AIM OF THE PROJECT

My Ph.D. project makes part of the “Italian project of Hereditary Optic Neuropathies (IPHON): from genetic basis to therapy", a program funded by the Italian Ministry of Health which is based on the collaboration between the University of Parma and the Institute of Neurological Sciences, Bellaria, Bologna (iItaly). This research project has two main aims:

- identification of new mutations causing the HON pathology trough NGS techniques and patient-derived fibroblasts analysis.

- validation of the pathological mutations, using the model organism *Saccharomyces cerevisiae*, provided that the identified mutations can be studied in such model

These two aims are the subject of two different Ph.D. theses. The former concerns the identification of the mutations in patients and the subsequent characterization of the disease, exploiting patient-derived fibroblasts. The latter, which is the object of the study here reported, regards the validation of the mutations identified in patients, by introducing them in the model organism *S. cerevisiae* and evaluating the effect on mitochondrial functionality. Since the data concerning the studies performed on fibroblasts are under embargo, only the results obtained in yeast will be discussed in this thesis. This project began with the genetic screening of almost 200 patients affected by HON, carried out at the Institute of Neurological Sciences in Bologna, where about 100 new cases are followed each year. The selection of patients was carried out based on their genetic characterization, focusing on subjects in which the disease is not due to the classic main known genetic determinants, already associated with HON. For the identification of patients with these characteristics, a custom panel based on the Illumina sequencing platform of nuclear genes already described or suspected to be related to hereditary optic neuropathies, syndromic or non-syndromic, was designed. For this purpose, a specific panel of 36 genes was created: *ACO2, AFG3L2, AIFM1, AOX1, ATP1A3, C12ORF65, C19ORF12, CISD2, DNM1L, IBA57, MFN1, MFN2, MTFR1, MTFR2, MTPAP, NEFH, NR2F1, NUTF2, OMA1, OPA1, OPA3, PHB, PHB2, PMPCA, PRPS1, RTN4IP1, SDHA, SFXN4, SLC25A46, SPG7, TFG, TIMM8A, TMEM126A, TSFM, WFS1, YME1L1*. 183 unrelated probands were investigated with this custom panel genes, and in negative cases, whole-exome sequencing (WES) was performed, prioritizing mitochondrial genes. In most cases, the patients presented mutations in genes already described to be associated with HON, except for two variants in homozygosis in the

MTFMT and *MECR* genes. Furthermore, the analysis performed with the panel identified novel mutations, not yet described in the literature, in the *SDHA* and *ACO2* genes. Although these genes are known to be associated, when mutated to HON, these novel variants were studied in this work.

In this screening, 13 variants were identified:

- 4 variants in the *SDHA* gene coding for the catalytic subunit of the succinate dehydrogenase
- 1 variant in *MECR* coding for the Mitochondrial Trans-2-Enoyl-CoA Reductase enzyme, involved in the mitochondrial biosynthesis of fatty acids
- 1 variant in *MTFMT*, encoding an enzyme that catalyzes the formylation of the first methionine during mitochondrial protein synthesis.
- 7 variants in *ACO2* coding for the aconitase, an enzyme of the Krebs cycle.

Once the allegedly pathological mutations have been identified, it is necessary to have a validation system that definitively links the patients' HON phenotype with these variants. Since the main purpose of this thesis is to assess whether these mutations are the direct cause of diseases in patients, it is necessary, therefore, to proceed with the validation process in yeast. In table1, the human variants, the condition in which they were identified (heterozygosis or homozygosis) and the conservation of this residues in yeast are reported:

	Human gene	cDNA variant	Human Protein change	Genotype	Yeast Gene	Residue conservation	Yeast Protein change
1	*SDHA*	c.1127T>C	L376P	HT	*SDH1*	Conserved	L367P
2	*SDHA*	c.1351C>t	R451C	HT	*SDH1*	Conserved	R444C
3	*SDHA*	c.1799G>A	R600Q	HT	*SDH1*	Conserved	R671Q
4	*SDHA*	c.1877C>A	T626N	HT	*SDH1*	Conserved	T602N
5	*MECR*	c.772C>T	R258W	HM	*ETR1*	Conserved	R256W
6	*MTFMT*	c.518C>T	T173I	HM	*FMT1*	Conserved	T173I
7	*ACO2*	c.935G>A	R312Q	HT	*ACO1*	Conserved	R308Q
8	*ACO2*	c.1420A>G	R474G	HT	*ACO1*	Conserved	R471G
9	*ACO2*	c.1438A>G	N480D	HT	*ACO1*	Conserved	N477D
10	*ACO2*	c.1454A>G	E485G	HT	*ACO1*	Non-conserved	Q482G
11	*ACO2*	c.1949A>C	Y650S	HT	*ACO1*	Conserved	Y647S
12	*ACO2*	c.2011C>T	R671W	HT	*ACO1*	Conserved	R668W
13	*ACO2*	c.2012G>A	R671Q	HT	*ACO1*	Conserved	R668Q

Table1: list of variants identified. HT indicates variants in Heterozygosis with the wild type allele and HM indicates variants in Homozygosis

Once the mutations are modeled in *S. cerevisiae*, firstly, the impact of the mutations on mitochondrial activity will be evaluated, analyzing oxidative growth and respiratory activity. A defect in the OXPHOS suggests that the mutation is the probable cause of the pathology in patients. After verifying the presence of a defect in the OXPHOS metabolism, the yeast model will be used for studies aimed to understand the molecular mechanisms causing the disease in patients and, when possible, to find molecules that could improve the phenotype. Thus, an approach based first on validation and then on understanding the molecular defect will be used.

1.8 OVERVIEW OF GENES IDENTIFIED AS A POSSIBLE CAUSE OF HON STUDIED IN THIS WORK

1.8.1 *SDHA* and Succinate dehydrogenase

Complex II of the respiratory chain (succinate-ubiquinone oxidoreductase or succinate dehydrogenase, SDH) is a flavoprotein located in the inner membrane of the mitochondrion. This complex represents the only direct link between the citric acid cycle and the electron transport chain, since it catalyzes the oxidation of succinate to fumarate, transferring electrons directly to ubiquinone to produce ubiquinol. The structure of the 124 kDa porcine mitochondrial complex II, the first SDH structure of a mammalian organism to be solved, was determined in 2005 (PDB ID: 1ZOY) (Sun et al. 2005). The respiratory chain SDH complex consists of two distinct regions: a hydrophilic peripheral dimeric domain and a hydrophobic dimeric region that anchors the entire complex to the IMM. The hydrophilic domain is composed of a flavoprotein subunit (Fp) with a typical Rossmann fold structure in an extended conformation, containing one FAD molecule bonded to a histidine side chain (Cecchini et al. 2002), and a 29-kDa iron-sulfur subunit (Ip) which connects Fp to the membrane anchor. It consists of three different clusters Fe-S ($[2Fe\text{-}2S]^{2+1+,}$ $[4Fe\text{-}4S]^{2+1+}$ and $[3Fe\text{-}4S]^{1+0}$), implicated in the electron transfer between FAD and ubiquinone (Sun et al. 2005). In all eukaryotic complexes, the hydrophilic domain, anchored to the inner mitochondrial membrane through hydrophobic subunits, locates in the mitochondrial matrix (Figure 1.8) (Ackrell 2000).

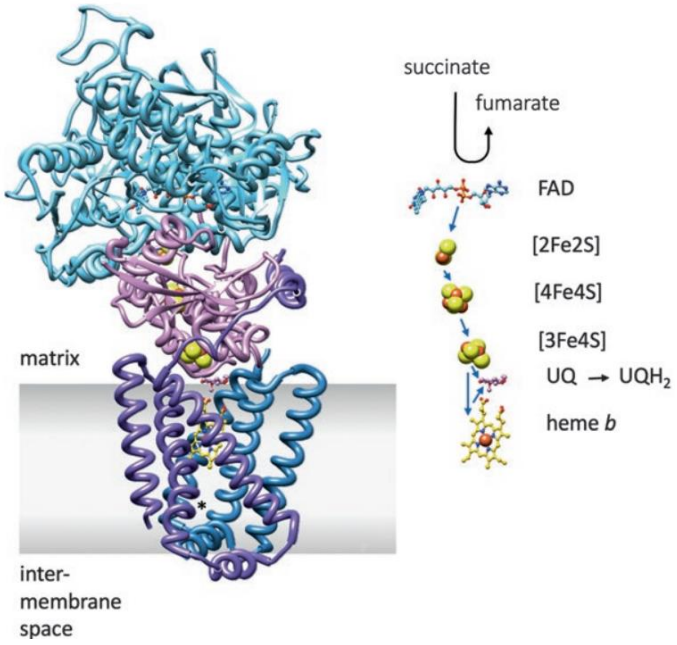

Figure 1.8: succinate dehydrogenase complex structure and electron flow direction from succinate to ubiquinone (Moosavi et al. 2020)

SDH is a heterotetrameric complex, composed of four subunits that are encoded by *SDHA-D* nuclear genes in mammals (corresponding to the *SDH1-4* genes in yeast): these genes are generally considered as housekeeping since they are expressed in all tissues (Parfait et al. 2000). Each subunit undergoes a maturation process starting from a precursor composed by a mitochondrion N-terminal targeting sequence, which is removed by proteolytic cleavage (Sharma et al. 2019). SDHA and SDHB subunits (corresponding to Sdh1 and Sdh2 in yeast, respectively) form the catalytic dimer which contains the active site, FAD and the three Fe-S clusters. SDHC and SDHD (corresponding to Sdh3 and Sdh4 in yeast, respectively) are integral membrane proteins containing the heme group and ubiquinone reduction sites. In yeast, the catalytic subunit Sdh1 is a 70 kDa protein encoded by the *SDH1* nuclear gene, located on chromosome XI. Through computational analysis, the presence of a highly conserved paralog gene *SDH1b* has been identified. The encoded proteins Sdh1 and Sdh1b share 84% identity; however, it was shown that *SDH1b* complements the deletion of the *SDH1* gene only when inserted in a multi-copy plasmid. On the contrary, under physiological conditions, the Sdh1b levels are 100-500-fold lower than those of Sdh1, with a low contribution to the catalytic activity (Colby, Ishii, and Tzagoloff 1998). The assembly process of the four subunits is a delicate mechanism and therefore is supported by helper proteins, called assembly factors, that guarantee the correct recognition and positioning of these SDH subunits. The first specific assembly factor for succinate dehydrogenase, SDHAF1, was discovered analyzing the genotype of young patients with progressive leukoencephalopathy associated with a significant decrease in SDH activity (Alston et al. 2012; Ghezzi et al. 2009). SDHAF1 is characterized by peculiar tripeptide motifs Leu-Tyr-Arg (LYR), which represents a signature for proteins involved in Fe-S metabolism (Sharma et al 2019). SDHAF1 plays likely an important role in the insertion or retention of the Fe-S centers inside the protein backbone of complex II (Na et al. 2014). The human *SDHAF1* gene is the ortholog of the yeast gene *SDH6,* and its deletion in yeast leads to 60-70% reduction in SDH activity (Ghezzi et al. 2009). Failure to incorporate the Fe-S centers can inhibit the formation or destabilize the holocomplex structure, leading to a decreased enzymatic activity. SDHAF2, another recently isolated assembler, which corresponds to Sdh5 in yeast, is involved in the insertion of FAD cofactor into the catalytic subunit of the enzyme (Hao et al. 2009). Yeast studies revealed that Sdh7, ortholog to SDHAF3 in human, another SDH assembly factor, act together with Sdh6, to promote Sdh2 maturation by binding

Sdh1/Sdh2 intermediate, protecting it from the deleterious effects of oxidants (Na et al. 2014). Therefore, since the role of complex II is crucial for mitochondrial metabolism, it is easy to understand that mutations and defects in genes that encode for the SDH subunits complex and their assembly factors lead to relevant pathologies, such as:

- Leigh's syndrome, an early-onset encephalopathy caused by homozygous or compound heterozygous mutations in *SDHA* gene (Parfait et al. 2000)

- paragangliomas (Baysal et al. 2000; Amar et al. 2021), tumors associated with the sympathetic nervous system, and pheochromocytomas (Astuti et al. 2001; Gill 2018), tumors connected to the chromaffin cell of the adrenergic glands, characterized by loss of heterozygosity in genes encoding for the subunits B, C and D of SDH complex

- Hereditary optic neuropathies (HON), mitochondrial pathologies characterized by deterioration of the retinal ganglion cells and optic nerve atrophy, already identified in several studies (Courage et al. 2017; Zehavi et al. 2021)and discussed in this thesis.

Previous studies in our laboratory (Panizza E., Ph.D. thesis, unpublished) on heterologous complementation studies have demonstrated the inability of *SDHA* human allele to complement the deletion of *SDH1* gene in yeast, probably due to the inability to interact correctly with the other subunits of the yeast complex or with the assembly factors. Despite this, as demonstrated in several studies, it was possible to create yeast models for the validation of *SDHA* pathological mutations, exploiting the homologous complementation approach. As an example of this, Burnichon and collaborators studied the effect of R589W mutation in *SDHA* gene, identified in patient affected by extra-adrenal paraganglioma, by inserting the pathological substitution directly into the corresponding yeast positions of Sdh1. The analysis of the phenotype of the mutant strain shows that the mutation leads to the inability to use non -fermentable carbon sources probably due to a total destabilization of the mutated protein,

evidenced through western blot analysis, validating the metabolic defect associated with this variant (Burnichon et al. 2010). Furthermore, in yeast, mutations in one of the four subunits of the complex, destabilize the other components which take part in the succinate dehydrogenase. In fact, mutations in the catalytic subunit Sdh1 are associated to deficient levels of Sdh2, the subunit with which it closely interacts (Bannon et al. 2017).

1.8.2 *MECR* and Mitochondrial fatty acids biosynthesis (mtFASII)

Fatty acids synthesis (FAS) is a process conserved from bacteria to eukaryotes including humans. In cells, FAS has several functions, among which the main ones are the production of triglycerides and phospholipids: the former are stored as energy stocks and the latter are the essential constituents of the membranes. This process takes place in two different compartments: cytosol and mitochondrion (Hiltunen et al. 2010). The presence of a second mitochondrial pathway for fatty acid synthesis (mtFAS) has been considered marginal for many years, with a negligible role in the production of these molecules. However, the identification of mutations in genes encoding for enzymes involved in this biosynthetic pathway, associated with neurodegenerative diseases, has restored the curiosity in understanding the true contribution of mtFAS in fatty acids production (Heimer et al. 2016). The cytosolic FAS type I pathway comprises one (a homodimer of α_2-subunits in higher eukaryotes) or two (a heterododecamer of $\alpha_6\beta_6$-subunits in fungi) multifunctional polypeptides generated as a consequence of a genes fusion (McCarthy and Hardie 1984; Wernig et al. 2020), whereas the mitochondrial pathway comprises independent monofunctional polypeptides that carry out individual steps in FAS (type II) (Hiltunen et al. 2009). Yeast has been a useful tool for understanding and characterizing the mtFAS pathway. The process starts from Acetyl-CoA, a fundamental and highly regulated hub of the mitochondrial processes. The elongation cycle is schematized in Figure 1.9. The first step involves a carboxylation reaction catalyzed by Acetyl-CoA carboxylase enzyme (Hfa1 in yeast and ACC in humans) which by means of an ATP-dependent reaction adds a carbon unit to the substrate, generating Malonyl-CoA (Hoja et al. 2004; Kearsey 1993; Kaushik et al. 2009). The malonyl-CoA:ACP transferase enzyme Mct1 (MCAT in humans), catalyzes the transfer of the malonyl moiety from malonyl-CoA to the free thiol group of the phosphopantetheine arm of the mitochondrial Acp1 protein (NDUFAB1 in

humans) (Schneider et al. 1997). Acp1 is a soluble scaffold for the formations of acyl intermediates during the stepwise process of *de novo* fatty acid synthesis (Van Vranken et al. 2016). The 3-Chetoacyl-ACP synthase enzyme Cem1 (OXSM in humans) is responsible for the chain elongation step in fatty acid biosynthesis, forming the elongate acyl-chains containing 2–14 carbon atoms with malonyl moieties attached to an acyl carrier protein. During this step, two carbon atoms are added to the fatty acid chain (Harington et al. 1993). The subsequent reaction, catalyzed by 3-Chetoacyl-ACP-reductase Oar1 (OXSM in humans), involves an NADPH-dependent reduction of the ketone group 3-oxoacyl-[ACP] to (3R)-hydroxyacyl-[ACP] (Venkatesan et al. 2014). The product of the previous reaction undergoes a dehydration reaction, catalyzed by hydroxyacyl-thioester dehydratase type 2 Htd2 (HTD2 in humans), which leads to the elimination of an H_2O molecule with the formation of trans-2-enoyl-ACP (Kastaniotis et al. 2004). Etr1 (MECR in humans) catalyzes the last step of the cycle, a NADPH-dependent reaction that leads to the formation of Acyl-ACP (Miinalainen et al. 2003). At this point, the cycle can restart with a new condensation reaction starting from Mct1 enzyme (the second enzyme of the pathway), elongating the fatty acid chain to form (C8) octanoyl-ACP, the most important intermediate that can be transformed into lipoic acid.

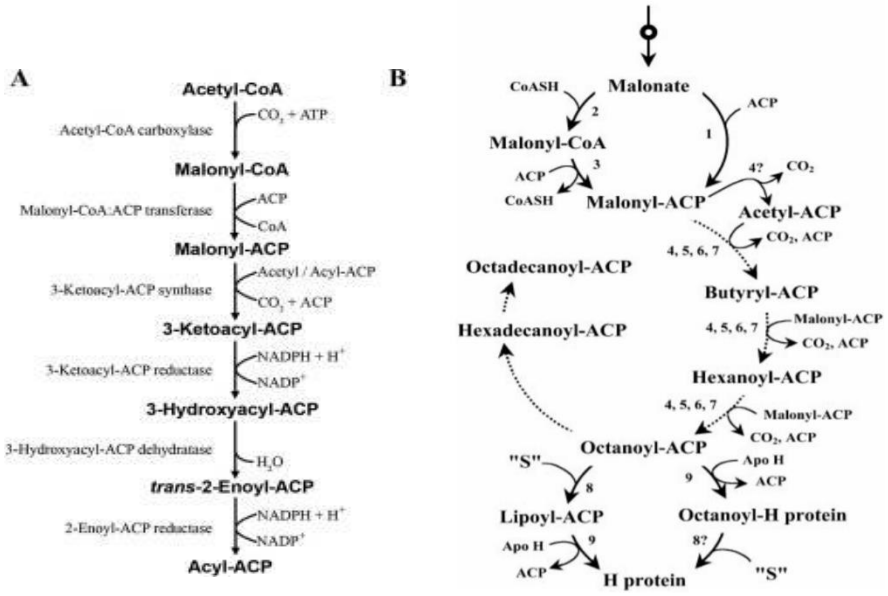

Figure 1.9: Schematic representation of the mtFAS II pathway. Fatty acids single cycle of elongation (A) and an overview of the entire biosynthetic pathway (B) (Gueguen et al. 2000; Hiltunen et al. 2009).

mtFAS has a marginal role in both phospholipids and triglycerides production, but rather is the main producer of lipoic acid, essential for many mitochondrial processes (Nowinski et al. 2018). Lipoic acid is a small amphipathic molecule composed of eight carbon atoms, two oxygen atoms in the carboxylic group and two sulfur atoms. It exists in two forms, as a cyclic disulfide (oxidized form) or as dihydrolipoic acid (reduced form), with two sulfhydryl groups in positions 6 and 8. However, the two forms are easily interconvertible through redox reactions. Due to these chemical characteristics, lipoic acid participates in various antioxidant mechanisms such as the reduction of glutathione (GSH) and ascorbic acid (P. Chen et al. 2011; Shay et al. 2009). Lipoic acid, besides being a powerful compound able to limit the ROS damaging action, plays an important role in the mitochondrial oxidative phosphorylation and in mitochondrial translation, through a tRNA maturation process linked to mtFAS (Hiltunen et al 2009). Mitochondrial tRNAs are cleaved from the initial multigenic transcripts by tRNA 3' endonuclease (Mörl and Marchfelder 2001) and mitochondrial RNAse P, which cuts the 5' leader sequences of tRNAs (Walker and Engelke 2006). This process is well detailed in yeast. *S. cerevisiae* mitochondrial RNAse P is composed of a nuclear-encoded protein Rpm2 (Morales et al. 1992)and RPM1, a mitochondrially encoded RNA subunit. *RPM1* is transcribed from different promoters: FP promoter, which transcribes *RPM1* with the upstream $tRNA_f^{Met}$ and the downstream $tRNA^{Pro}$, or SP promoter with only $tRNA^{Pro}$ (Stribinskis 2001). Following the tRNA removal from the RNA precursor, the sequence of RPM1 is processed by Pet127 (Ellis, Schonauer, and Dieckmann 2005) in the 5' end, and by 3'-to-5' exonuclease Dss1/Suv3 and/or by other enzymes not yet characterized (Dziembowski et al. 2003). These data suggest that the production of mature RPM1 RNA requires the activity of a variety of mitochondrial RNA processing factors, including RNase P itself. It was demonstrated that disruption of the mitochondrial FAS II pathway in yeast results in inefficient processing at the 5' ends of mitochondrial tRNAs by RNase P (Schonauer et al. 2008). Specifically, in FAS II yeast mutant strains, in which the cleavage of $tRNA^{Pro}$ from the 3' end of the pre-RPM transcript is abolished, low levels of mature RPM1 are observed, leading to a damaged mitochondrial translation (Schonauer et al. 2008).Besides having an important role in the regulation of mitochondrial oxidation state and mitochondrial synthesis, lipoic acid is also used as an essential cofactor for enzymes involved in glycine metabolism and α-ketoacids oxidative decarboxylation (Perham 2000; Burger, Gray, and Lang 2003). In yeast, there are three well-known lipoate-dependent enzyme systems: the glycine cleavage system (GCV), the α-ketoglutarate dehydrogenase (KGDC) and the pyruvate dehydrogenase (PDH) (Schonauer et al.

2009). GCV is involved in the cleavage of glycine to ammonia and C1 units, which is fundamental to using glycine as a sole source of nitrogen (Sinclair and Dawes 1995; Piper et al. 2002). KGDC catalyzes the oxidative decarboxylation reaction, converting 2-oxoglutarate into succinyl-CoA, the precursor of several amino acids and source of succinate, a molecule which links the respiratory chain to Krebs cycle (Repetto and Tzagoloff 1991; Vatrinet et al. 2017). PDH catalyzes the oxidative decarboxylation of pyruvate, linking cytosolic glycolysis pathway and mitochondrial respiration (Boubekeur et al. 1999; van Rossum et al. 2016). Gcv3p, Kgd2p, and Lat1p are the subunits of GCV, KGDC, and PDH, respectively, which are covalently bonded to lipoate (Nagarajan and Storms 1997; B. Chen et al. 2020). To generate the lipoylated-bonded subunits Gcv3p, Kgd2p, and Lat1p, a two-step conversion mechanism has been hypothesized for lipoic acid synthesis and protein attachment in yeast mitochondria (Hermes and Cronan 2013). Lip2p and Lip3p encode for octanoyltransferases enzymes, that utilize octanoyl-ACP or octanoyl-CoA to attach the octanoyl group to the apo-form of lipoate-dependent proteins. (Marvin, Williams, and Cashmore 2001; Hermes and Cronan 2013). The bounded octanoyl group is subsequently modified through lipoyl synthase Lip5p, which catalyzes the insertion of two sulfur atoms into the octanoate carbon chain (Sulo and Martin 1993; B. Chen et al. 2020). Lipoic acid is bound to Gcv3p, Kgd2p, and Lat1p via an amide linkage between the epsilon amino group of a lysine residue of these proteins and its carboxyl group (Sulo and Martin 1993; B. Chen et al. 2020). Interestingly, it has been discovered that Lip2p and Lip5p are required for lipoylation of all three proteins, while Lip3p is essential for lipoylation of Kgd2p and Lat1p but not Gcv3p (Hermes and Cronan 2013). A model in which Lip2, Lip3 and Lip5 together with Gcv3 take part in the same complex with lipoyl-transferase activity has been proposed (Hermes and Cronan 2013). In fact, lipoylation of Gcv3, and not the glycine cleavage activity, has been reported to be required for lipoylation of the other two target proteins (Lat1 and Kgd2), but several details on the mechanism are still lacking (Schonauer et al. 2009). In literature, some cases of *MECR* mutations associated with childhood-onset dystonia characterized by a distinctive MRI pattern in the basal ganglia and optic atrophy, have been reported (Heimer et al. 2016). Heimer and collaborator identified the *MECR* R258W variant in compound heterozygosity with a frameshift mutation; the same mutation was found in our patients' cohort in homozygous condition with recessive inheritance, as described below. In this thesis, this potentially pathological variant will be studied in yeast to understand the real effect on the mitochondrial metabolism. Based on previous results, some of the variants identified in the Heimer work (p.G232E and Y285*) were validated using a heterologous complementation approach, by inserting a multi-copy plasmid carrying the mutated

h*MECR* cDNA in a yeast *ETR1* deleted strain (Miinalainen et al. 2003; Heimer et al. 2016). Phenotypic analysis concerning oxidative growth of these strains demonstrated that the presence of the mutated h*MECR* alleles is associated with defects in oxidative growth and alteration of Krebs cycle enzymes activity, due to the lack of lipoylation of α- keto-glutarate and pyruvate dehydrogenase subunits (Heimer et al. 2016). The R258W variant was not validated in this study, probably because being in compounded with a truncated protein, it could have a marginal role in the patient's pathological phenotype.

1.8.3 MTFMT and mitochondrial translation

Protein synthesis begins with a methionine residue or with a formyl-methionine derivative (Kozak 1983; Gualerzi and Pon 1990). In prokaryotes and mitochondrion, the first methionine residue is formylated, through a transfer reaction, catalyzed in humans by MTFMT, in which a formyl group derived from 10-Formyltetrahydrofolate (10-CHO-THF) is covalently bound to the methionine residue. A single $tRNA^{Met}$ type is produced in the mitochondria, able to load methionine through a specific aminoacyl-tRNA synthetase (MetRS), generating Met-$tRNA^{Met}$ (Figuccia et al. 2021). After this aminoacylation reaction, the Met-$tRNA^{Met}$ may become the substrate of MTFMT, the human mitochondrial methionyl-tRNA formyltransferase, which binds a formyl group to the methionine. At this point, two different species of methionine-binding tRNA are present, formylated (fMet-$tRNA^{Met}$) and non-formylated (Met-$tRNA^{Met}$), used during the initiation or the elongation, respectively. Many studies have focused on understanding how these two tRNA species could be discriminated and chosen (Tucker et al. 2011). fMet-$tRNA^{Met}$ has been shown to have a higher affinity for mitochondrial initiation factor mtIF2 (Spencer and Spremulli 2004; F. Wang et al. 2021), which is recruited to the ribosome in the early stages of the synthesis. On the contrary, the Met-$tRNA^{Met}$ has a preferential affinity for mitochondrial elongation factor mtEF-Tu, recruited to the ribosome during the elongation (Takeuchi et al. 1998; Mai, Chrzanowska-Lightowlers, and Lightowlers 2017) (Figure 1.10).

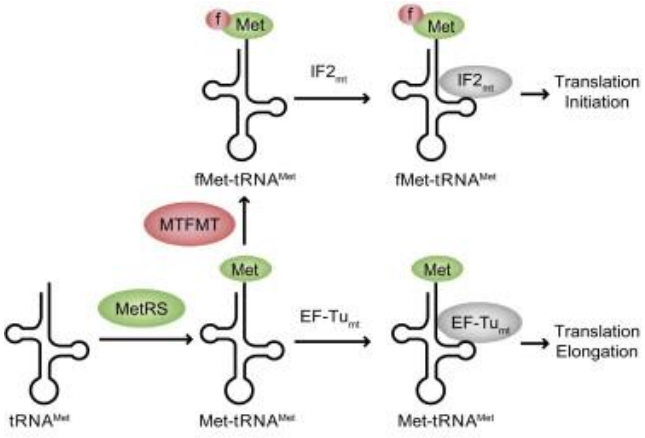

Figure 1.10: Selection process of methionine-loaded tRNAs for the elongation and initiation phases of mitochondrial synthesis

The importance of the first methionine residue formylation in human mitochondrial synthesis was demonstrated by several patients carrying mutations in *MTFMT*, identified by genetic screening and associated with Leigh syndrome (Tucker et al. 2011; Haack et al. 2014; Neeve et al. 2013). The discovery of fMet-tRNA^{Met} in the yeast *Saccharomyces cerevisiae* suggested that protein synthesis is also initiated with formyl-methionine (Kuzmenko et al. 2014). Yeast has an ortholog of the human *MTFMT* gene, *FMT1*, which encodes for a protein of 393 amino acids, which contains a mitochondrial targeting sequence and a highly conserved motif in the N-terminal proposed to be the binding site for the N10-formyltetrahydrofolate (10-formyl-THF), source of formyl group. The C-terminal contains a sequence with a putative Met-tRNA binding domain (Li et al. 2000) (Figure 1.11).

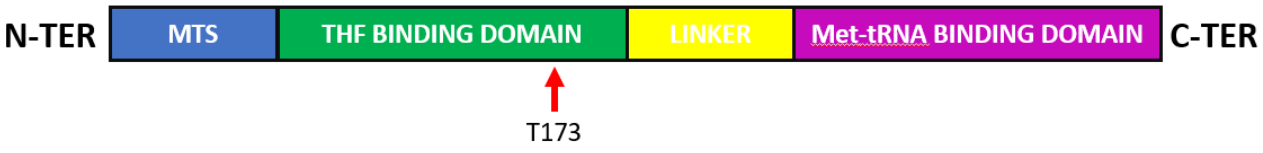

Figure 1.11: Human MTFMT protein organization

Although yeast has retained this function, it is not fundamental for mitochondrial synthesis under physiological conditions. In fact, studies carried out on yeast strain deleted in the *FMT1* gene do not show any defects in mitochondrial protein synthesis and oxidative growth (Franco et al. 2019). Based on this consideration, the function of *FMT1* can be bypassed in physiological conditions, but it was demonstrated that remain indispensable in heat-stress or starvation conditions (Li et al. 2000). Since the deletion of the *FMT1* gene leads to a mild defect in mitochondrial phenotypes only at high temperature, no *MTFMT* mutation has been validated using the yeast model. The purpose of this thesis is, if possible, to build a yeast model of *MTFMT* and find conditions in which the pathological phenotype of the mutations identified are highlighted.

1.8.4 *ACO2*

Aconitase is the second enzyme of the Krebs cycle and catalyzes the reversible isomerization of citrate to isocitrate, through the formation of the cis-aconitate intermediate.

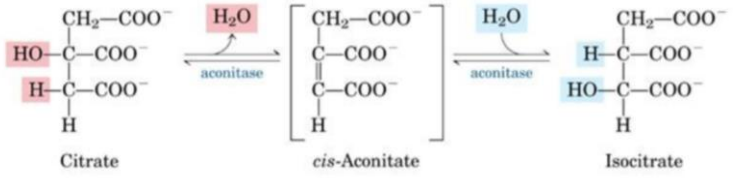

Figure 1.12: Aconitase enzymatic reaction

The substrate of the reaction is citrate which, following a dehydration reaction, loses a proton and OH group becoming cis-aconitate. The second step of the reaction is rehydration of the double bond of the cis-aconitate to form isocitrate. The structure of *Sus scrofa* mitochondrial aconitase (PDB ID: 5ACN), the first mammal aconitase to be solved, was deposited in 1990 (Robbins and Stout 1989), allowing to gain information on protein organization. The primary protein sequence is divided in four domains and a one linker region: 1-202 (domain I), 203-320 (domain II), 321-513 (domain III), 538-755 (domain IV) while residues 514-537 form the linker region which connects domains 3 and 4 (Figure 1.13). The unorganized structure of this region permits hinged movements which are

fundamental for the catalysis of the reaction (Robbins et al 1989). In the active site of the enzyme, there is an iron-sulfur center [4Fe-4S] which presumably coordinates the OH group of the citrate, to facilitate its elimination. This Fe-S center could act both in the substrate binding to the active site and in catalytic removal of water. Three cysteine residues, positioned within the active site, bind the inactive form of the cluster [3Fe-4S], while a fourth Fe atom is subsequently added and coordinated with the citrate (Robbins and Stout 1989; Artymiuk and Green 2006).

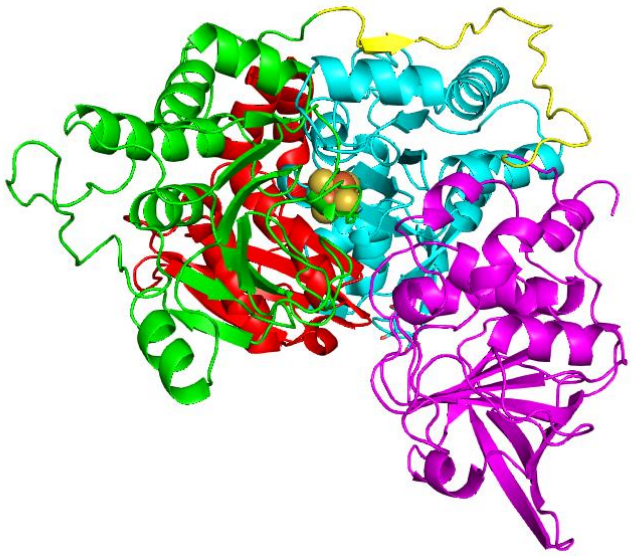

Figure 1.13: Cartoon representation of the porcine mitochondrial aconitase (PDB ID: 5ACN): domain I in light blue; Domain II in red; Domain III in green; Domain IV in magenta; Linker region in yellow

The integrity of this iron-sulfur center is essential for the enzymatic activity of aconitase (Xin Jie Chen et al. 2005). In humans, besides the mitochondrial aconitase (ACO2), there is also a cytoplasmic form (ACO1) with a different function. Human cytoplasmic aconitase (ACO1) acts as an iron regulator protein (IRP-1) (Artymiuk and Green 2006). The main feature of the cytoplasmic isoform is the presence of a labile [4Fe-4S] cluster. In fact, in absence of the latter, the interconversion of citrate into isocitrate is blocked and the protein becomes an IRP protein able to bind RNA (Wachnowsky et al. 2019). The IRPs are located in eukaryotic cells' cytosol, where they act

as post-transcriptional regulators, binding the hairpin structures of RNA known as IREs (iron response elements) (J. Wang and Pantopoulos 2011). Specifically, IRP1 recognizes IRE in the 5' UTR of the mRNA for ferritin, a protein involved in the iron storage inhibiting its own translation (negative regulation) (Zhou and Tan 2017). On the contrary, when the IRE in the 3' UTR of the transferrin receptor mRNA is recognized, the stability of the mRNA is improved (positive regulation) (Rupani and Connell 2016). In iron deprivation conditions, the necessity to increase the absorption of this ion, up-regulating transferrin receptors and down-regulating ferritin level, is satisfied by post-transcriptional regulation mediated by IRP1 (J. Wang and Pantopoulos 2011). IRP1s could be considered intracellular iron sensors, regulating the translation of proteins involved in the iron homeostasis through the assembly and disassembly of iron-sulfur clusters. In *Saccharomyces cerevisiae*, mitochondrial aconitase Aco1 is a bifunctional protein: an enzyme involved in the TCA cycle and a component of the nucleoid. Aco1 has a crucial role in ensuring the distribution and propagation of the mitochondrial genome, suggested by the fact that yeast strain deleted in *ACO1* quickly loses mtDNA (X. J. Chen, Wang, and Butow 2007). In addition, the overexpression of the *ACO1* gene suppresses the mtDNA instability in cells lacking the mtDNA packaging factor Abf2p, although the function in the mitochondrion of Aco1p and Abf2p do not completely overlap (X. J. Chen, Wang, and Butow 2007). Aco1 expression is finely regulated through two different pathways: the HAP system (heme activator protein), which is enhanced in cells with normal respiratory activity; and the retrograde system (RTG), which is activated in cells with compromised or dysfunctional mitochondria (Mao and Chen 2019; X. J. Chen, Wang, and Butow 2007). Inactivation of these two pathways leads to a decrease in the expression of *ACO1* resulting in point mutations and nick accumulation in the single strand mtDNA. These events can promote the reduction of recombination and replication stalling, which consequently leads to the complete loss of mitochondrial genomes. Under glucose repression conditions, Abf2p is essential for mtDNA maintenance, probably for its DNA packaging function (Chakraborty et al. 2017). Since Aco1 binds ssDNA, it is hypothesized that Aco1, but not Abf2, can protect ssDNA sites from ROS species during the replication (Vozáriková et al. 2020). All these considerations validate the conclusion that Aco1 stabilizes mtDNA during the replication, recombination and repair events through physical interaction with the ssDNA, even when the ability to convert the citrate into isocitrate is absent (X. J. Chen, Wang, and Butow 2007). Mutations in the human *ACO2* gene are identified in patients with a broad range of symptoms correlated to neurodegenerative diseases, including cortical atrophy, optic nerve atrophy, cerebellar atrophy, hypotonia, seizures and intellectual disabilities. (Spiegel et

al. 2012; Metodiev et al. 2014; Neumann et al. 2020; Sharkia et al. 2019). *S. cerevisiae* has proved to be an excellent model for the study of mutations associated with the *ACO2* gene. The sequence similarity allows using a homologous complementation approach for the insertion of the potentially pathological variant directly into the yeast gene *ACO1*, in fact, Sharkia and collaborators exploited this approach to validate the H596R and R684W mutations identified in compound heterozygosity in a patient with optic atrophy. These variants are inserted into the corresponding residues in the yeast *ACO1* gene, encoding the mitochondrial aconitase. H596R and R684W mutations are studied both in homozygous and compound heterozygous conditions. From these validation studies, it emerged that both variants lead to enzymatic activity deficit, dissecting the contribution of each of these mutations to the pathological phenotype of the patient (Sharkia et al 2019). However, the ability of the *ACO2* human gene to complement the absence of the *ACO1* yeast gene, when inserted in a multicopy plasmid context, was demonstrated (Metodiev et al. 2014). These finding allows studying mutations in non-conserved amino acids between the two species. The variants L74V, G259D, G661R, K736N were validated using heterologous complementation approach. Yeast, in this case, has confirmed the role of mutations in mitochondrial metabolism dysfunctions, leading to pleiotropic phenotypes such as the inability to use non-fermentable carbon sources, reduced respiratory rate, mtDNA instability and defect of aconitase activity(Spiegel et al. 2012; Metodiev et al. 2014; Neumann et al. 2020). Furthermore, the growth phenotype defects of the different yeast mutant strains showed a good correlation with the severity of the disease in patients. (Metodiev et al. 2014).

CHAPTER 2: RESULTS AND DISCUSSION SECTION I

2.1 *SDHA* MUTATIONS MODELING AND YEAST STRAINS CONSTRUCTION

As reported in the introduction, next-generation sequencing on HON patients led to the identification of four mutations in the *SDHA* gene, in compound heterozygosis with the wild type allele, encoding the catalytic subunit of succinate dehydrogenase. In particular, the mutations identified in patients are L376P, R451C, R600Q, T626N. To verify whether these amino acid substitutions, identified in patients, are the effective cause of the disease or neutral polymorphisms, several analyses are carried out. Before starting the validation iter of these mutations in the model organism *S. cerevisiae*, molecular docking studies were performed, to evaluate the region in which the variants lie. Thanks to the high sequence identity (about 95%) between porcine and human SDHA catalytic subunits and the available structure of porcine succinate dehydrogenase complex (PDB ID: 1ZOY), it was possible to discriminate where the mutations are positioned in the protein folding. The human mutated residues L376, R451, R600 T626, corresponding to the porcine L334, R409, R558, T584 respectively, are highlighted in figure 2.1

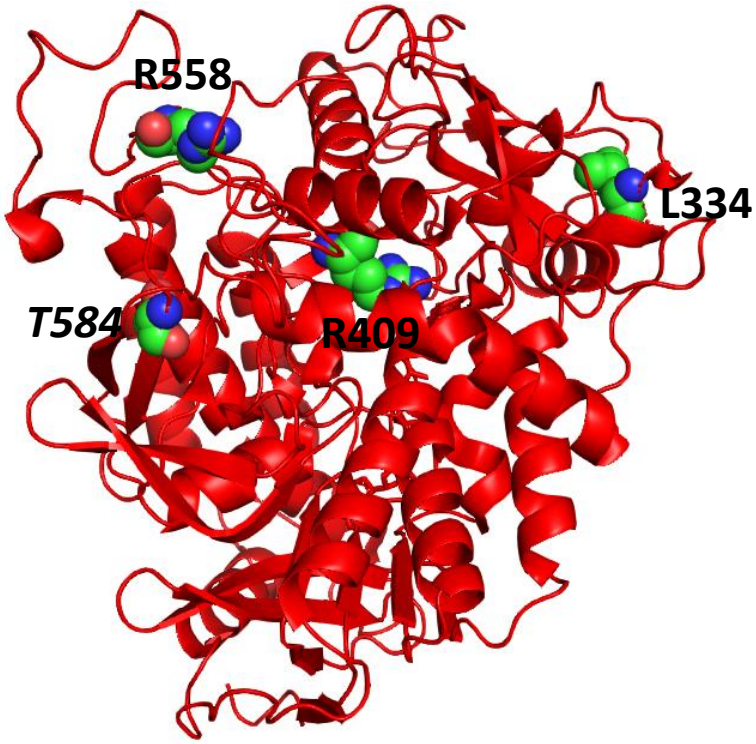

Figure 2.1: Cartoon representation of the SDHA structure of *S. scrofa* (PDB ID: 1ZOY), highlighting the position of corresponding mutated residues identified in the patients

From the row analysis of the structure, three of these residues (L334, R558 and T584) fall into superficial regions that do not show a peculiar structural organization. On the contrary, the arginine 409 has an internal localization in the structure, making contact with succinate, the SDH complex substrate. In literature, a catalytic mechanism was proposed through which the electrons and protons from the succinate are transferred to FAD (Figure 2.2) (Sharma et al. 2018; Birch-Machin et al. 2000).

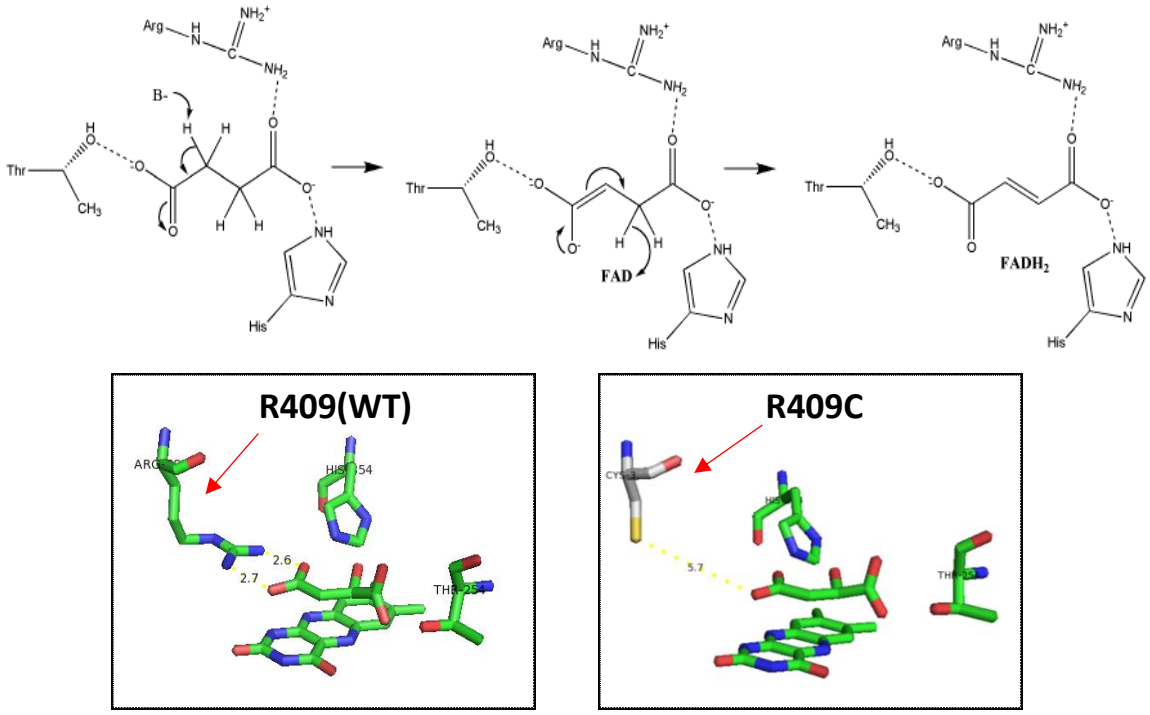

Figure 2.2: Proposed mechanism of the conversion of the succinate to fumarate with the consequent formation of $FADH_2$ (above). Analysis of the structural role of the R451 residue in the catalytic site of SDHA and the change induced by the R451C mutation(below).

This model predicts the presence of a catalytic triad formed by arginine, threonine and histidine within the catalytic site of the human SDHA subunit. The arginine residue 451, highly conserved during evolution, corresponds to amino acid R409 of the porcine structure, represented in figure 2.2. Being a nucleophilic molecule, succinate is stabilized within the catalytic site by the positive charges present on the nitrogen atom of the arginine side chain, which allowed correct positioning and subsequent FAD nucleophilic attack. Structural analysis shows that succinate and arginine 409

were contiguous (2,7 Å) in the enzymatic pocket. The replacement of arginine 409 with cysteine, an amino acid with completely different chemical-physical characteristics in the side chains, causes a loss of the proximity effect but also an ineffective stabilization of the substrate charges within the catalytic site. The mutation affecting the human R451 residue seems to have a clear impact on the protein functionality: however, for the other mutations falling into poorly structured regions, it is not possible to gain information on the possible correlation with the patient's HON phenotype. Nevertheless, all the variants identified require careful validation in *S. cerevisiae* to evaluate the impact of these on mitochondrial activity *in vivo*. Previous studies have reported the inability of the human *SDHA* gene to complement the *SDH1* deletion (Introduction, section 1.8.1), so, in this specific situation, only a homologous complementation approach is allowed. Using bioinformatics tools, the flavoprotein (FP) subunit of succinate dehydrogenases from different organisms has been aligned to evaluate the conservation degree of the residues in analysis during evolution. The multiple alignment represented in figure 2.3 clearly shows that the amino acids under investigation are highly conserved from bacteria to humans, assuming a retained function of these amino acids in the complex. The human SDHA and the yeast ortholog Sdh1 proteins share a high identity percentage, of about 60%. Moreover, all the four human amino acids under analysis are conserved in yeast and correspond to L367, R444, R593 and T602, making it possible to perform a homologous complementation approach.

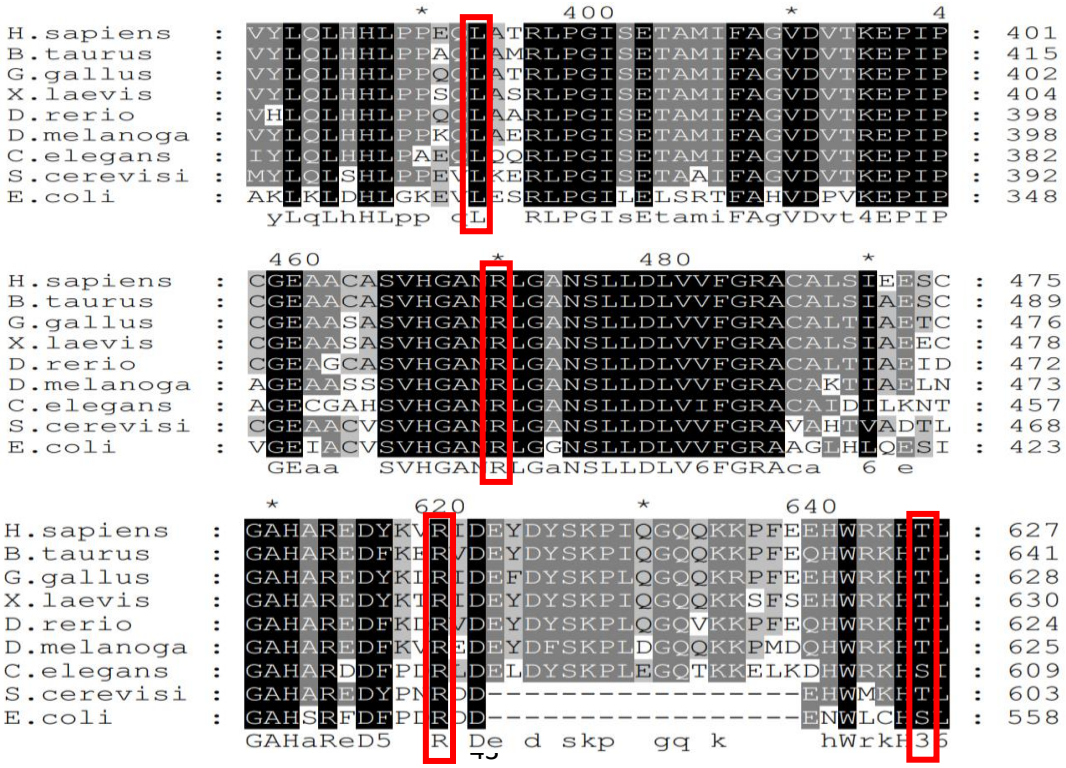

Figure 2.3: Multiple alignments of succinate dehydrogenase flavoprotein subunit sequences from different organisms. In red are highlighted the residues under analysis. The alignment was performed with cluster X and displayed with GeneDoc tool. The accession numbers related to the selected sequences are: *H. sapiens* NP_004159.2; *S. cerevisiae* CAA8198.1; *G. gallus* NP_001264327.1; *X. laevis* AAH47261.1; *E. coli* CAD6019009.1; *B. taurus* AAI05358.1; *D. rerio* AAI64560.1; *D. melanogaster* NP_477210.1; *C. elegans* NP_509446.1

To study the effect of *SDHA* mutations, it is necessary to insert the *SDH1* mutant alleles in a yeast strain bearing the deletion of the *SDH1* genomic gene. The specific deletion cassette for the *SDH1* gene (*sdh1::kanMX4*) was amplified starting from the genomic DNA extracted from the BY4741 *sdh1Δ* strain (Brachmann et al. 1998) through a preparative PCR reaction using the *SDH1*DFw and *SDH1*DRv primers. The 5' and the 3' regions of the amplicon share homology with the upstream and downstream region of the *SDH1* ORF, which allows the recognition of the correct locus and the subsequent integration by homologous recombination; the central fragment contains the gene for resistance to kanamycin, used for the selection. The cassette was then inserted into the W303-1B strain through "high-efficiency yeast transformation protocol" (Daniel Gietz and Woods 2002) to produce the deletion of *SDH1* in the W303-1B genetic background (producing W303-1B *sdh1Δ*). To generate the mutated alleles, the *SDH1* gene and its downstream and upstream regulatory regions were PCR amplified using genomic DNA of the W303-1B strain as a template and the primers *SDH1*Fw and *SDH1*Rv, containing respectively the restriction sites recognized by *Sac*I and *Sal*I. The amplicon was then digested with the *Sac*I and *Sal*I enzymes and cloned in the centromeric vector pFL38, digested with the same enzymes to obtain the construct pFL38*SDH1*. Subsequently, the *SDH1* mutant alleles containing the amino acid substitutions, corresponding to those found in patients, were prepared through overlap PCR. This reaction, described in the materials and methods section, allows, through a series of reactions, to make site-specific mutagenesis targeting the site of interest on the template. Starting from pFL38*SDH1* template and using primers listed in 6.5 paragraph (material and method section), the *sdh1*^{L367P}, *sdh1*^{R444C}, *sdh1*^{R593Q}, *sdh1*^{T602N} alleles were produced. The mutant alleles, besides harboring the mutation of interest, contain at the 5' and 3' ends the sites recognized by the *Sac*I and *Sal*I restriction enzymes inserted during the amplification phases. This allows, after digestion, cloning the mutant alleles into the centromeric plasmid pFL38. Once the mutant and wild type alleles have been prepared, they can be used to transform the W303-1B *sdh1Δ* yeast strain. The wild type and the mutant strains thus constructed were used to evaluate the effects

of mutations on some mitochondrial phenotypes such as oxidative growth, respiratory activity and SDH enzymatic activity.

2.2 Analysis of oxidative growth in *SDH1* mutant strains

Succinate dehydrogenase plays a pivotal role within the mitochondrion, as it is part of both oxidative phosphorylation and the Krebs cycle, the main processes involved in energy production in this organelle. Yeast is an excellent tool to highlight defects in energy production with simple experiments, such as the analysis of oxidative growth on non-fermentable carbon sources. The ability of mutants and wild type strains to grow in the presence of several non-fermentable carbon sources such as ethanol, glycerol, acetate, lactate that allows exclusively oxidative growth in the presence of mitochondrial functionality, has been tested. Through spot assay analysis, serial dilutions of the different strains were spotted on SC-URA supplemented with these non-fermentable carbon sources or glucose 2%. The plates were incubated at 28°C, the physiological temperature of growth, and 37°C to highlight temperature-dependent defects. The results obtained were very similar in all the conditions tested; here, only spot assays on medium supplemented with ethanol is reported (figure 2.4)

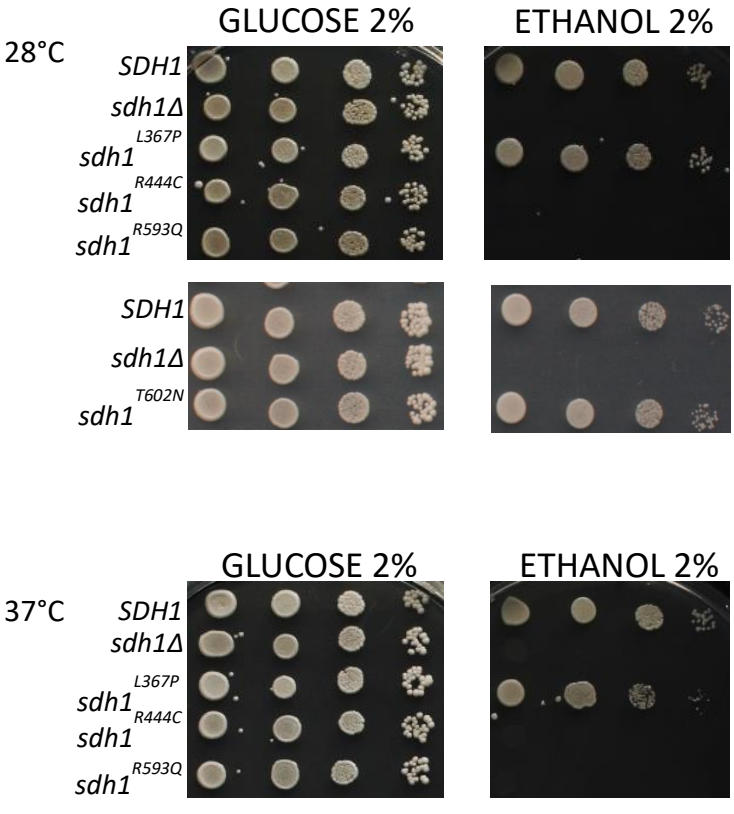

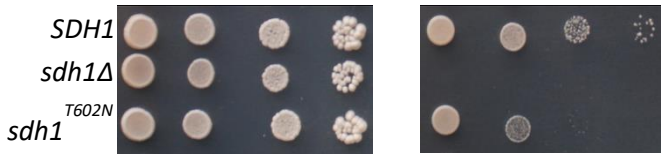

Figure2.4: Oxidative growth analysis of W303-1B *sdh1Δ* strains containing the wild type *SDH1* gene, empty vector and mutated alleles at 28 and 37 °C.

The analysis of oxidative growth on medium supplemented with ethanol allows dividing the mutations into two groups: severe and mild mutations. Severe mutations R444C and R593Q exhibited total ablation of oxidative growth both at 28 and 37 °C, showing the same phenotype of the strain transformed with the empty plasmid. These results demonstrated that the presence of the substitutions leads to severe dysfunction of mitochondrial activity, probably due to the impairment of succinate dehydrogenase complex and the consequent block of the Krebs cycle leading to the inability to metabolize ethanol. The strains harboring L367P and T602N mild mutations at 28°C on ethanol plates show a growth trend comparable to that of the wild type strain. However, in a stress condition due to the temperature increase (37°C), these strains exhibit slight reduction in oxidative growth compared to the wild type strain, indicating thermosensitive abnormalities in mitochondrial activity. However, to confirm these hypotheses further analyses are necessary.

2.3 Evaluation of the respiratory rate in *SDH1* mutant strains

SDH complex takes part both in the Krebs cycle and in the electron transport chain so that pathological mutations could have an effect not only on the enzymatic activity but also on the ability of complex II to exchange electrons with the other components of the respiration chain. To gain a broader view of the OXPHOS metabolism defects and to validate this hypothesis, the ability of the yeast mutants to reduce molecular oxygen to H_2O was evaluated. The analysis of respiratory activity was performed in the strains W303-1B *sdh1Δ* transformed with *SDH1* wild type or mutant alleles and empty vector, grown at 28 and 37 °C in SC-URA supplemented with 0,5% glucose. The oxygen consumption rate was measured after total exhaustion of glucose available in the medium to

promote respiratory metabolism, and within one hour to avoid metabolic shift induced by ethanol. Figure 2.5 showed the results obtained.

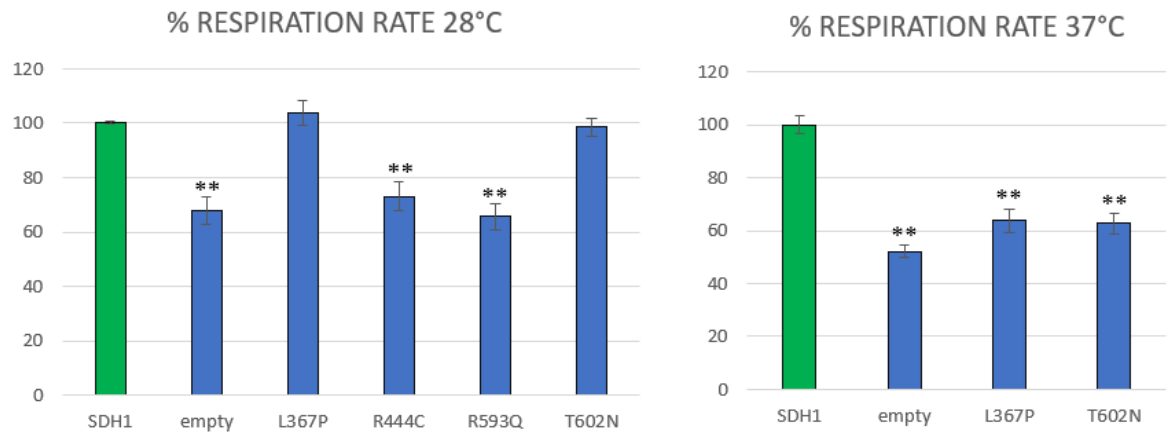

Figure 2.5: Oxygen consumption of W303-1B *sdh1Δ* harboring the plasmid pFL38 *SDH1*, pFL38*sdh1*^{L367P}, pFL38*sdh1*^{R444C} pFL38*sdh1*^{R593Q} pFL38*sdh1*T^{602N} at 28 and 37°C. The green bar indicates the wild type strain (positive control). Values are represented as the mean of at least three values ± SD. P values are obtained using one-way analysis of variance followed by Bonferroni's test, **P<0.01

The first significant data that can be observed from this analysis is that the absence of the catalytic subunit of complex II, does not lead to a total reduction in oxygen consumption. In fact, in the null strain, the absence of the catalytic subunit of complex II leads to a reduction in respiratory rate of about 40% at 28°C and 50 % at 37°C, compared to the wild type strain. This particular result cannot be attributed to the presence of the paralogue gene *SDH1B*, which, as described in the introduction section, seems to poorly contribute to the SDH functionality. A more realistic explanation lies in the nature of the respiratory chain. In fact, complex II can be bypassed and the electrons coming from the reduction of NADH, accomplished by the internal Ndi1 enzyme, can flow directly to complex III and will continue the chain until the reduction of molecular oxygen. Analyzing the behavior of mutant strains, it is possible to observe good parallelism between oxidative growth and respiration. The strains bearing the severe mutations R444C and R593Q have a similar reduction in respiratory rate compared to the null mutant, while the mild mutations L367P and T602N confirm the thermosensitive phenotype, showing defects in oxygen consumption only at 37°C. These thermosensitive mutations have a greater impact on respiration than on oxidative growth, as the respiratory rate is comparable to that of the null mutant, while oxidative growth presents an intermediate phenotype between the wild type and the deleted strains. The growth observed on

non-fermentable carbon sources is the result of multiple factors converging together, including respiration, Krebs cycle and the ability of the mutated enzyme to catalyze the reduction of succinate to fumarate. The partial retention of oxidative growth may be due to residual enzymatic activity of the mutated proteins which could not block the progress of the Krebs cycle, allowing the use of ethanol to grow. To better dissect this hypothesis, the enzymatic activity of the mutated SDH complexes is measured and discussed in the next paragraph. The data coming from oxidative growth and respiratory rate analysis highlights defects in mitochondrial activity, establishing a positive correlation between the mutation identified in the screening and the clinical phenotype in patients.

2.4 How does it work? Molecular investigations in *SDH1* mutant strains

Once it is clarified that these mutations are the effective cause of disease in patients, it is possible to investigate the molecular mechanisms through which they act. The phenotypes analyzed so far show that all the variants are associated with respiratory phenotypes compatible with an altered SDH complex II functionality, with several degrees of severity. Using a mitochondrial protein extract, it was possible to quantify these defects, through an enzymatic assay of the SDH complex. This analysis was performed on yeast strains grown in SC-URA medium in a limiting 0.5% glucose condition at both 28 and 37°C. To determine the ability of the mutated SDH complexes to catalyze the reaction, an in vitro reaction was prepared, containing the following molecules:

- Succinate, the enzyme-specific substrate
- KCN, an inhibitor of the complex IV
- DCPIP (2,6-Dichlorophenolindophenol)
- Decylubiquinone

In particular, the electrons generated by the reduction of succinate are conveyed to the final acceptor of the reaction, the DCPIP. KCN, a specific inhibitor of complex IV, blocks the electron flow through the mitochondrial transport chain, directing all the electrons produced to the DCPIP. Decylubiquinone, the initiator of the reaction, is involved in the transmission of electrons from succinate to DCPIP. The results obtained are shown in figure 2.6. Since malonate is a strong inhibitor

of the succinate dehydrogenase, at the end of each reaction was added, to ensure the specificity of the reaction and as expected the reaction stopped (data non shown).

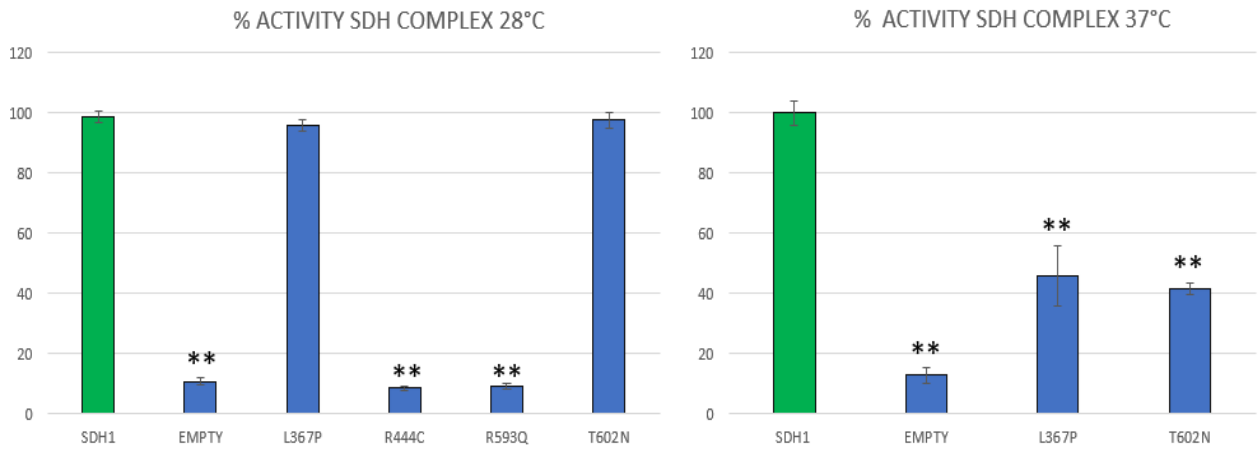

Figure 2.6: Enzymatic activity at 28 and 37 °C of the W03-1B *sdh1Δ* strain transformed with wild type and mutant alleles, and empty plasmid as a negative control. Values are represented as the mean of at least three values ± SD. P values are obtained using one-way analysis of variance followed by Bonferroni's test, **P<0.01;

The analysis of the enzymatic activity of the SDH complex provided data that agree with those obtained from the analysis of the OXPHOS metabolism. In fact, the severe mutations R444C and R593Q lead to a reduction of the enzymatic activity of succinate dehydrogenase similar to that observed in the null strain. The absence of catalytic activity may explain the deficit both in oxidative growth and respiratory activity, seen in the previous paragraphs. In fact, the inability to convert succinate into fumarate constitutes a limiting stage for the Krebs cycle, probably leading to a strong reduction of the produced intermediates. The block of the Krebs cycle could be associated with the inability to use ethanol as a carbon source. The consequent decreased quantity of molecules with high reducing power, such as NADH and $FADH_2$, could explain the reduced respiratory rate observed. The mild mutations L367P and T602N exhibit a trend similar to the wild type strain at 28 °C and a decrease in enzymatic activity only in a heat-stress condition. In fact, at 37°C these mutations lead to a reduction of SDH complex enzymatic activity, confirming once again the thermosensitivity of these mutations. The proteins harboring the mild mutations, although presenting an evident defect,

maintained an enzymatic activity of about 40/45%, which could explain the intermediate growth phenotype seen in the previous paragraph. To evaluate whether the decreased enzymatic activity could be related to a decreased Sdh1 steady state levels, western blot analysis was performed. For this purpose, the cells were grown under the same conditions in which the enzymatic defect was detected. After 18 hours of growth at both 28 and 37°C, the cells were harvested, and the TCA protein extraction protocol was performed. The western blot was carried out on these extracts and the Sdh1 protein was detected using ANTI-SDHA antibody, able to recognize both human SDHA and yeast Sdh1 proteins. Por1, the mitochondrial porin, was used as housekeeping, and the signal was measured with an antibody against yeast Por1. The normalized values of the Sdh1 protein content in the different strains analyzed are shown in figure 2.7.

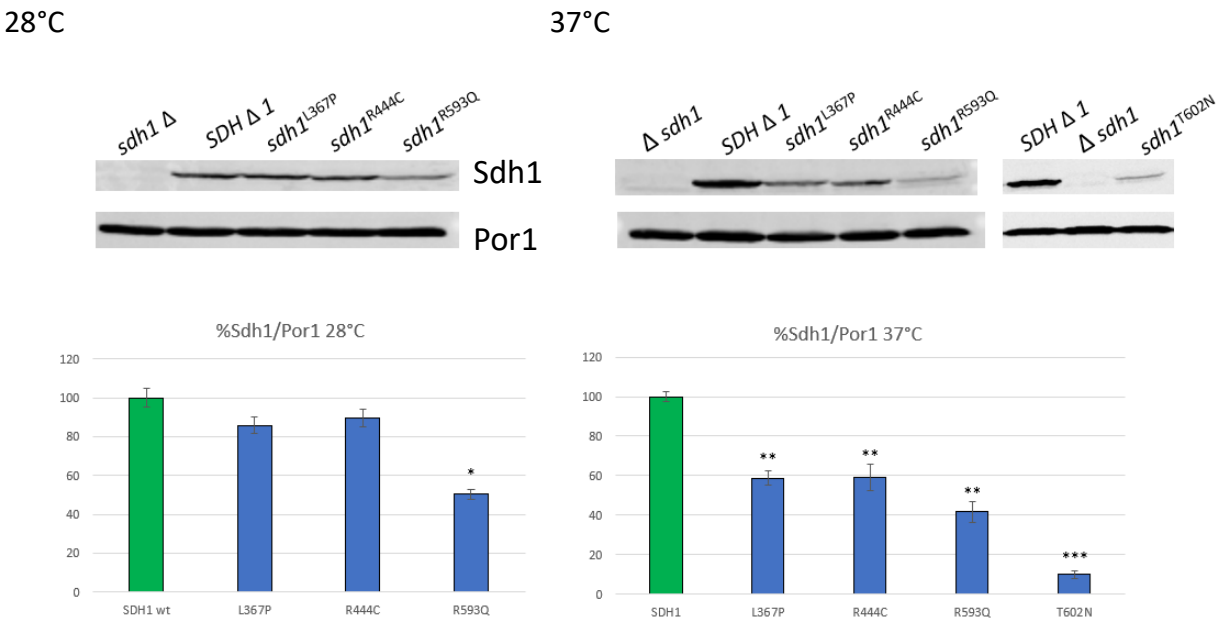

Figure 2.7: Western blot performed at 28 and 37 °C on *SDH1* wild type, deleted and mutant strains, and related quantification graphs using Por1 as housekeeping to quantify the Sdh1 content. Values are represented as the mean of at least three values ± SD. P values are obtained using one-way analysis of variance followed by Bonferroni's test, *P<0.05; **P<0.01; ***p<0.001

At 28°C the R593Q mutation in Sdh1 protein leads to a moderate decrease in its levels (about 50%), compared to the control. All the other mutant variants analyzed, including R444C, show Sdh1 level similar to the strain transformed with the wild type allele. Since from the previous analysis, the severe mutations (R444C and R593Q) exhibit a phenotype comparable to that of the null mutant, it is possible to conclude that the instability of the protein carrying the R593Q mutation together with other factors, such as the catalytic deficiency, lead to the expression of the pathological phenotype. Regarding the R444C mutation, it is possible to hypothesize that the disease in patient is due to a pathogenetic mechanism not correlated with the reduction of the Sdh1 levels. At 37°C, the L367P and T602N mutations confirm their thermosensitive phenotype, showing a decreased Sdh1 protein levels. Based on these data, it is therefore possible to associate the decreased levels of Sdh1 carrying the L367P and T602N mutations with the defects in the enzymatic activity and OXPHOS phenotypes analyzed before. However, as previously mentioned in the docking analysis paragraph, the severe mutation R444C acts following another pathogenic mechanism close correlated with its function in the catalysis. The pivotal role of the arginine residue 451 in the human catalytic site, and consequently of the arginine residue 444 in yeast, can explain the severe phenotype associated with the R444C substitution. In fact, in the presence of this mutation, the enzymatic activity of the succinate dehydrogenase complex is almost null, probably due to the inability of the mutated catalytic site to stabilize the substrate. Although for the R444C mutation the mechanism of action is quite clear, for the other substitutions other details are necessary. Since the Sdh1 subunit is part of a tetramer, and in particular interacts specifically with Sdh2, forming the hydrophilic dimer with a catalytic function, the presence of mutations in Sdh1 could lead to a defect in the assembly of Sdh1-Sdh2 dimer and therefore a reduction in the stability of the other subunit (Sdh2 for example). The assembly of the dimer is not autonomous but is helped by assembly factors that facilitate the process. The Sdh2 subunit contains 3 Fe-S clusters which act as a link for the electrons transport from the catalytic subunit Sdh1 to coenzyme Q, the final acceptor. To maintain the electron transport continuous, the assembly of these subunits must be a rigorous process, ensuring contiguity between the portion containing the FAD in the Sdh1 subunit and the region of Sdh2 containing the Fe-S centers. Based on these considerations, the stability of the Sdh2 protein in the yeast *SDH1* mutant strains was evaluated through Western blot. Using the same protein extracts prepared for the evaluation of Sdh1 stability, a second western blot analysis was performed. The detection of the Sdh2 subunit was carried out using a primary anti-SDHB antibody, able to recognize also the yeast orthologous protein Sdh2. The results obtained are reported in Figure 2.8.

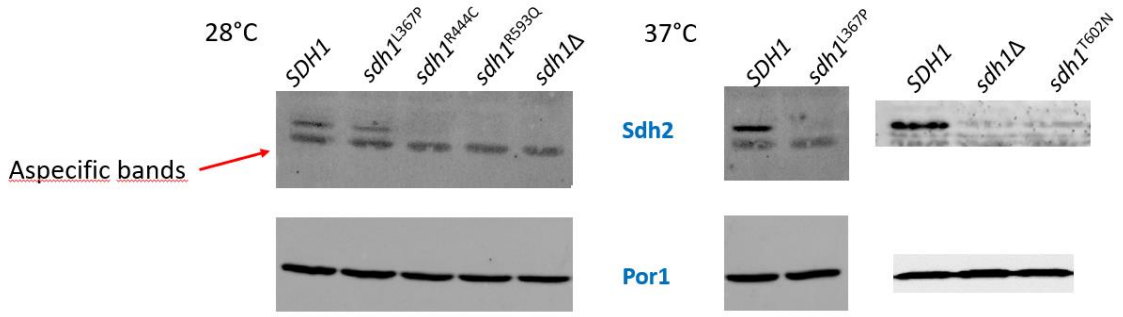

Figure2.8: Evaluation of Sdh2 levels, through western blot, performed at 28 and 37°C on strains W303-1B containing empty plasmid and *SDH1* wild type and mutated alleles. Por1 was used as housekeeping. The red arrow indicates an aspecific band.

The results show that the Sdh2 protein, at 28°C, is present only in wild type and the mutant strain containing the L367P substitution, a condition in which no defects, related to mitochondrial activity, are observed. In all the other mutants, no bands related to Sdh2 subunits are detected. Since the L367P and T602N mutations in the previous analysis have shown a thermosensitive phenotype, the experiment was repeated at 37°C. In this stress condition, almost no detectable levels of Sdh2 are present in the line corresponding to the thermosensitive mutants. These results highlight the intrinsic instability of Sdh2. In fact, Sdh2 is completely absent in null mutants (R444C and R593Q) but is still present in mild mutant L347P at 28°C, while a 37°C both L367P and T602N lost this subunit. These results could establish a correlation between the functionality of the catalytic subunit SDH1 and Sdh2 stability. To stably maintain Sdh2 in cells, it must be associated in a functional catalytic tetramer/dimer and when this condition is not satisfied, for example in the case of the mutants analyzed in this thesis, the levels of the Sdh2 protein drastically drop. Further confirmations come from previous studies reported in literature on patients who also showed instability of the SDHB subunit in the presence of mutations in the SDHA (Bannon et al. 2017).

2.5 INHERITANCE ASSOCIATED WITH MUTATIONS IN *SDH1*

All the mutations here analyzed induce mitochondrial defects and thus led to the pathological phenotype in patients. Once this has been demonstrated, it is possible to investigate the type of inheritance associated with these mutations. All variants identified in *SDHA* gene are heterozygous in patients, each mutated allele was in compound with the corresponding wild type allele. The yeast

S. cerevisiae can be a useful tool to obtain information regarding the genetic mechanism associated with inheritance; for example, in the case of dominant mutations, it may be useful to highlight negative dominance or haploinsufficiency. For this purpose, diploid strains were constructed. The first step was the selection of a strain with the same genetic background of W303-1B with an opposite mating type, allowing the formation of a diploid yeast (2n). The isogenic strain W303-14A was chosen. These strains share all five genetic markers (*ade2, leu2, trp1, ura3, his3*) leading to auxotrophies for adenine, leucine, tryptophan, uracil and histidine. To create a functional yeast model to study the inheritance, both strains must contain the deletion of the genomic *SDH1* gene: i) W303-1B *sdh1Δ* strain constructed to study haploid mutations (paragraph 2.1) was used; ii) W303-14A strain was transformed with the deletion cassette (*sdh1::kanMX4;* paragraph 2.1) to obtain the W303-14A *sdh1Δ* yeast strain. The *SDH1* gene cloned in the pFL38 plasmid (paragraph 2.1) was subcloned into another monocopy plasmid with a different selection marker (pFL39 containing the *TRP1* marker). W303-14A *sdh1Δ* strain was transformed with the plasmids pFL39*SDH1* and empty pFL39. Diploid heteroallelic strains were constructed by crossing the haploid W303-1B *Matα sdh1Δ* strain transformed respectively with the plasmids pFL38*SDH1*, empty pFL38, pFL38*sdh1*^{L367P}, pFL38*sdh1*^{R444C}, pFL38*sdh1*^{R593Q} and pFL38*sdh1*^{T602N} with the isogenic W303-14A *Mata sdh1Δ* strain transformed with the empty pFL39 or pFL39*SDH1* plasmids. The crossing has been carried out using the "drop on drop" technique in YPD medium, and a subsequent incubation for three days. Diploids were selected through replication on SD medium, supplemented with adenine, histidine and leucine, exploiting the complementation of the *URA3* and *TRP1* genes present on the plasmids contained in the starting strains. At the end of this selection, the following diploid strains were obtained (W303-1B *sdh1Δ* xW303-14A *sdh1Δ*):

pFL38*SDH1*/ pFL39*SDH1*

pFL38/pFL39*SDH1*

pFL38/pFL39

pFL38*sdh1*^{L367P}/pFL39 *SDH1*

pFL38*sdh1*^{R444C}/pFL39*SDH1*

pFL38*sdh1*^{R593Q}/pFL39*SDH1*

pFL38*sdh1*^{T602N}/pFL39*SDH1*

To investigate the effects of the mutated alleles in the presence of the *SDH1* wild type copy, the oxidative growth of diploid strains on non-fermentable carbon sources was evaluated. This analysis was performed through spot assay, following the same experimental procedure adopted for haploid cells. Serial dilutions of cells were plated on SC-U-W medium, selective for the maintenance of pFL38 and pFL39 plasmids, alternatively supplemented with glucose or non-fermentable carbon sources (ethanol, glycerol, Na-acetate, lactate). The plates are incubated for several days at 28 and 37 °C and the phenotypes obtained are shown in figure 2.9. The results obtained are comparable in all the sources tested: the NA-acetate plates are reported here because in this condition the diploid strains show a more evident defect.

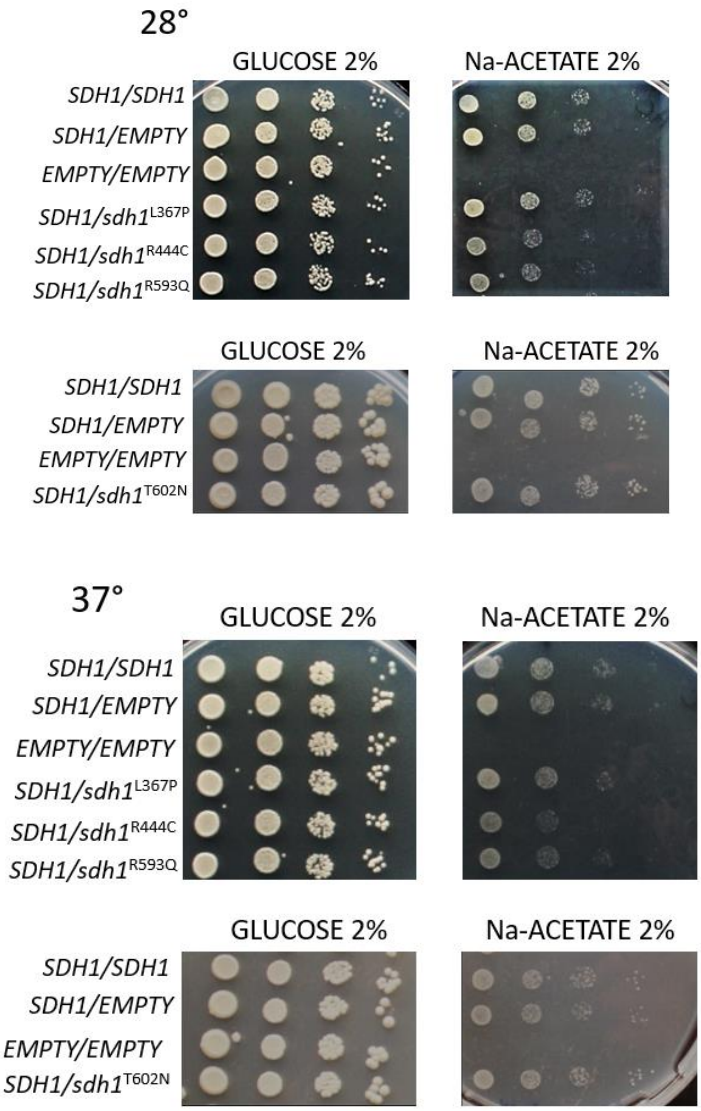

Figure 2.9: oxidative growth of diploid strains containing wild type and mutated *SDH1* alleles at 28 and 37°C on Na-acetate and glucose as control

The analysis of oxidative growth allows drawing several conclusions. The mutations R444C and R593Q are also in this case associated with a more severe growth defect. Comparing the growth of the diploid strain harboring these mutations with the homoallelic (*SDH1*/*SDH1*) and hemiallelic (*SDH1* / empty) control strains, an oxidative growth slight reduction is observed. Both mutations lead to growth reduction compared to the hemiallelic strain, containing only one copy of the *SDH1* gene, indicating that the presence of the mutated alleles carrying the R444C and R593Q mutations has a detrimental effect on the wild type *SDH1* allele. These results highlight a negative dominant effect associated with these mutations. On the other hand, the mild mutations L367P and T602N exhibit a similar growth behavior to the homoallelic strain, containing two copies of *SDH1,* both at 28 and 37 °C. In this case, the presence of the wild type *SDH1* allele complements the effect of the mutations on oxidative growth, suggesting that these mutations in yeast are recessive. However, this type of analysis allows doing a qualitative investigation, useful for highlighting significant differences, but could be less sensitive in detecting the effect of mutations with a mild phenotype. More sensitive and detailed analyses, which allow a quantification of the defect associated with the mutations, are necessary. One of the possible alternatives is certainly to measure the SDH enzymatic activity in diploid strains, which allows quantifying the enzymatic SDH complex defect. The protocol followed is the same used for the haploid strains: the cells are grown for 18 hours at both 28 and 37°C on SC-U-W medium, to allow the maintenance of the pFL38 and pFL39 plasmids. The results obtained are shown in figure 2.10.

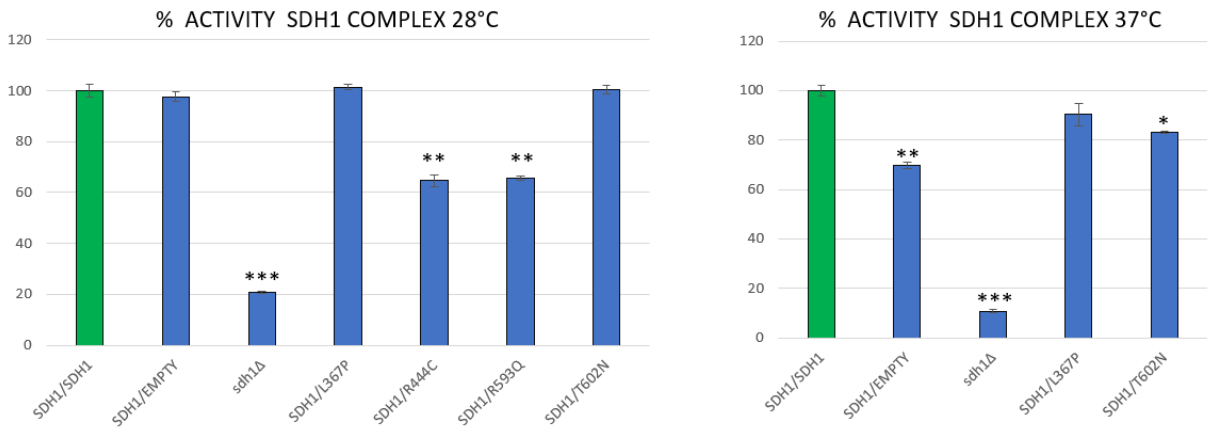

Figure 2.10: Enzymatic activity at 28 and 37 °C of the diploid strains containing wild type and mutant alleles, and empty plasmid as a negative control. Values are represented as the mean of at least three values ± SD. P values are obtained using one-way analysis of variance followed by Bonferroni's test, *P<0.05; **P<0.01; ***p<0.001

The results obtained confirm the negative dominance of the R444C and R597Q mutations at 28 °C, since the enzymatic activity of the diploid strains containing these variants shows a significant reduction compared to both the homoallelic and hemiallelic strains, containing respectively two and one copy of the *SDH1* wild type allele. It is therefore confirmed that the presence of these mutated alleles leads to a negative effect on the *SDH1* wild type allele, suggesting that the pathogenetic mechanism in patients bearing these mutations is associated with a negative dominant effect. The thermosensitive mutations L367P and T602N at 28 °C, as expected, do not show any difference in enzymatic activity compared to the homoallelic diploid strain. At 37°C, indicating a greater sensitivity of this analysis, it is observed that there is a significant difference in enzymatic activity between the homoallelic and the hemiallelic strains, in which only one copy of the *SDH1* gene is present. Consequently, it is possible to affirm that in stressing condition in yeast, a single copy of the *SDH1* gene is not able to support the maximum succinate dehydrogenase activity, indicating a haploinsufficiency condition. By the analysis of the behavior of the mild L367P mutation, no significant difference is observed compared to the control homoallelic strain, assuming a recessive inheritance in yeast, in contrast with the data obtained from the patient. On the other hand, the diploid strain containing the T602N mutation exhibits an intermediate behavior, with a value of enzymatic activity significantly different from that of both homoallelic and hemiallelic strains, which could explain the dominance related to this mutation with a mechanism linked to haploinsufficiency.

To have a further confirmation of the negative dominance associated with the R444C and R593Q mutations, a second spot assay experiment was set up to evaluate the oxidative growth in a strain overexpressing the mutant alleles, which allows to better visualize the effect of negative dominant variants. First, the *SDH1* wild type gene and all the mutants under analysis were subcloned into a YEpLac195 multicopy vector; subsequently, these plasmids were introduced in a W303-1B yeast strain containing the genomic copy of *SDH1*. The heteroallelic strain thus constructed carried the wild type *SDH1* allele at the genomic locus and plasmids that overexpress wild type or mutated alleles. If a mutant variant, expressed at the physiological level, has a dominant negative effect, it would be expected that the overexpression of the same mutant variant will lead to the exacerbation of this defect. Based on this concept, the ability of this strain to use non-fermentable carbon sources was evaluated at 28 and 37°C, the results are shown in figure 2.11.

28°C

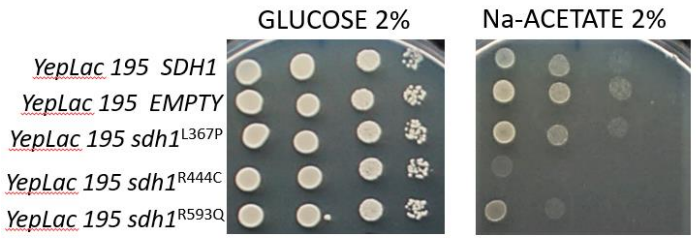

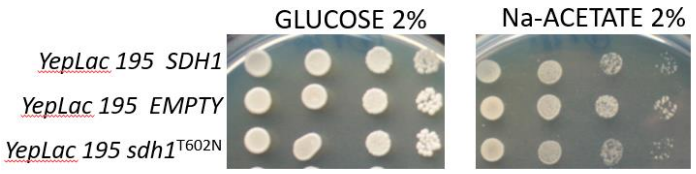

37°C

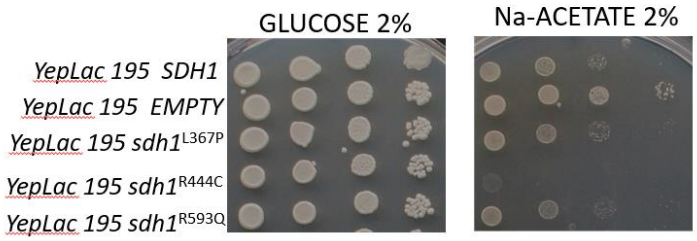

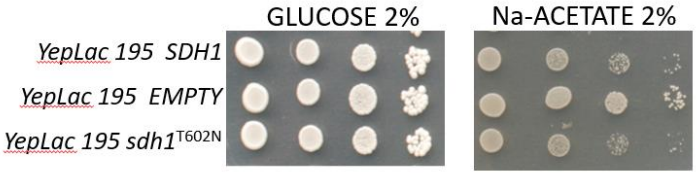

Figure 2.11: Oxidative growth of heteroallelic strains containing wild type and mutated *SDH1* alleles in a multicopy vector at 28 and 37°C on Na-acetate and glucose as control

Analyzing the phenotype of the strains transformed with the empty plasmid or the wild type *SDH1* allele, a difference in growth is present. The explanation of this phenomenon lies in the gene overexpression consequences that, even in the wild type form, is often an unfavorable event compared to the physiological condition (strain transformed with empty plasmid). The overexpression of the pathological R444C variant in a heteroallelic context leads to almost total repression of oxidative growth, confirming the severe negative effect of the mutated Sdh1 isoform on the wild type protein. Overexpression of the R593Q variant also shows a reduction in oxidative growth, which is less severe compared to that associated with the R444C variant, suggesting also in this case a negative effect of the mutated protein on the wild type counterpart. Both the recessive L367P and haploinsufficient T602N variants show oxidative growth at 28 and 37°C comparable to that of the strain overexpressing the wild type *SDH1* allele. The data obtained in this experiment further confirmed the negative dominance of the R444C and R593Q mutations and demonstrated that the L367P and T602N mutations, at least in yeast, exhibit another hereditary pathway, as shown in the previous experiments.

2.6 DISCUSSION

This first part of the thesis concerns the study of mutations in the *SDHA* gene, coding for the catalytic subunit of succinate dehydrogenase complex, identified in patients with a typical clinical characterization of hereditary optical neuropathies (HON). The yeast *S. cerevisiae* is an excellent model organism to study diseases associated with mitochondrial dysfunctions, as it is one of the very few eukaryotes viable in the absence of mitochondrial functionality. Several studies have described mutations in the *SDHA* gene, validated in yeast exploiting the homologous complementation approach, due to the inability of the human gene to complement the absence of *SDH1*. The sequence alignment of the human SDHA and yeast Sdh1 proteins shows a high degree of similarity, which also involves the potentially pathological residues identified in the patients. This similarity allows, using the homologous complementation approach, inserting the pathological

substitutions in the corresponding yeast residues to study their effect on a series of mitochondrial phenotypes (Figura 2.12).

MUTATION	OXIDATVIVE GROWTH DEFECT	T (°C)	ENZYMATIC ACTIVITY	RESPIRATION RATE	PROTEIN STABILITY	INHERITANCE
sdh1^{L367P}	LOW	37	MODERATE	MODERATE	MODERATE	RECESSIVE
sdh1^{R444C}	HIGH	28	HIGH	MODERATE	LOW	DOMINANT
sdh1^{R593Q}	HIGH	28	HIGH	MODERATE	MODERATE	DOMINANT
sdh1^{T602N}	MODERATE	37	MODERATE	MODERATE	HIGH	DOMINANT

Figure2.12: Summary of the phenotypes analyzed in yeast of in SDH1 mutations

The models constructed are used to test the oxidative growth on non-fermentable carbon sources, which allows highlighting defects related to OXHOS metabolism. Two of the mutations identified, R444C and R593Q, induced a total loss of oxidative growth, assuming a severe defect of mitochondrial metabolism. On the other hand, the L367P and T602N mutations allow a growth similar to that of the wild type strain at the physiological temperature, presenting a moderate defect in oxidative metabolism only at 37 °C. To better understand the different behavior of the mutations, molecular, biochemical and computational analyzes are performed. In particular, the severe defects in the mutants containing the R444C and R593Q mutations are associated with a strong reduction of the SDH catalytic activity, which leads to the stall of the metabolic pathway of the Krebs cycle. The arginine residue R444, highly conserved between species, is part of the catalytic site of succinate dehydrogenase and is involved in the stabilization of succinate. If this stabilizing effect is lost in the presence of the R444C substitution, the catalytic reaction could be blocked. The R593 amino acid, on the other hand, does not show a strictly catalytic role, since it localizes on the external surface of the protein. However, the yeast mutant carrying the R593Q mutation shows a strong reduction in the activity of complex II. This behavior can be explained, in part, by the poor stability of the protein in the presence of the mutation, but other mechanisms could be involved. In fact, arginine

R593, being a surface residue, could play an important role in the interaction with the other subunits of the complex or with the various assembly factors involved in the subunits association. Yeast is also a very useful tool to define the type of inheritance involved in the pathogenetic mechanism of the diseases. Assuming that all mutations in patients are heterozygous and therefore dominant, yeast has been used in this study to identify the dominance mechanism. The severe mutations (R444C and R593Q) exert their dominance through a negative dominant mechanism, indicating that the mutated allele influences the activity of the wild type allele. For the mild T602N mutation, dominance in yeast is associated with haploinsufficiency. On the other hand, for the L367P mutation, there is no concordance between yeast and humans, since the heterozygous mutation in patients is recessive in yeast. Based on these considerations, it is possible to think that patient data may be incomplete, and that the dominant pathological phenotype in patients could be due to the combination of L367P mutation in *SDH1* with another mutation in a different gene: alternatively, this mutation cannot contribute to the pathological phenotype at all. However, it is important to underline that yeast can confirm the pathological role of a mutation, but if no defects are observed, it could still remain the cause of the pathology in patients. Besides this, three of the four identified mutations have a positive correlation, and the alleged dominance in patients iss also confirmed in yeast, demonstrating that *S.cerevisiae* is an excellent model to highlight mitochondrial dysfunctions.

CHAPTER 3: RESULTS AND DISCUSSION SECTION II

3.1 MECR MUTATIONS MODELING, YEAST STRAINS CONSTRUCTION AND COMPLEMENTATION ASSAY

In the second part of the thesis, the attention will be focused on the recessive mutation identified in homozygosity through NGS in *MECR*, which codes for the Mitochondrial Trans-2-Enoyl-CoA Reductase. In particular, the identified amino acid substitution in the patient is R258W. As mentioned in the introduction part, this mutation has already been reported in a previous study, in heterozygosity with an allele harboring a long deletion and, therefore, probably null (Heimer et al. 2016). This variant has never been validated in a model organism, since the contribution of this substitution to the pathological phenotype was considered marginal, and completely due to the truncated protein. In our patient cohort, however, the R258W substitution was identified in homozygous condition, assuming a possible involvement in the patient's HON phenotype. For these reasons, careful validation in a model organism is required. The presence in the database of the human MECR structure (PDB ID: 1ZSY) allows performing docking analysis on the mutation Figure3.1.

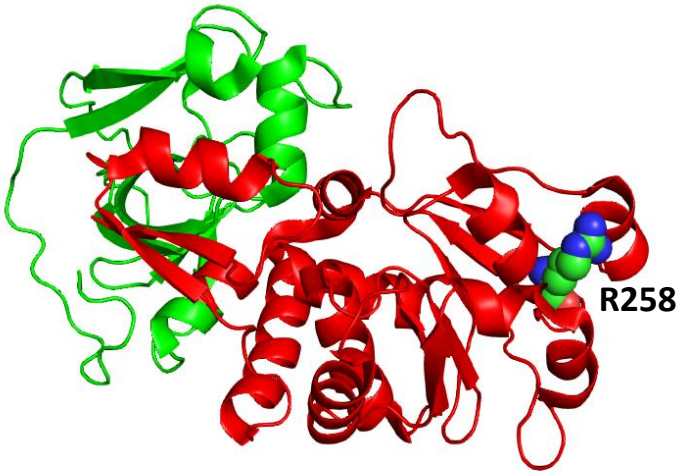

Figure3.1: Cartoon representation of human MECR protein. The N-terminal domain is represented in green and C-terminal domain is colored in red.

Human MECR is divided into two domains, an N-terminal (Arg42–Val166) with catalytic activity and a C-terminal (Asn167–Trp311) which contains a NADH cofactor binding site and the fatty acyl-acyl carrier protein (ACP) recognition regions (Z.-J. Chen et al. 2008). In the fatty acyl–ACP substrate, the fatty acyl molecule is covalently bound to the pantetheine moiety of ACP. MECR acts as a homodimer in the catalysis of the last step of the mitochondrial fatty acid biosynthesis pathway. The homodimer organization forms a groove of about 15 Å in which the pantetheine, a molecular group of the fatty acyl-ACP complex, is accommodated. The arginine 258 residue is one of the structural components of this groove, and, therefore, mutations in this residue can lead to the loss of interaction between pantetheine and MECR, blocking the mitochondrial fatty acids biosynthesis. (Z.-J. Chen et al. 2008). Although this hypothesis is plausible, validation in an in-vivo system, such as a yeast, is necessary. The multiple alignment of mitochondrial Enoyl-[acyl-carrier-protein] reductase sequences from different organisms, shows the high conservation degree of the human R258 residue during the evolution, assuming a function conserved between species (Figure 3.2).

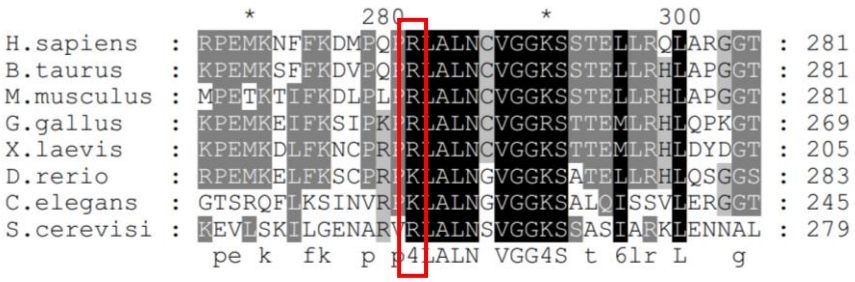

Figure3.2: Multiple alignments of mitochondrial Enoyl-[acyl-carrier-protein] reductase sequences from different organisms. In red are highlighted the residues under analysis. The alignment was performed with cluster X and displayed with GeneDoc tool. The accession numbers related to the selected sequences are: *H. sapiens* NP_057095.4; *S. cerevisiae* QHB06797.1; *G. gallus* XP_040546107.1; *X. laevis* XP_041438071.1; *B. taurus* NP_858055.1; *D. rerio* NP_001017852.1; *C. elegans* CAA19533.1; *M. musculus* NP_079573.2

Comparing MECR protein sequence with Etr1, the respective orthologous proteins in yeast, the conservation of the arginine under study is observed, although the whole sequence identity of the two proteins is low (around 30%), with large non-overlapping areas. As described in the introduction part, it was previously reported that the deletion of *ETR1* is partially complemented by overexpression of human *MECR* (Heimer et al. 2016).

Based on the low identity percentage between MECR and Etr1 proteins and the knowledge coming from literature, it was chosen to build the corresponding *MECR* yeast models, using a heterologous complementation approach, in which the mutation pathological effect, if present, is directly demonstrated by introducing the mutated human allele into a yeast strain deleted in the corresponding orthologous gene. The deletion cassette *etr1::kanMX4* was amplified through a preparative PCR using the primer pairs *ETR1*DFw / *ETR1*DRv and the genomic DNA, extracted from the BY4741 *etr1Δ* strain, as the template (Brachmann et al. 1998). The amplified DNA contains external fragments, corresponding to the regions flanking *ETR1* ORF, where integration must occur and kanamycin resistance gene for the selection. The deletion cassette was used to transform the yeast strain W303-1B, producing the W303-1B *etr1Δ* strain. To evaluate whether the human allele is able to complement the deletion of the yeast ortholog *ETR1*, *MECR* cDNA (GenBank ID: BC001419.2) was cloned into both single-copy and multi-copy expression vectors. The human cDNA, purchased from an external company, was amplified through a preparative PCR reaction using the primer pairs *MECR*CNotFw/*MECR*CNotRv, producing *MECR* cDNA containing *Not*I restriction sites at the 5' and 3' ends. The amplicon was digested with the *NotI* restriction enzymes and cloned in the pFL39*TET*off and *YepLac112TET*off vectors, digested with the same enzymes. In both cases, the cDNA was cloned under the strong and repressible *TET*off promoter, consisting of *CYC1* yeast promoter preceded by seven doxycycline repressible regulatory elements. The use of both single-copy centromeric (pFL39*TET*off) and multicopy episomal (YepLac112*TET*off) plasmids is due to the attempt to optimize the expression of the human gene in yeast, in order to provide a good level of complementation. These recombinant plasmids containing human *MECR* allele were used to transform the respective strain W303-1B *etr1Δ,* producing the humanized yeast strain. To evaluate the complementation, it was necessary to construct the control strain, containing the orthologous yeast gene under its natural promoter. Starting from the genomic DNA extraction of W303-1B strain, the *ETR1* gene was amplified using the respective *ETR1*CBamFw/*ETR1*CPstRv primer pairs, which introduces *Bam*HI and *Pst*I restriction sites at the 5' and 3' ends. Yeast gene *ETR1,* digested with *Bam*HI and *Pst*I, was cloned into the centromeric plasmid pFL38, digested with the same restriction enzymes. The produced vector pFL38*ETR1* was used to transform the W303-1B *etr1Δ* strain. Once the strains have been prepared, it was possible to perform the study of complementation. To assess the ability of the human *MECR* gene to complement the absence of the *ETR1* orthologue gene in yeast, the oxidative growth of the humanized and yeast wild type strains was analyzed. In this case the ability of the human protein to restore the growth phenotype of the null strain must be

evaluated at first. Through the spot assay technique, strains were plated on media supplemented with non-fermentable carbon sources, which allow highlighting defects of oxidative metabolism. The growth phenotype was comparable on all the sources tested and the results obtained in medium supplemented with 2% ethanol are shown in figure 3.3.

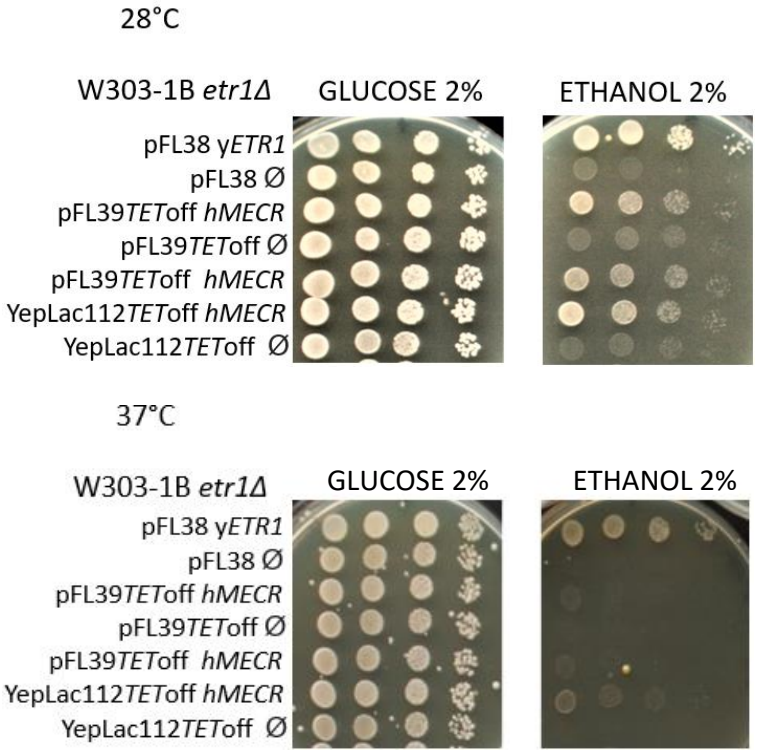

Figure3.3: Oxidative growth analysis to evaluate the complementation of human *MECR* gene.

At 28°C, both constructs, lead to a restoration of oxidative growth in the *ETR1*-deleted strain, with an effect dependent on the amount of gene product available in the cell. In fact, comparing the oxidative growth of the strain containing the multicopy plasmid YepLac112*TET*off*MECR* with that of the strain containing pFL39*TET*off*MECR*, a better degree of complementation is observed in the

presence of a greater quantity of gene product, guaranteed by a multicopy plasmid contest. At 37°C, on the other hand, the complementation is weaker. The strain harboring *MECR* gene within the centromeric plasmid, shows a growth phenotype almost comparable to the null mutant, whereas a partial complementation is observed using *MECR* overexpressing plasmid. These results well parallelize with the results shown by Heimer and collaborators. Based on these considerations, it was decided to study the effect of the R258W mutation, using the YepLac112*TET*off *MECR* multicopy vector. Once the complementation of the human gene is established, the *MECR*-related yeast model carrying the mutation identified in patient was constructed. In fact, exploiting a site-specific mutagenesis PCR technique, called "Quik change® PCR", the mutation was inserted directly into the constructs previously prepared. To introduce the R258W mutation, a mutagenic PCR was performed, using the plasmid YepLac112*TET*off *MECR* as a template and the primers pair *MECR*R258WFw and *MECR*R258WRv. The recombinant mutated plasmid YepLac112*TET*off $MECR^{R258W}$ was selected and used to transform the yeast strain W303-1B *etr1Δ*, producing the mutant strain for the validation of the putative pathological mutation.

3.1.1 VALIDATION OF *MECR* R258W MUTATION IN HUMANIZED YEAST MODEL

The validation process is a well-defined workflow: after the construction of the strain bearing the mutation, putative defects associated with the OXPHOS metabolism must be analyzed. Following the same pattern described for the *SDH1* mutations in the previous chapter, the ability of the mutant strains to use non-fermentable carbon sources was investigated, in order to correlate the presence of the mutation with mitochondrial dysfunctions. Using the spot assay technique, serial cell dilutions were plated on media supplemented with non-fermentable carbon sources. This analysis was performed at 28°C, the temperature at which a better degree of complementation occurs. The results of this analysis were similar in all conditions tested, and the results on medium supplemented with ethanol 2% are reported in figure 3.4.

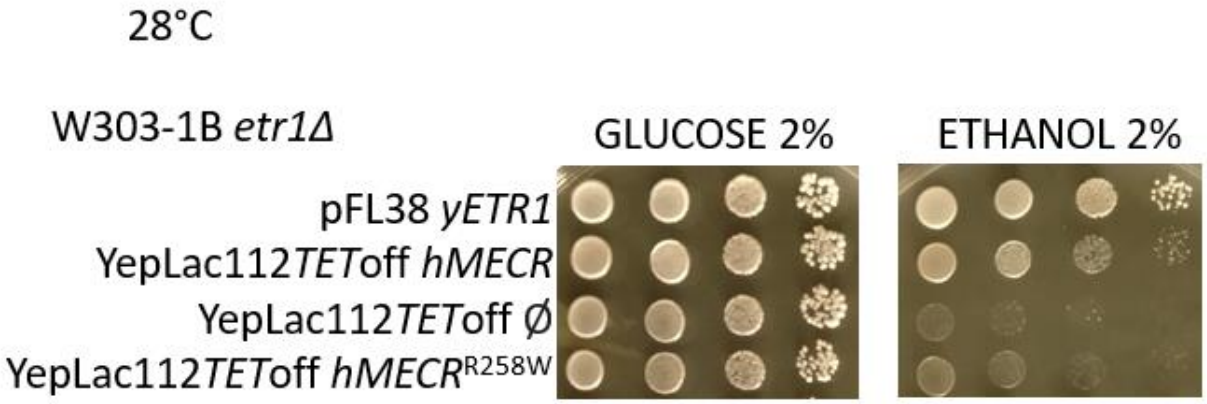

Figure3.4: Oxidative growth analysis of W303-1B *etr1*Δ strain containing *MECR* wild type/mutated alleles and empty vector (negative control) at 28°C.

The strain containing *MECR* R258W mutation, shows a reduction of oxidative growth compared to that of the strain containing the wild type *MECR* allele, similar to that of the strain transformed with the empty plasmid. So, this phenotype could be compatible with the pathology observed in patients. Since *MECR* is involved in the biosynthesis of the mitochondrial fatty acids, it does not have direct involvement in the mitochondrial respiration. However, secondary effects caused by the malfunctioning of the pathways in which it participates could influence oxygen consumption rate. To evaluate this hypothesis, the respiratory capacity of wild type and mutant strains was measured. Since the growth in ethanol of *MECR*-related strains is slow, these strains were inoculated in YP medium supplemented with 0.5% glucose at 28 °C for 18 hours. The results of this analysis are shown in figure3.5.

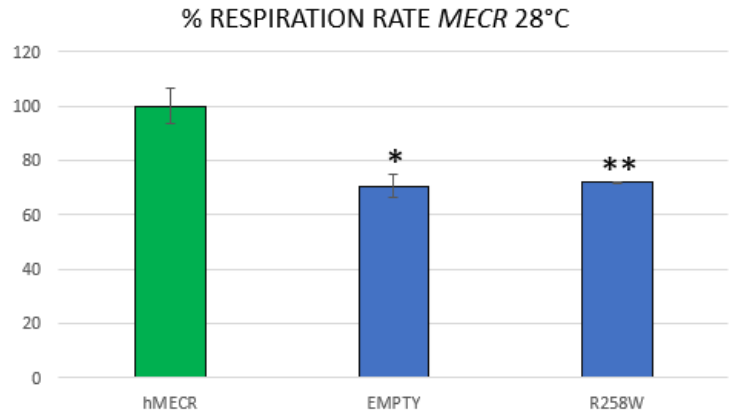

Figure 3.5: Oxygen consumption rate of strain carrying *MECR* wild type, null and mutant alleles at 28 °C. Green bar indicates the wild type strain, which was set to 100%. Values were normalized to the wild type strain value and are represented as the mean of at least three values ± SD. p values are obtained using one-way analysis of variance followed by Bonferroni's test, *P<0.05; **P<0.01;

The deleted strains W303-1B *etr1Δ* shows a respiratory activity of about 70% compared to the wild type. The respiratory activity of the R258W mutant is similar to the deleted strain. These results confirm the association between the R258W mutation and defects related to the mitochondrial activity, indicating that it is *bona fide* the direct cause of the disease in patient. To evaluate whether the deleterious effects of the mutation could be due to a decreased level of the mutated protein, a western blot experiment was set up to detect human MECR protein (Figure 3.5). For this purpose, *MECR* strains were inoculated in YP medium supplemented with 0.5% glucose and incubated overnight at 28 °C. The proteins were extracted through TCA extraction protocol, and subsequently loaded on polyacrylamide gel and incubated with an anti-MECR primary antibody, able to detect human protein. Por1 was used as a loading control.

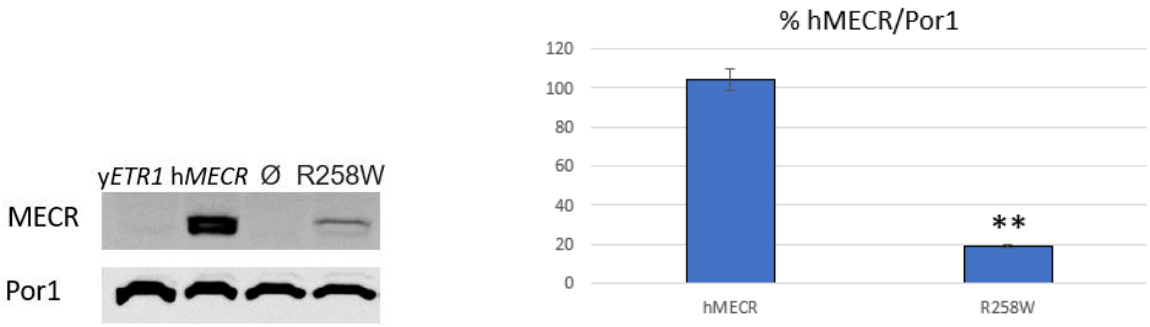

Figure 3.6: Western blot performed at 28°C on strains carrying *ETR1*, wild type *MECR*, the empty plasmid and the MECR mutant allele, and relative quantification graphs using Por1 as housekeeping to normalize the MECR levels. Values were normalized to the wild type *MECR* strain value and are represented as the mean of at least three values ± SD. P values are obtained using one-way analysis of variance followed by Bonferroni's test, *P<0.05; **P<0.01

The representative image of the western blot shows the absence of bands in the *ETR1* and null yeast strains. In fact, the antibodies used, probably for a low degree of sequence conservation, recognized only the human protein and not the yeast one. The R258W mutation leads to a drastic decrease in protein content (about 80%), suggesting that the defects seen in the previous phenotype analyzed, may be due to the low level of MECR in the presence of the R258W substitution. MECR presents a mitochondrial targeting sequence of approximately 40 amino acids, which is removed once the protein is translocated into the mitochondrion. Looking at the image in detail, two contiguous bands were present: based on the sizes, the bands may correspond to the MECR pre-protein and the mature forms. In the lane corresponding to the strain containing the wild type *MECR* allele, similar levels between the precursor and the mature form are observed. On the contrary, in the mutated strain, most of the protein detected seems to be in the unprocessed form, assuming defects in the maturation process linked to the R258W mutation. However, to confirm the hypothesis of stability or turn-over protein defects, pulse-chase experiments, not investigated in this thesis, would be necessary. Besides, it cannot be excluded that the two bands could be the mature protein and a degradation product respectively, due to overproduction or just heterologous expression in yeast. Nevertheless, these results taken together indicate that protein scarcity may be the cause of mitochondrial defects detected in yeast, and therefore the factor that strongly contributes to the patients' HON phenotype.

3.1.2 LIPOYLATION ANALYSIS OF THE ENZYMES INVOLVED IN THE KREBS CYCLE AND POTENTIAL THERAPEUTIC APPROACH

MECR encodes the last enzyme involved in the biosynthesis of mitochondrial fatty acids, which catalyzes the NADPH-dependent reduction of trans-2-enoyl thioesters. As widely discussed in the introduction of this thesis, the main product of this biosynthetic pathway is lipoic acid. This compound plays two main roles in cells, acting both as a scavenger against various oxygen radicals (ROS) and as a cofactor for some enzymes important for the respiratory metabolism, such as pyruvate dehydrogenase (PDH) and α-ketoglutarate dehydrogenase (α-KGD). A study on fibroblasts derived from patient with severe defect in lipoic acid production, due to compound heterozygous mutation in *LIPT1* gene, which catalyzes the transfer of the lipoyl group to the target protein, demonstrates a reduction in PDH activity by 70% and, even if to a lesser extent, a reduction in KGD activity (Ni et al. 2019). Yeast well replicates the human condition: it has been shown that the Lat1, Kgd2 and Gcv3 subunits, whose function is reported in the introduction section, are covalently bonded to the lipoate group, which directly participates in the enzymatic reaction. Some studies reported that the deletion of the *LIP3* gene, involved in the biosynthesis of lipoic acid in yeast, leads to total ablation of the enzymatic activity of both pyruvate and α-ketoglutarate dehydrogenases (Schonauer et al. 2009). These data coming from literature, further underline the importance of the lipoylation of target proteins Lat1, Kgd2 and Gcv3. Starting from these considerations, it was decided to evaluate the lipoylation state of the Lat1 and Kgd2 subunits in the *ETR1* deleted strain transformed with empty plasmids or wild type/mutant *MECR* allele. For this purpose, a western blot analysis was carried out, using an antibody able to recognize lipoic acid covalently linked to proteins. Unfortunately, this type of antibody fails to detect lipoylated Gcv3, and for this reason the focus will be pointed to the two other target proteins. The strains were grown at 28 °C in YP medium supplemented with 2% of ethanol for 18 hours, until the exponential phase, and subsequent TCA protein extraction was performed. The proteins were separated on a polyacrylamide gel and transferred into the membrane, which was subsequently incubated with the primary anti-Lipoic Acid antibody. Por1 was used as the housekeeping loading control. The western blot results are shown in figure 3.7.

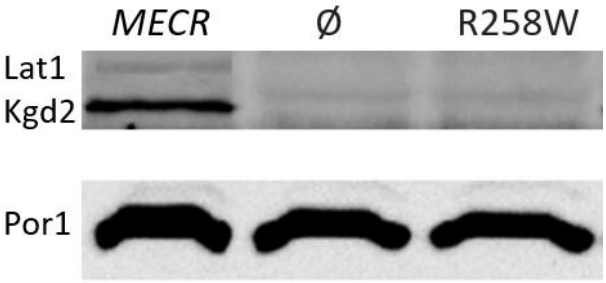

Figure 3.7: Western blot analysis to evaluate the lipoylation state of the Lat1 and Kgd2 subunits in W303-1B *etr1Δ* strain transformed with plasmids containing wild type *MECR*, and*MECR*^{R258W} alleles, and the empty plasmid.

The gel image shows the absence of lipoylated Lat1 and Kgd2 subunits in the null and R258W-mutated strains, probably due to irreversible damage to mtFASII which leads to the inability to produce a sufficient amount of lipoic acid. This type of test allows measuring only the lipoylation levels of Lat1 and Kgd2 in the different strains analyzed, but does not allows obtaining any information on the levels of these subunits. However, the conclusive result is that the levels of the lipoylated subunits are decreased. As previously mentioned, lipoylation of Lat1 (pyruvate dehydrogenase) and Kgd2 (α-ketoglutarate) subunits, permits the catalytic efficiency of these enzymes. The absence of detectable levels of lipoylated subunits observed well parallelized with the oxidative growth and respiration defects observed in the previous analyses. Specifically, the reduced ability of the null and the mutated strains, to use non-fermentable carbon sources could be the result of the weak functionality of the pyruvate dehydrogenase and α-ketoglutarate enzymes, due to the absence of lipoylation. From the information drawn so far, it is clear that the lipoic acid deficit maybe the fulcrum of all defects observed. Since in the mutant containing the R258W mutation, the lipoylated subunits of the pyruvate dehydrogenase and of the α-ketoglutarate dehydrogenase enzymes are absent, it has been evaluated whether supplementation with lipoic acid is able to bypass the defects, increasing the lipoylation levels of Lat1 and Kgd2. To test this hypothesis, wild type, null and mutant strains were grown 18 hours at 28°C in YP medium supplemented with 2% ethanol, with or without lipoic acid at different concentrations (40 μg/ml, 4 μg/ml and 0.4 μg/ml). The concentrations used were selected from data available in literature, identified in studies that have demonstrated the lipoic acid beneficial effect on the mitochondrial DNA polymerase mutants (Mip1) (Baruffini et al. 2006; 2012). Cells were harvested for subsequent TCA protein extraction to

assess the lipoylation levels of Lat1 and Kgd2 through western blot in the same conditions described above, and the results are shown in figure 3.8.

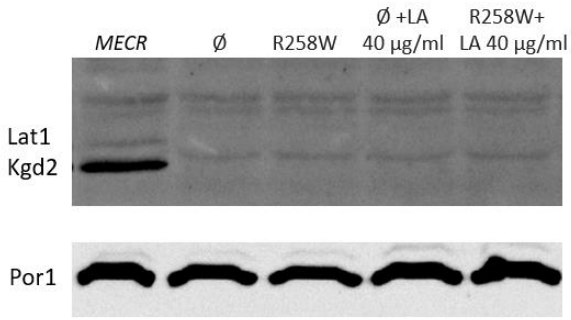

Figure 3.8: Western blot analysis on W303-1B *etr1Δ* strain transformed with plasmids containing *MECR*, empty, *MECR*^{R258} alleles to evaluate the effect of lipoic acid 40 µg/ml treatment on the lipoylation state of Lat1 and Kgd2 subunits.

As is possible to observe, the treatment with lipoic acid does not affect the lipoylation levels of the Kgd2 and Lat1 subunits, which are still absent. Then, the ability of lipoic acid to rescue the reduced growth phenotype observed on media with non-fermentable carbon sources, was analyzed. The deleted, wild type and mutant strains were plated on YP supplemented with 2% ethanol without or withlipoic acid at different concentrations (40 µg/ml, 4 µg/ml and 0.4 µg/ml). Figure 3.9 shows the results related to the administration of Lipoic acid 40 µg /ml (comparable data were obtained with the other two concentrations).

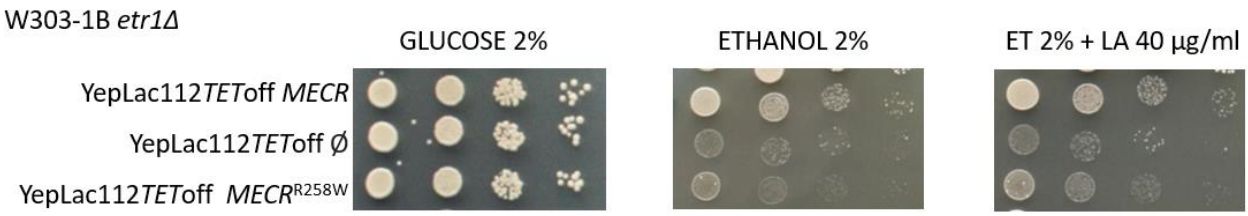

Figure 3.9: Evaluation of the lipoic acid effects, supplemented at 40 µg / ml, on the oxidative growth of the wild type, deleted and mutant *MECR* strain

The results obtained show that 40 µg/ml lipoic acid does not lead to a significant rescue of the pathological phenotype associated to the R258W allele, indicating, again, that the supplementation of lipoic acid cannot bypass the enzyme defect associated with the MECR mutation. A hypothesis to explain this result is dependent on the administered form of lipoic acid, which may not be recognized and bounded by the enzymatic system that catalyzes the binding of the lipoate group on the target subunits. Another important role of lipoic acid within cells is the antioxidant function against reactive oxygen species (ROS). In fact, the characteristic structure of lipoic acid consents the switch to two forms, oxidized and reduced, allowing the exchange of electrons with other compounds to defuse the hazard linked to oxygen radicals. The scarcity of lipoic acid in the yeast mutant containing the R258W mutation, could, therefore, be associated with an increased levels of oxidative stress To validate this hypothesis, a method to highlight the deficit associated with oxidative stress, induced by exposure to different concentrations of H_2O_2, was tuned. At first, the growth assay was set up, in which the wild type, mutant, and deleted strains were plated on YP medium supplemented with 2% glucose, without or with 2 mM H_2O_2 (Figure 3.10A). In the latter condition, it is observed that both deleted end mutant strains show growth defects compared to the wild type strain. This experiment provided a qualitative evaluation of hypersensitivity to ROS-inducing agents in the presence of fatty acids metabolism dysfunctions. To better quantify H_2O_2 sensitivity, after the treatment with 0.5, 1 or 2 mM H_2O_2, an equal number of cells derived from mutant, wild type and deleted strains were plated on YP media supplemented with 2% glucose and incubated at 28 °C. The survival cell rate was determined by counting the number of colonies (Figure 3.10B).

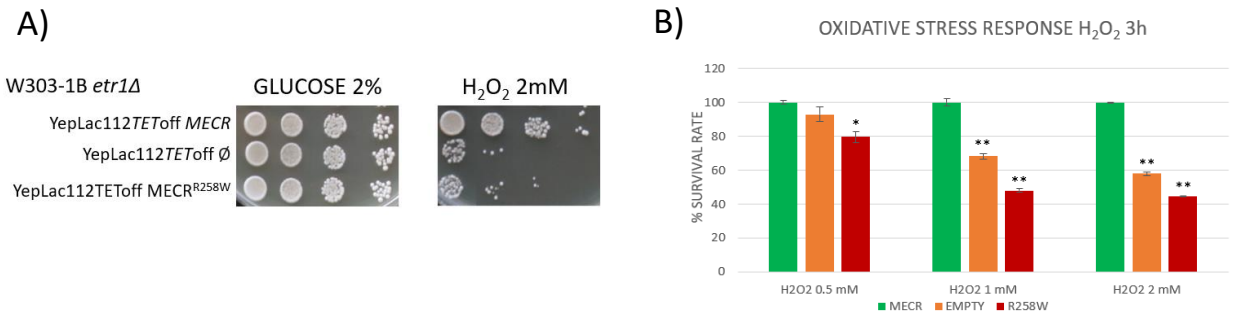

Figure 3.10: Evaluation of hypersensitivity to ROS-inducing agents of wild type, null and mutant *MECR* strains. (A) Cell growth assay performed at 28 °C in the presence of 2mM H_2O_2. (B)Survival rate percentage after the exposure to 0,5 or 1 or 2 mM of H_2O_2 for 3 hours. The values were normalized to the wild type strain, to which an arbitrary survival rate value of 100% was assigned. Values are represented as the mean of at least three values ± SD. P values are obtained using one-way analysis of variance followed by Bonferroni's test, *P<0.05; **P<0.01;

In all conditions tested, a greater sensitivity to H_2O_2 of deleted and mutant strains is observed, showing a significant decrease in the survival rate compared to the wild type. Intriguingly, at all the concentration tested, the lethality was slightly higher in the MECR mutant strain than in the null strain. When H_2O_2 concentration rises, the gap, in terms of survival rate, between the mutant and wild type strains proportionally increased. In fact, at low concentrations of H_2O_2 (0.5 mM), the strain containing the R258W mutation shows an increase in mortality of 20% compared to the wild type, while at the higher concentration tested (H_2O_2 2mM) the increase in mortality was 60%. These data confirmed the high sensitivity of the mutant and the deleted strains to oxidizing agents, showing the inability to respond to increasing concentrations of H_2O_2. This series of experiments allow, by counting the total colonies, quantifying the defect associated with hypersensitivity to H_2O_2, confirming the oxidative demage associated with mitochondrial fatty acid biosynthesis disfuncition. To validate the hypothesis that lipoic acid may be associated with better management of oxidative stress in the mutant strain, a second cell viability experiment, after H_2O_2 treatment, was set up. The wild type and mutant strains were inoculated in YP medium supplemented with 2%, glucose and the mutated strain was supplmented with different concentrations of lipoic acid (40 µg/ml, 4 µg/ml and 0.4 µg/ml); the cells were incubated overnight at 28°C and subsequently exposed to two different concentrations of H_2O_2. The cells were treated independently with 1 mM H_2O_2 for 2 hours or with 2 mM H_2O_2 for 3 hours, to induce a mild and a more severe oxidative stress conditions. Subsequently, the same number of cells was plated and the survival rate was calculated. The results of this analysis are shown in figure 3.11.

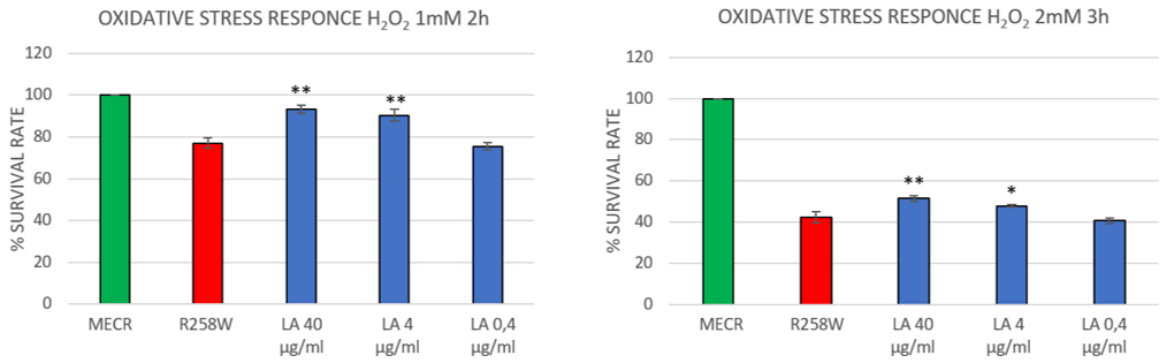

Figure 3.11: Lipoic acid supplementation effect on ROS-inducing agents treatment of wild type, null and mutant *MECR* strains. Survival rate percentage analysis after the exposure to 1mM H_2O_2 for 1 hour (A) . Or after the exposure to 2 mM H_2O_2 for 3 hours (B) . The values were normalized to the wild type strain, to which the arbitrary survival rate value of 100% was assigned. Values are represented as the mean of at least three values ± SD. P values are obtained using one-way analysis of variance followed by Bonferroni's test, *P<0.05; **P<0.01

Mild stimulation with 1 mM H_2O_2 for one hour leads to an increase of 25% in cell mortality in the mutant compared to the wild type. 40 and 4 µg/ml lipoic acid supplementation show an almost total recovery of this defect, while the administration of 0.4 lipoic acid µg/ml showed no effect on mortality. The more severe condition with 2mM H_2O_2 for 3h is associated with a deep defect in mutant viability, with a 60% decrease in the survival rate. The beneficial effect of lipoic acid is observed also in this condition, since supplementation with 40 µg/ml leads to a significant decrease of 15% in cell mortality. It is important to underline that the enzymatic defect associated with the R258W mutation cannot be bypassed, since the administration of lipoic acid does not lead to both an improvement in the oxidative growth and restoration of the lipoylation state of Lat1 and Kgd2 subunits of the mutant. However, these data confirm the antioxidant power of lipoic as a general scavenger molecule, which is able to contrast the oxidative stress generated in MECR/Etr1 deficiency, reducing the sensitivity of the R258W mutant strain to the oxygen radical species (ROS) exposure. Lipoic acid is a low toxic compound that can be integrated through the oral use of tablets. Given the results here reported, the data from literature and the safety of lipoic acid, the molecule has been tested directly in the patient harboring *MECR* mutation to evaluate putative beneficial effects on the disease progression.

3.2 MTFMT MUTATIONS MODELING, YEAST STRAINS CONSTRUCTION AND COMPLEMENTATION ASSAY

The NGS screening carried out on patients' cohort led to the identification of another mutation in homozygous condition. Specifically, the T178I substitution in *MTFMT* gene, coding for the Mitochondrial Methionyl-TRNA Formyl transferase, was identified. *MTFMT*, as reported in the introduction part of this thesis, is the enzyme involved in the formylation of the initial methionine residue in the mitochondrial protein synthesis process. Unfortunately, the structure of the human MTFMT protein (or other mammalian) protein has not yet been resolved, and information on the domain's organization is obtained by homology with the well-characterized bacterial Methionyl-TRNA Formyl transferase. hMTFMT protein is composed of 393 amino acids and contains the initial mitochondrial targeting sequence, a highly conserved motif that forms the N10-formyltetrahydrofolate (10-formyl-THF) binding site at the N-terminal region and a putative Met-tRNA binding domain in the C-terminal part of the protein (Li et al. 2000). The threonine 173 residue lies in the N-terminal domain, implicated in the recognition and binding of 10-formyl-THF, the substrate of the reaction and donor of the formyl group. The replacement of threonine, which possesses a polar side chain with a hydroxyl group, with isoleucine, containing a bulky apolar side chain, could leads to a weak recognition of the substrate and a defect in the enzymatic activity. However, this little information available does not allow discerning between a pathological mutation or a neutral polymorphism, making it necessary to validate the T173I substitution in a model organism. The multiple alignment of mitochondrial Methionyl-TRNA Formyl transferase sequences from different organisms shows the high degree of conservation of the human T173 residue during the evolution, assuming a critical function of this residue among different species (Figure3.12).

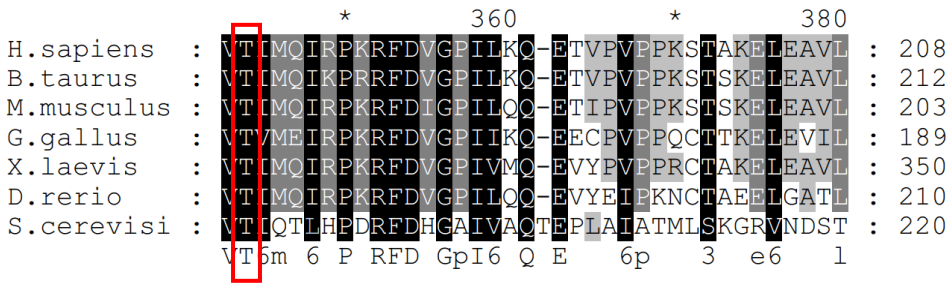

Figure 3.12: FigureX: Multiple alignments of mitochondrial methionyl-tRNA formyltransferase sequences from different organisms. In red are highlighted the residues under analysis. The alignment was performed with cluster X and displayed with GeneDoc tool. The accession numbers related to the selected sequences are: *H. sapiens* NP_640335.2; *S. cerevisiae* NP_009540.2; *G. gallus* XP_040536165.1; *X. laevis* XP_018108772.1; *B. taurus* NP_001159995.1; *D. rerio* NP_001071010.2; *M. musculus* AAH19509.1

Although the amino acid is conserved in human and yeast, the whole identity percentage of the two proteins is low (around 30%) with large non-overlapping areas. Based on the low conservation, it was chosen to construct a disease model, associated with this gene, using a heterologous complementation approach, thus introducing the mutated *MTFMT* human allele into a yeast strain deleted in the orthologous gene *FMT1*. In literature, no evidence of complementation of *MTFMT* in *FMT1*-deleted strain is available, and therefore the purpose of this thesis, besides the validation of the mutation, is to evaluate the ability of *hMTFMT* gene to complement the lack of *FMT*1 gene. The deletion cassette *fmt1::kanMX4* was amplified through a preparative PCR using the primer pairs *FMT1*DFw / *FMT1*DRv, and the genomic DNA extracted from the BY4741 *fmt1Δ* strain as the template (Brachmann et al. 1998). The amplicon fragment contains external portions, homologous to the region flanking the *FMT1* ORF, and kanamycin resistance gene for the selection. To induce the deletion of *FMT1* gene, the deletion cassette was used to transform the yeast strain W303-1B, producing the W303-1B *fmt1Δ* strain. To evaluate whether the human allele can complement the deletion of the yeast orthologs, *MTFMT* cDNA was cloned into both centromeric and episomal expression vectors. The human cDNA (Gene Bank ID: BC016630.1), purchased from an external company, was amplified by exploiting a preparative PCR reaction using the primer pairs *MTFMT*CNotFw /*MTFMT*CNotRv, producing *MTFMT* cDNA containing *Not*I restriction sites at the 5' and 3' ends. The amplicon was digested with *NotI* restriction enzymes and cloned in the pFL39*TET*off and *YepLac112TET*off vectors, digested with the same enzyme. These recombinant plasmids containing *MTFMT* were used to transform the respective deleted strain W303-1B *fmt1Δ,* producing the humanized yeast strain. To evaluate the complementation, it was necessary to construct the strain containing the orthologous yeast gene regulated by its physiological promoter inserted in a centromeric plasmid as a control. Starting from the genomic DNA extraction of the W303-1B strain, *FMT1* gene was amplified using the *FMT1*CBamFw/*FMT1*CPstRv primer pairs, which introduces *Bam*HI and *Pst*I restriction sites at the 5' and 3' ends. Yeast gene *FMT1* digested with *Bam*HI and *Pst*I was cloned into the monocopy plasmid pFL38, digested with the same restriction enzymes. The

pFL38*FMT1* vector thus produced was used to transform the W303-1B *fmt1Δ* strains. Once the strains have been prepared, it was possible to perform the study of complementation. To assess the ability of the human *MTFMT* gene to complement the lack of *FMT1* orthologue genes, the oxidative growth of the humanized and yeast wild type strains was analyzed. Using the spot assay technique, the strains were plated on media supplemented with non-fermentable carbon sources which allow highlighting mitochondrial defects related to the oxidative metabolism. The results were consistent across all sources tested, and glycerol is the source in which the complementation is more evident. (Figure3.13).

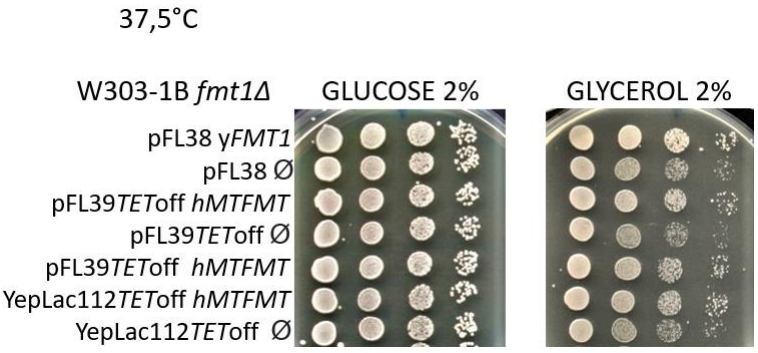

Figure 3.13: Oxidative growth analysis to evaluate the complementation of the human *MTFMT* gene.

The complementation of human *MTFMT* has never been reported in the literature. However, it is well established that the respiratory deficient phenotype of the strain deleted in *FMT1* is very weak (Franco et al. 2019). In fact, there is a partial reduction of oxidative growth only at high temperatures, above 37°C. For this reason, the complementation analysis was performed only in this condition, to better visualize the difference in the growth phenotype between the deleted and wild type strains. Both constructs inserted in the *fmt1Δ* strain, pFL39*TET*off*MTFMT* and YEplac112*TET*off*MTFMT*, are able to complement the deletion of *FMT1* gene. It was decided to continue this analysis using the centromeric plasmid, more stable inside the cell and which produces a lower amount of protein, sufficient to guarantee the best possible complementation. Once the complementation of the human gene was established, the *MTFMT*-related yeast model carrying the

mutation identified in patients was constructed. In fact, using "quik change® PCR", the mutation of interest was inserted directly into the construct pFL39TEToff *MTFMT*. The T173I mutation was introduced into the plasmid using the primers pair *MTFMT*T173IFw / *MTFMT*T173IRv. The recombinant mutated plasmid FL39*TET*off *MTFMT*^{T173I} was used to transform the yeast strain W303-1B *fmt1Δ*, producing the yeast model useful for the validation of the putative pathological mutation.

3.2.1 VALIDATION OF T173I *MTFMT* MUTATION IN HUMANIZED YEAST MODEL

Once the ability of *MTFMT* gene to complement the *FMT1* deletion was ascertained, the impact of the mutation on mitochondrial activity is assessed, evaluating the oxidative growth and respiration of the mutant strain. The oxidative growth evaluation through spot assay allows having a quick qualitative demonstration of mitochondrial defect associated with a particular genetic background. This analysis was performed at 37.5°C in medium supplemented with 2% glycerol, since only at high temperatures the possible defect associated with the mutation can be detected. The results of this analysis are shown in figure 3.14.

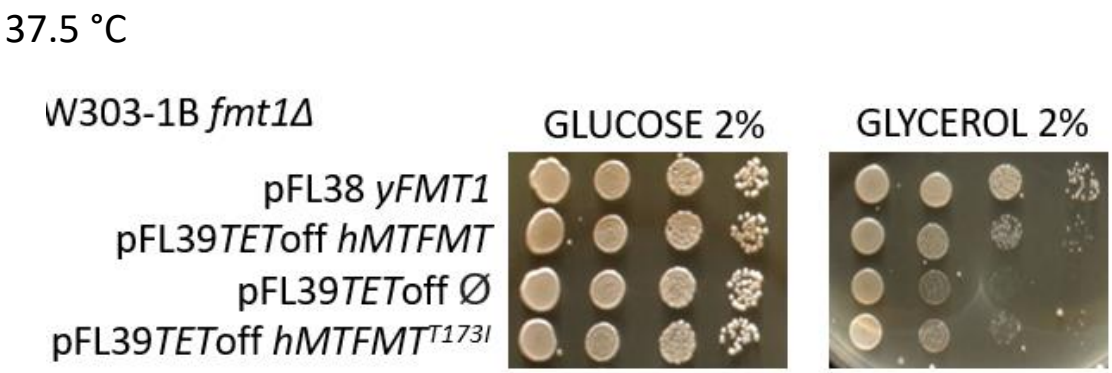

Figure 3.14: Oxidative growth analysis of W303-1B *etr1*Δ and W303-1B *fmt1*Δ strains containing *MECR* or *MTFMT* wilt type/mutated alleles and empty vector (negative control) at 28 and 37.5 °C, respectively.

The strain containing the *MTFMT* T173I mutation showed a reduction in oxidative growth compared to the wild type strain. Since this analysis does not allow a quantification of the mitochondrial defect, offering only a rapid and qualitative overview of mitochondrial activity, the evaluation of the respiratory rate was performed. Although *MTFMT* is not directly involved in respiratory metabolism, secondary effects, for example due to defects in mitochondrial protein synthesis, could be related to a deficit in respiratory ability in the mutant strain. To evaluate this hypothesis, the respiratory capacity of the wild type and mutant strains was measured in heat stress condition.*MTFMT*-related strains were grown for 18 hours in YP medium supplemented with 0.5% glucose at 37.5°C. The results of this analysis are shown in figure 3.15.

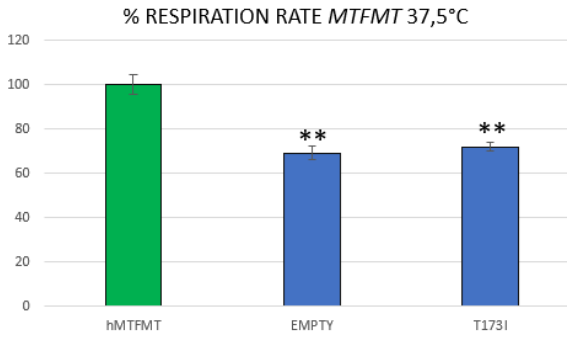

Figure 3.15: Oxygen consumption rate of strains carrying *MTFMT* wild type or mutant alleles, or the empty plasmid, at 37.5°C, respectively. The green bar indicates the wild type strain, which was set to 100%. Values were normalized to the wild type strain value and are represented as the mean of at least three values ± SD. p values are obtained using one-way analysis of variance followed by Bonferroni's test, *P<0.05; **P<0.01;

The deleted strain W303-1B *fmt1Δ* shows a residual respiratory activity, with a reduction of about 30% compared to the strain containing the wild type allele. The T173I mutant shows a phenotype similar to the deletant strain, indicating that the mutated protein is unable to complement the partially defective respiratory phenotype of the null mutant. However, this residual 70% respiratory activity in null and T173I mutants could explain the slight oxidative growth reduction phenotype, compared to the control strain, observed in the previous analysis. All these considerations lead to the association of the T173 mutation with defects related to the mitochondrial activity in yeast, indicating that it could be the direct cause of the disease in patient. To evaluate whether the

detrimental effects of the T173I substitution could be due to a decreased level in the mutated protein, western blot analyses were set up to detect MTFMT protein (Figure 3.16). For this purpose, the strains were inoculated in YP medium supplemented with a limiting source of glucose (0.5%) and incubated overnight at 37.5 °C. The proteins were extracted using TCA extraction protocol, loaded on a polyacrylamide gel and subsequently incubated with a primary anti-MTFMT antibody, able to detect human proteins. Por1 was used as a loading control.

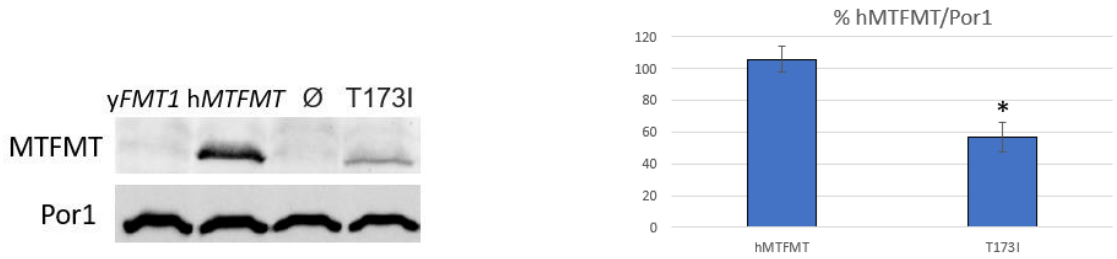

Figure 3.16: Western blot performed at 37.5°C on strain carrying *MTFMT* wild type, null and mutant alleles and relative quantification graphs using Por1 as housekeeping to quantify the MTFMT contents. Values were normalized to the wild type strain value and are represented as the mean of at least three values ± SD. P values are obtained using one-way analysis of variance followed by Bonferroni's test, *P<0.05; **P<0.01

The image of the western blot highlighted the inability of the antibody to detect the yeast protein Fmt1, since no bands are detected in the *FMT1* wild type strain. Protein levels of wild type and mutated MTFMT are also measured, and a significant reduction in the MTFMT mutated protein content (50%) is observed, suggesting that protein scarcity may contribute to the pathological phenotype. It is important to underline that the mutant strain shows a respiratory rate comparable to that of the null strain, therefore the reduction of the protein content of about 50% may be an important contribution to the patients' pathological phenotype; however other factors are likely involved.

3.2.2 MITOCHONDRIAL PROTEIN SYNTHESIS DEFECTS IN THE YEAST MODEL OF *MTFMT*

Mitochondrial translation normally requires formylation of the initiator Met-tRNA^{Met}. While this process in humans has been widely demonstrated to play a pivotal role in the stability of proteins produced within the mitochondrion, it seems largely unnecessary in yeast. As previously mentioned, at physiological temperature, the deletion of *FMT1* gene did not affect mitochondrial activity. However, this process tends to acquire importance in stress conditions, such as starvation and high temperature. Based on this information, it was decided to evaluate the ability of deleted, wild type and mutant *MTFMT* strains to synthesize mitochondrial proteins *in vivo*. The yeast strains were grown at 37.5°C for 18 hours, the condition in which the oxidative defect was detected, in minimal SC-TRP medium supplemented with 2% galactose and 0.2% glucose. Galactose is the standard source for measuring the protein synthesis, 0.2% glucose was added since the growth on galactose medium is slow. The cells were harvested and the ability to incorporate the radioactive methionine and cysteine containing the ^{35}S isotope into mitochondrial proteins in the presence of cycloheximide, a specific inhibitor of cytoplasmic synthesis, was evaluated. The proteins were extracted and subsequently loaded into the polyacrylamide gel and transferred on a nitrocellulose membrane, which was used to impress the autoradiography film. The results are represented in figure 3.17.

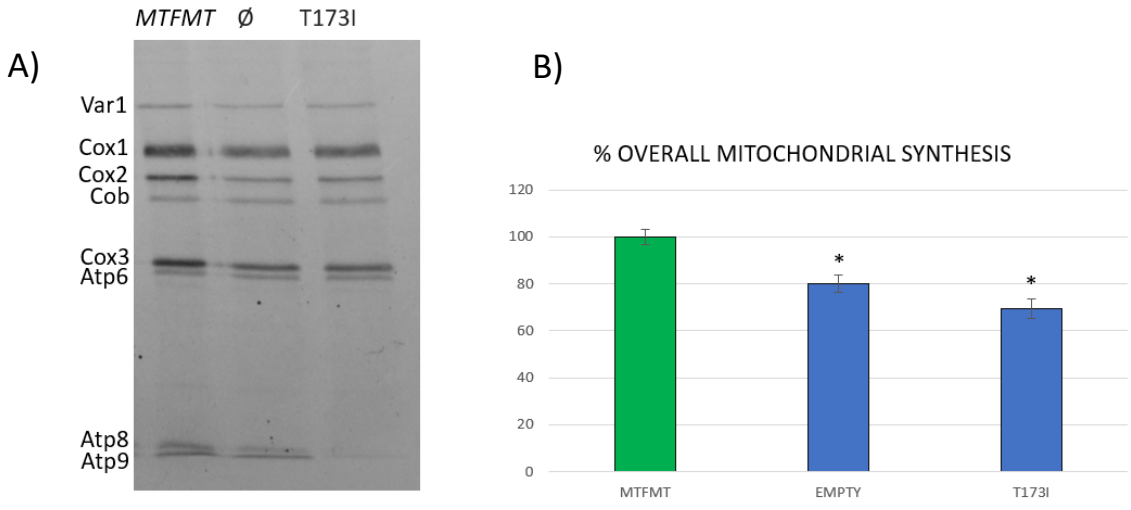

C

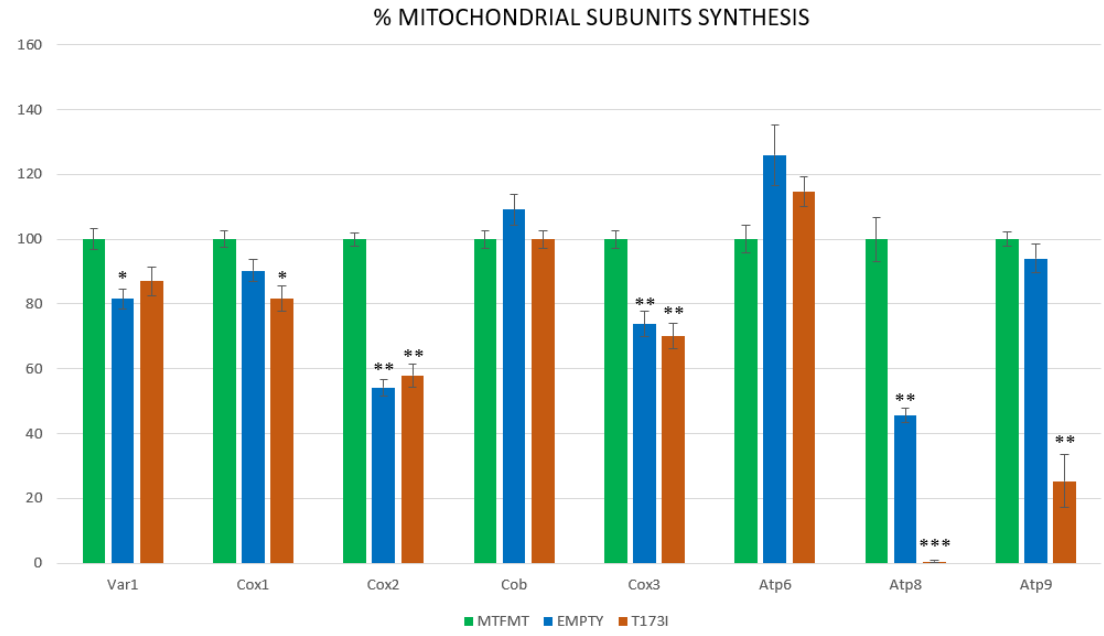

Figure 3.17: Mitochondrial protein synthesis in *MTFMT* wild type, deleted and mutant strains at 37.5°C. (A) Representative image of mitochondrial synthesis. (B) Quantification of the overall mitochondrial synthesis (C) Relative quantification of proteins codified by mtDNA. Values were normalized to the wild type strain value and are represented as the mean of at least three values ± SD. P values are obtained using one-way analysis of variance followed by Bonferroni's test, *P<0.05; **P<0.01; ***p<0.001

In the presence of the T173I mutation, a significant decrease in the overall mitochondrial protein synthesis is observed. In detail, the proteins that showed a greater reduction are Cox2 and Cox3, which are subunits to the cytochrome c oxidase (complex IV), and Atp8 and Atp9, which are subunits of the ATP synthase (Complex V). Analysis performed on muscle fibroblasts derived from the patient carrying the T173I mutation confirmed the deficiency in complex IV. This result is further confirmed by evidence in the literature that associates dysfunctions of the formylation process with anomalies of cytochrome C oxidase (Hinttala et al. 2015). Based on this consideration, the attention was focused on complex IV. To have further confirmation of the data obtained concerning the synthesis deficit in the subunits of complex IV, the Cox2 subunit levels were detected by western blot, and subsequently, using spectrophotometric enzymatic assay, the activity of complex IV *in vitro* was evaluated (figure 3.18). Experimentally, the cells were inoculated in SC-TRP medium supplemented with 0.5% glucose and incubated at 37.5 °C in a thermostatic bath for 18 hours. At the end of the

growth, the cells were collected; a part of them was for the TCA protein extraction with the aim to evaluate the Cox2 levels, whereas the remaining cells were used for the zymolyase mitochondria extraction to evaluate the enzymatic activity of complex IV.

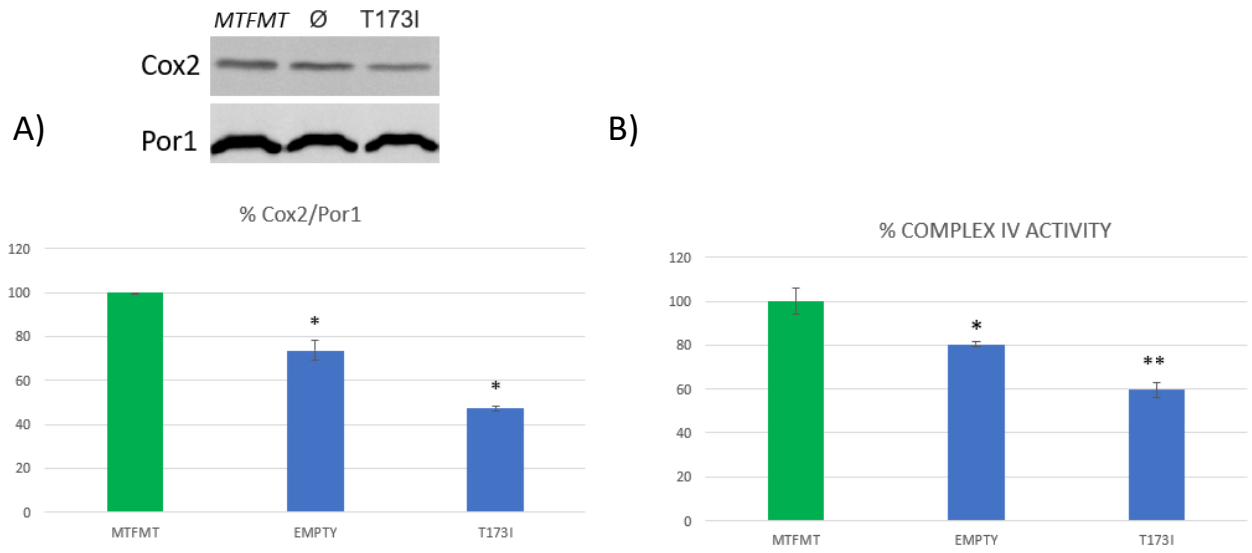

Figure 3.18: analysis of complex IV defects in mutant, null and wild type *MTFMT* strains at 37.5° C. (A) Western blot analysis on the stability of the Cox2 subunit and relative quantification using the housekeeping Por1. (B) Evaluation of the enzymatic activity of complex IV. Values were normalized to the wild type strain value and are represented as the mean of at least three values ± SD. P values are obtained using one-way analysis of variance followed by Bonferroni's test, *P<0.05; **P<0.01

Western blot confirmed the data obtained from the mitochondrial synthesis assay: the levels of Cox2 subunit of complex IV are reduced in both mutated and *MTFMT*-lacking strains, with a greater reduction of about 50% in the mutated strain. The analysis of the complex IV enzymatic activity, in agreement with the previous considerations, shows a 40% reduction in the strain carrying the T173I mutation compared to the wild type. This evidence supported the hypothesis that the deficit in the synthesis of mitochondrial proteins and the consequent decrease of the complex IV activity could lead to the symptomatology observed in the patients. However, the residual activity of the COX complex is 60%, thus allowing a partial activity of the electron transport chain, a result that well parallelize with the mild phenotype of the null and the MECR mutant strain. An hypothesis to explain

the decreased mitochondrial protein synthesis and, as secondary effect, the defect observed in complex IV activity could involve the maturation and quality control processes of newly synthesized proteins. The nascent polypeptide chain is immediately recognized by PDF, a deformylase associated with ribosomes that removes the formyl group, allowing the correct folding of the protein (Giglione et al. 2000). Furthermore, the proteins that escape to the PDF action, still exposing the residue of formylated methionine, are recognized and degraded by fMet/N-recognin/protease. The absence of formylation could lead to an incorrect folding, due to the loss of interaction between PDF and native protein, but also can deregulate the quality control system of newly synthesized peptides, leading to reduced protein stability. In yeast, these quality control mechanisms are probably switched off at physiological temperature and subsequently activated only in response to heat prolonged stress. Therefore, mutant strains defective in formylation may lose the ability to respond to these environmental stimuli, and consequently, defects in the stability of mitochondrial proteins are observed.

3.3 DISCUSSION

In the second part of this thesis the process of validation in yeast of *MECR* R258W and *MTFMT* T173I recessive mutations, identified in two different HON patients in homozygosis, is described. The study of the mutation was performed using a heterologous complementation approach, in which the human pathological allele is inserted directly into the yeast context bearing the deletion of the respective ortholog. Regarding *MTFMT* gene, encoding the enzyme that catalyzes the formylation reaction of the first methionine residue in mitochondrial synthesis, no experimental pieces of evidence from literature, on the ability of the human allele to complement the deletion of the yeast *FMT1* ortholog, are available. The results obtained firstly confirmed the ability of the human *MTFMT* allele to partially complement the *FMT1* deletion, and also identify the experimental conditions in which the pathological phenotype of the mutated allele could be evaluated. In fact, it has been shown that the methionine formylation process in yeast, despite being bypassed at physiological temperature, plays a fundamental role in heat-stress conditions. At 37.5°C, the strain containing the T173I variant shows defects of the OXPHOS metabolism with a deficit in oxidative growth and respiration, thus confirming that the patient pathological phenotype is due to the mutation under analysis. Molecular studies aimed at understanding the pathogenetic mechanism related to the mutation show that T173I substitution leads to a decrease in the overall mitochondrial protein

synthesis, with a greater effect on the subunits that take part in cytochrome c oxidase (Complex IV) and ATP synthase (Complex V). Enzymatic assays on mitochondrial extracts supported the complex IV enzymatic defects in the presence of the mutation. Studies on patient fibroblasts derived from the patient carrying the T173I substitution confirm a deficient assembly and activity of cytochrome c oxidase. The formyl group of the first methionine residue could be important for the recognition of native peptides in the folding phase by proteins that facilitate this process. The formylated methionine residue is immediately recognized by PDF, a deformylase enzyme that removes the formyl group, probably recruiting multi-protein machinery with a chaperone-like action, favoring the folding process. The absence of formylation could lead to the loss of these interactions and therefore to the lower stability of the mitochondrial proteins produced. This work demonstrates the complementation of the human *MTFMT* allele and the existence of a defect linked to the absence of formylation in yeast, hypothesizing a conserved maturation mechanism between humans and yeast, in which it is active only under stress conditions. However, two similar mechanisms of native protein maturation could coexist: i) one involved in the maturation of polypeptides under physiological conditions and ii) one involving the initial methionine formylation, active only under stress conditions. These considerations make yeast an excellent tool also for the validation of defects related to the formylation mechanism, allowing studying mutations in *MTFMT*. Regarding the other homozygous mutation, on the contrary, it had already shown that the overexpression of the human *MECR* allele, involved in the mitochondrial fatty acids biosynthesis (mtFASII), is able to complement the absence of the corresponding *ETR1* yeast ortholog*.* Also in our experimental conditions, the complementation using multicopy plasmids, leading to the overexpression of *MECR,* is observed. After the construction of mutant strain containing the R258W mutation, a series of phenotypes related to oxidative metabolism are evaluated. Also in this case, defects in oxidative growth and respiration are observed, confirming that the R258W mutation could be the cause of the disease in patient. The mtFASII, in which *MECR* is involved in the final step of the pathway, has lipoic acid as the main product. In cells this compound has several functions, it is a powerful antioxidant agent but also an essential cofactor for the subunits of key enzymes in OXPHOS metabolism, such as pyruvate dehydrogenase and α-ketoglutarate dehydrogenase. The lipoylation levels of the Lat1 and Kgd2 yeast subunits, which respectively take part in these enzymes, were assessed by western blot. In the mutant strain carrying the R258W mutation, the total absence of lipoylated subunits emerged, probably leading to a lower residual activity of these enzymes, which could explain the observed defect in oxidative growth. Since defects in mtFASII cause a reduction in

lipoic acid production, the effects of lipoic acid supplementation on the oxidative growth of the mutant are tested. It is observed that the mutant treated with lipoic acid does not show improvement in oxidative growth. This result underlines the absence of a "salvage pathway" in yeast, capable to use exogenous lipoic acid, to rescue the lipoylation of target subunits. However, as previously mentioned, lipoic acid also has a scavenging action, aimed to contrast the oxidative stress induced by ROS. In this thesis it has been demonstrated that the mutant containing the R258W mutation, is associated with hypersensitivity to ROS-inducing agents, since the treatment with H_2O_2 has shown a different survival rate in mutant and wild type strains, assuming the inability to respond at oxidative stress sources in the presence of R258W mutation. The mutant strain treated with lipoic acid shows a significant increase in the survival rate after exposure to different concentrations of H_2O_2. All these results demonstrate the beneficial effect of lipoic acid on the mutant containing the R258W substitution, due to the intrinsic antioxidant capacity of this molecule rather than to the restoration of normal levels of lipoylation in Lat1 and Kgd2 subunits. Thanks to its low toxicity, lipoic acid is already used to treats several diseases in human such as diabetic retinopathy and acute optic neuritis (Nebbioso et al. 2013; Falardeau et al. 2019). Based on this consideration, lipoic acid is now administrated to the patient carrying the R258W mutation, to evaluate the allegedly beneficial effects on the progress of the disease.

CHAPTER 4: RESULTS AND DISCUSSION SECTION III

4.1 ACO2 MUTATIONS MODELING, YEAST STRAINS CONSTRUCTION AND COMPLEMENTATION ASSAY

The last part of the thesis concerns the mutations identified in the *ACO2* gene, coding for the mitochondrial aconitase which catalyzes the conversion of citrate to isocitrate. Interestingly, *ACO2* was the most frequent mutated gene in the patients' cohort analyzed. Seven variants in unrelated probands were identified in heterozygosis, which specifically lead to the following amino acid substitutions: R312Q, R474G, N480D, E485G, Y650S, R671W and R671Q. Following the same pattern used in the previous validation studies, the analysis started from the modeling of the mutations, exploiting mammalian mitochondrial aconitase crystallographic structure, available in the PDB database. The structure of human mitochondrial aconitase has not yet been solved, however, structures of other mammalian proteins, such as *Sus scrofa* (PDB ID: 7ACN), are available. The high percentage of identity between the human and porcine sequences, of about 97%, allows inserting the mutations identified in the patients in the respective residues of the *S. scrofa* protein, modeling them with an excellent confidence interval. In particular, the residues in the polypeptide structure of *S. scrofa*, corresponding to the substitutions identified in the patients, are listed in figure 4.1.

A)

HUMAN ACO2	PORCINE ACO2
R312	R258
R474	R447
N480	N453
E485	E458
Y650	Y623
R671	R644

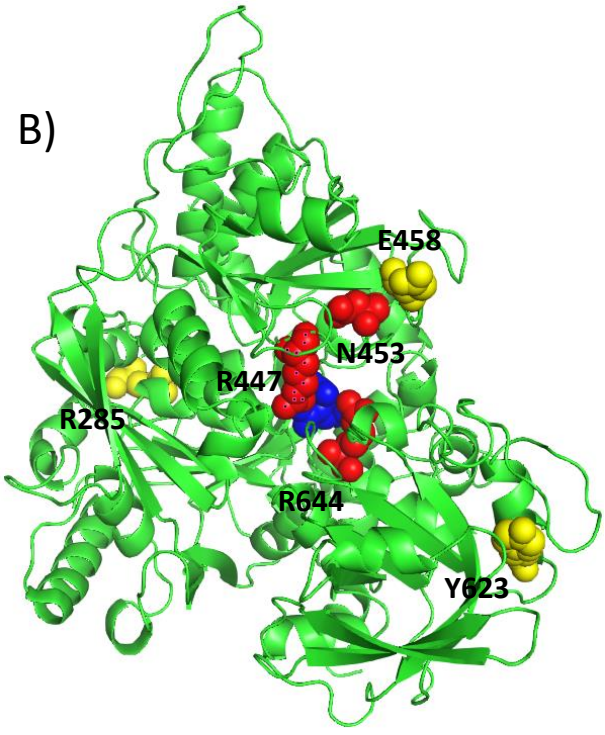

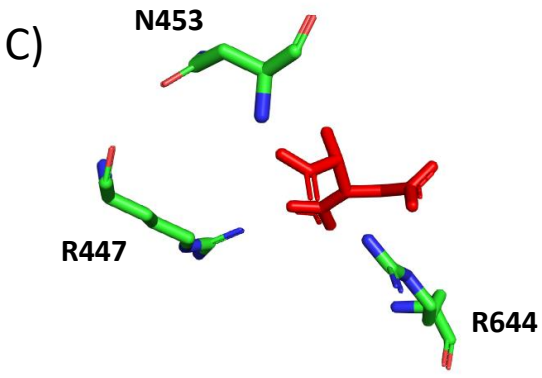

Figure 4.1: Modeling of human mitochondrial aconitase mutation in the *Sus scrofa* protein. A) correspondence between human residues, identified in the screening, and porcine amino acids. B) The mutations in close contact to the substrate are highlighted in red, citrate in blue, while the surface mutations are colored in yellow. C) Zoom on the interaction between the residues R474, N480, R671 and citrate.

Based on the model obtained, it is possible to cluster the mutations in two distinct groups. The residues R447, N453 and R644, corresponding to R474, N480 and R671 in human aconitase respectively, localize into the enzymatic pocket of the enzyme in close contact with citrate, the substrate of the reaction catalyzed by ACO2. Furthermore, it has been shown that the human arginine residues 474 and 671 are involved in both the binding of citrate and in the catalytic process of isocitrate formation. Analyzing the position of the human asparagine residue 480 (N453 in the porcine structure), although it does not seem to show a catalytic role, it is probably fundamental to recreate the optimal environment in which the reaction takes place, being close to the substrate. Therefore, mutations in these amino acids could lead to severe defects in aconitase activity. Instead, the second group of residues, including R285, E458 and Y623, corresponding to R312, E485 and Y650 in human protein, localize in superficial and unorganized stretches of the protein, hypothesizing a structural role rather than an involvement in the enzymatic reaction. For mutations that lie in the enzymatic pocket, the impact on the mitochondria aconitase functionality seems evident from the modeling information obtained; however, for all the mutations, especially those involving amino acids of the second group, analyses are necessary to verify whether they are the effective cause of the disease in patients. For this purpose, a yeast model was constructed to study the impact of all these mutations on mitochondrial functionality. The multiple alignment of mitochondrial aconitase sequences from different organisms shows the high conservation degree of the mutate amino acids during the evolution, assuming a very specialized function conserved among the species, except for amino acid E485 which is poorly conserved but lies in a conserved stretch (Figure 4.2). The mitochondrial aconitase sequences of human and yeast, phylogenetically distant organisms, show a high degree of similarity, with an identity percentage of about 67%.

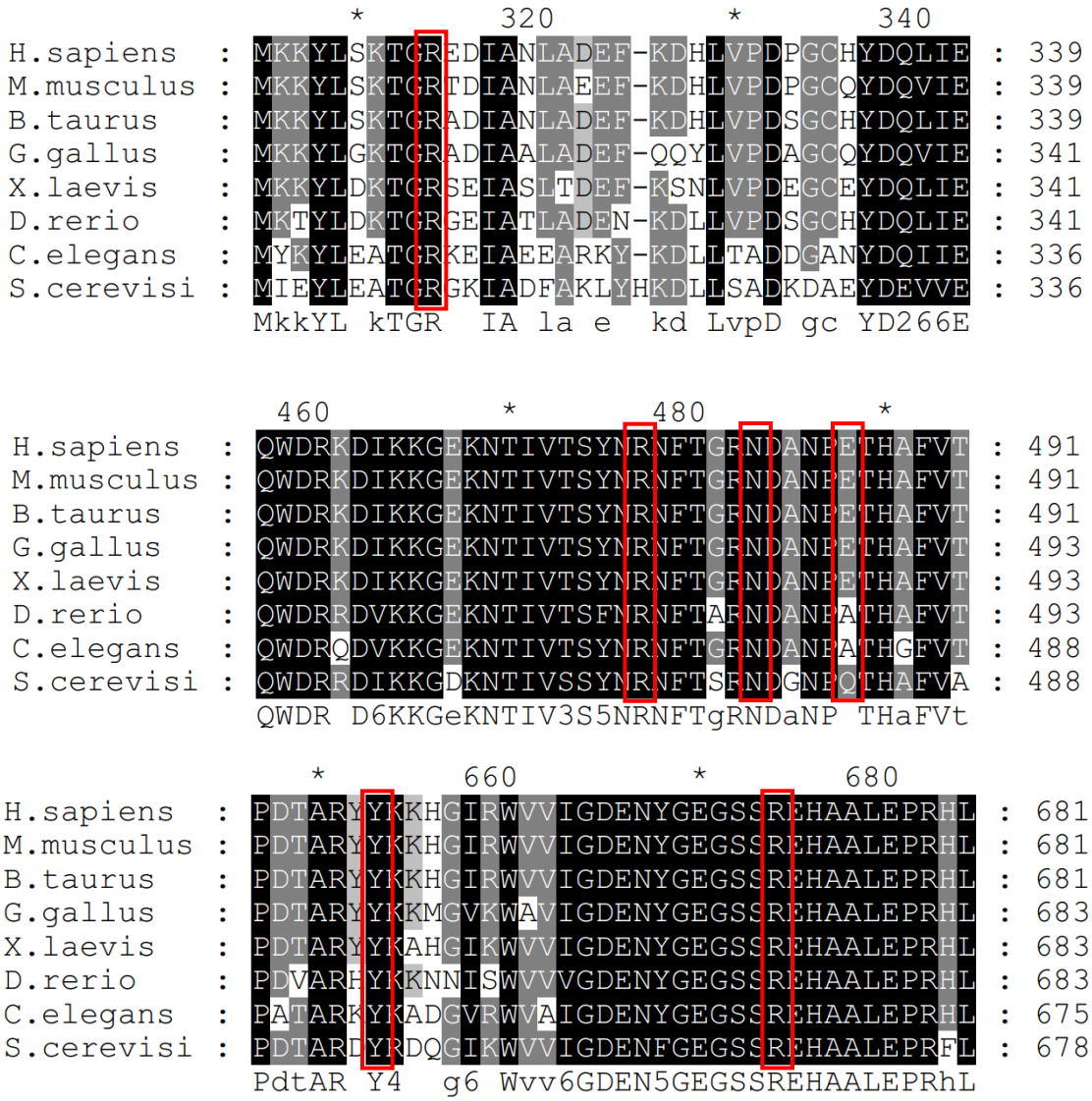

Figure 4.2: Multiple alignments of mitochondrial aconitase sequences from different organisms. In red are highlighted the residues under analysis. The alignment was performed with cluster X and displayed with GeneDoc tool. The accession numbers related to the selected sequences are: *H. sapiens NP_001089.1* ; *S. cerevisiae* NP_013407.1; *G. gallus* NP_989519.2; *X. laevis* NP_001337055.1 ; *B. taurus B.taurus AAI02643.1* ; *D. rerio NP_944590.1* ; *C. elegans* NP_741235.1; *M. musculus* NP_542364.1

Studies reported in the literature (Metodiev et al. 2014), have demonstrated the ability of the human *ACO2* allele, inserted into a multicopy plasmid, to complement the absence of the yeast ortholog *ACO1*. Based on these considerations, it was chosen to validate the mutations identified in patients exploiting the heterologous complementation approach, by inserting the mutated*ACO2* allele into an *aco1Δ* strain. However, it is necessary to optimize the complementation in our experimental conditions, and for this purpose, several strains were prepared. Since aconitase has a fundamental role within the mitochondrion, being part of both the Krebs cycle and a component of the nucleoid, *ACO1* deletion leads to irreversible loss of mtDNA, a condition that does not allow evaluating the complementation of the human allele. For this reason, to construct the yeast model related to the *ACO2* gene, it was necessary to perform the *ACO1* genomic allele deletion in the presence of a plasmid-borne wild type allele. Moreover, the strain bearing the *ACO1* gene deletion is auxotrophic for glutamate, therefore, to allow the mutants and deleted strain growth this amino acid must be present in the culture medium (Narahari et al. 2000). Considering this fundamental information, the model yeast strains were constructed. The *ACO1* gene with its promoter and terminator was amplified through PCR, using the genomic DNA extracted from the W303-1B strain as a template and the primers pair *ACO1*FwBamHI and *ACO1*RvHindIII. The amplicon was digested with *Hind*III and *Bam*HI and cloned in the centromeric plasmid pFL38, digested with the same enzymes, to obtain the construct pFL38*ACO1*. The plasmid thus constructed, was used to transform the W303-1B strain, generating the W303-1B pFL38*ACO1* strain. The *ACO1* deletion cassette (*aco1::KanMX4*) was prepared through PCR, carried out using the genomic DNA of the BY4741 *aco1Δ* strain (Euroscarf collection; Brachmann et al., 1998) as a template and the *ACO1*BamHIFw /*ACO1*HindIIIRv primers pair. Through "high-efficiency yeast transformation protocol" (Daniel Gietz and Woods 2002) the amplicon, containing regions for homologous recombination in the *ACO1* locus and the gene conferring kanamycin resistance, was used to induce *ACO1* deletion in the W303-1B pFL38*ACO1* strain. The *aco1::KanMX4* cassette could recognize either the *ACO1* gene present at the chromosomal locus or that contained in the plasmid. To distinguish between these two situations, plasmid shuffling on 5-FOA method was used to test the ability of the deleted clones to use a non-fermentable carbon source (ethanol). Clones harboring the genomic *ACO1* deletion, after growth on 5-FOA medium to induce loss of the plasmid pFL38 *ACO1*, are unable to grow on ethanol-supplemented medium; vice versa, clones with the deletion of plasmid-borne *ACO1*, due to the genomic *ACO1* copy maintenance, can grow on non-fermentable carbon sources. Furthermore, the clones were also selected on a medium supplemented with geneticin, since only the clones bearing

the *ACO1* deletion at the genomic locus were geneticin resistant, while the clones containing the plasmid *ACO1* deletion, after two 5-FOA cycles, lost their ability to grow on the antibiotic-containing medium. Based on the different growth characteristics, the positive clones, containing the deletion of *ACO1* genomic gene, were selected. To study the human *ACO2* mutations, it was necessary to investigate the complementation of *ACO2* human gene in our experimental condition. For this purpose, the *ACO2* cDNA was cloned in two different multicopy yeast expression vectors, containing two strong promoters: *TET*off promoter, consisting of *CYC1* yeast promoter preceded by seven doxycycline repressible regulatory elements, or *PGK* promoter, which controls the expression of the housekeeping phosphoglycerate kinase gene in yeast. The human *ACO2* cDNA (GenBank ID: BC014092.2), purchased from an external company, was amplified through preparative PCR using the h*ACO2*NotIFw and hA*CO2*NotIRv primers, introducing the *Not*I restriction site at the 5' and 3' ends. The amplicon was digested with *NotI* enzyme and cloned into YepLac112*PGK* or YepLac112*TET*off multicopy plasmids, digested with the same restriction enzyme. The two constructs thus prepared (YepLac112*PGK*A*CO2* and YepLac112*TET*offA*CO2*), were used to transform the strain W303-1B *aco1Δ* pFL38*ACO1.* To obtain the strains bearing only the human *ACO2*, 5-FOA plasmid shuffling was performed. These strains containing the cDNA under the control of two different promoters were tested for the oxidative growth ability, to evaluate which of these constructs lead to better complementation. To evaluate the growth phenotypes associated with these humanized strains, it is necessary to use a reference strain containing the *ACO1* gene in a centromeric plasmid with the same selection marker (*TRP1*). For this reason, *ACO1* gene was subcloned into the centromeric plasmid pFL39, exploiting the presence of restriction enzymes *Bam*HI and *Hind*III sites. The resulting construct pFL39*ACO1* was used to transform the strain W303-1B *aco1Δ* pFL38 *ACO1*. The subsequent loss of the plasmid pFL38*ACO1* was obtained through plasmid shuffling on a medium containing 5-FOA, obtaining the strain W303-1B *aco1Δ* pFL39*ACO1*. Once all the strains were constructed, the ability of the human *ACO2* allele, under the control of two different promoters, to complement the *ACO1* deletion was evaluated. Through spot assay analysis, the ability of the human *ACO2*, under the control of *TET*off and *PGK* promoters, to restore the growth phenotype of the *ACO1* deleted strain on non-fermentable carbon sources was analyzed. The different strains were spotted in YP medium supplemented with 2% glycerol and ethanol or 2% glucose, at 28 and 37 °C. The results obtained are shown in figure 4.3.

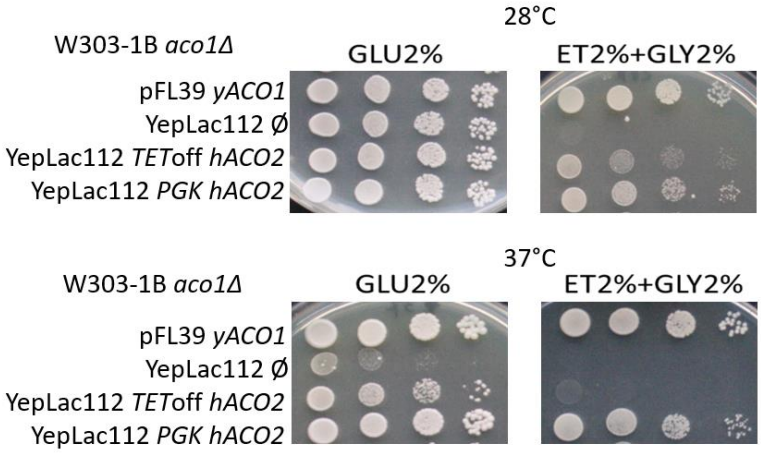

Figure 4.3: Oxidative growth analysis to evaluate the complementation of human *ACO2* gene at 28 and 37°C.

The results clearly exhibit a growth difference between the strains containing the human *ACO2* gene: better complementation of the strain harboring the construct containing the human gene under the control of the *PGK* promoter is observed, which almost completely restored the phenotype of the deleted strain both at 28 and 37°C. The different degree of complementation could be explained by the different levels of gene product formed from the two different promoters. In fact, previous studies in our laboratory have shown that the *PGK* promoter, compared to the *TET*off promoter, leads to a doubling of the gene product quantity, which could be the reason for the different complementation observed. Based on the results obtained, it was decided to study the effect of the pathological mutations identified in patients using the strain W303-1B *aco1Δ* YepLac112*PGKACO2* as a model. Once the best complementation condition was identified, the allegedly pathological mutations were inserted into the human *ACO2* gene within the construct YepLac112*PGK*off*ACO2* through Quik™ Change site-specific PCR, using the primer pairs shown in 6.5 paragraph (materials and methods section), producing:

- YepLac112*TET*off *ACO2*^{R312Q}
- YepLac112*TET*off *ACO2*^{R474G}
- YepLac112*TET*off *ACO2*^{N480D}
- YepLac112*TET*off *ACO2*^{E485G}
- YepLac112*TET*off *ACO2*^{Y650S}
- YepLac112*TET*off *ACO2*^{R671W}
- YepLac112*TET*off *ACO2*^{R671Q}

The mutant constructs were used to transform the strain W303-1B *aco1Δ* pFL38*ACO1*, thus producing heteroallelic strains containing one copy of the yeast wild type *ACO1* gene and the mutated copy of the human *ACO2* gene. Subsequently, plasmid loss of *ACO1* was induced by means of plasmid shuffling on 5-FOA plates, in the presence of and glutammate, to obtain haploid strains containing exclusively the mutated human allele (YepLac112*PGK ACO2**).

4.2 VALIDATION OF OXIDATIVE METABOLIC DEFECTS ASSOCIATED WITH *ACO2* MUTATIONS IN THE YEAST MODEL

Aconitase catalyzes the second reaction of the Krebs cycle, converting citrate into isocitrate through a two-reaction mechanism, in which dehydration is followed by subsequent rehydration reactions to form the final product. Furthermore, the role of aconitase in mtDNA stability has been also demonstrated, probably due to its SSB-like (single stand binding protein) activity. The mitochondrial processes in which this enzyme takes part are fundamental to sustaining the mitochondrial activity; thus, defects in these processes could be associated with impaired mitochondrial metabolism. To evaluate this hypothesis, the ability of wild type and mutant strains to use non-fermentable carbon sources (or combinations of them) were analyzed. Through spot assay analysis, the cells were spotted on YP medium supplemented with a combination of 2% glycerol and ethanol (the condition in which the complementation is maximal) or with 2% glucose and subsequently incubated at 28 or 37°C. Figure 4.4 shows the results obtain

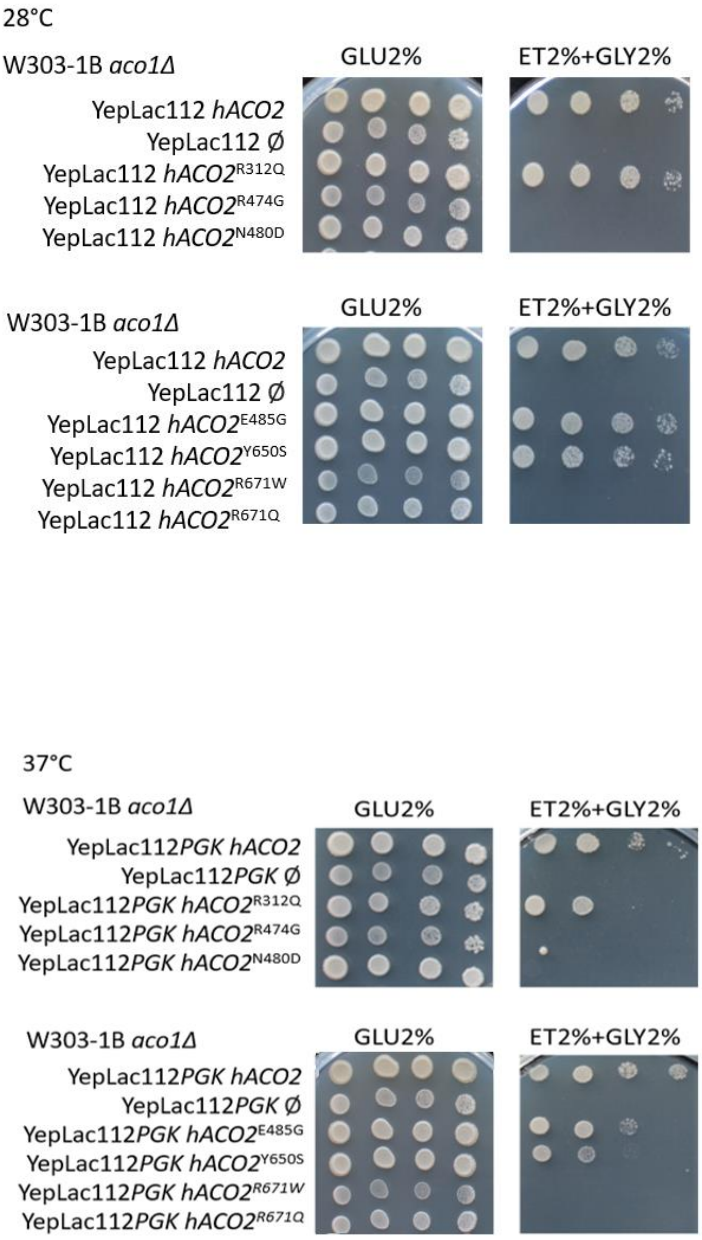

Figure 4.4: Oxidative growth analysis of W303-1B *aco1Δ* strains containing the wild type or mutated *ACO2* alleles and empty vector at 28 and 37°C.

Analyzing the growth phenotype of the mutants, it is possible to cluster the mutations into two categories, that well parallelize the pattern identified in the modeling analysis, dividing the mutations into severe and mild. The severe mutations R474G, N480D, R671W and R671Q inhibit completely the growth ability on media with non-fermentable carbon sources, with a consequent defect in mitochondrial activity, underlining that the involved amino acids could have a key role in

the protein functionality. In this analysis, the arginine 671 is affected by two different mutations, with the replacement of this amino acid with tryptophan and glutamine, leading to the same severe phenotype, thus confirming the pivotal role of this residue in the protein functionality. On the contrary, the mild mutations R312Q, E485G and Y650S, located in peripheral areas of the protein, are associated with a growth level comparable to the strain transformed with the wild type *ACO2* allele at 28°C, but show a thermosensitive moderate reduction of oxidative growth in a heat-stress condition at 37 °C. Further investigations are needed to confirm and explain the diversity of the defects associated with these mutations. Another analysis related to mitochondrial OXPHOS defects concerns the assessment of the respiratory activity. Since the Krebs cycle and the OXPHOS pathway are closely linked, the defects detected in the oxidative growth could have repercussions on the respiratory rate. To test this hypothesis, the strains were inoculated in YP medium added with 0.5% glucose, incubated for 18 hours at 28 and 37°C. Since the growth in media with ethanol and glycerol is slow, a limiting fermentable carbon source was added, and the analysis of the respiratory rate was performed after total exhaustion of glucose. The results obtained from the respiratory rate analysis are shown in the figure 4.5.

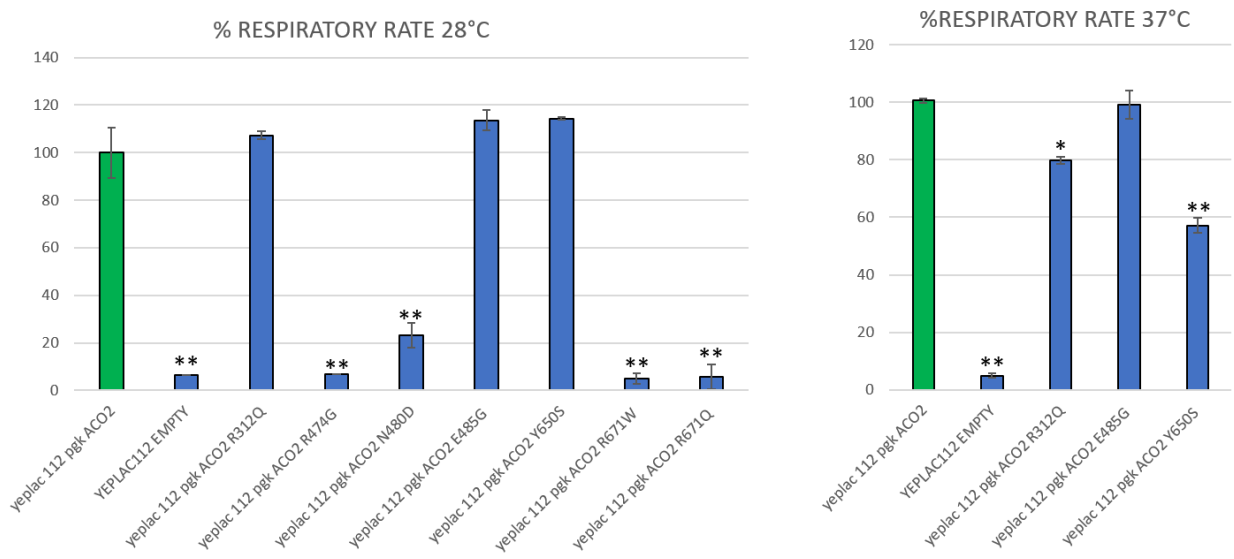

Figure 4.5: Oxygen consumption rate of W303-1B *aco1Δ* harboring the wild type or mutated *ACO2* allele and empty plasmid at 28 and 37°C. The green bar indicates the wild type strain, which respiratory activity was normalized to 100%. Values are represented as the mean of at least three values ± SD. p values are obtained using one-way analysis of variance followed by Bonferroni's test, *P<0.05; **P<0.01

The results obtained show that *ACO1* null strain loses any respiratory capacity, likely due to the loss of mtDNA, producing a *rho*^{0} strain. mtDNA encodes for some subunits of the respiratory complexes, in particular of complex III, IV and V; therefore, the absence of these proteins negatively affects the entire electrons transport chain process. Focusing on mutant strains, excellent parallelism is observed between oxidative growth and respiratory rate. In fact, mutant strains unable to grow on ethanol and glycerol plates at 28°C, show an oxygen consumption rate comparable to that of the null mutant, confirming also in this analysis the severe phenotype associated with these mutations. All variants that present a thermosensitive oxidative growth defect, except for E485G, also exhibit a reduction in respiratory activity at 37°C. In particular, the strain containing the R312Q mutation shows a slight reduction in the respiratory activity (~ 20%) compared to the wild type, while the Y650S mutation is associated with a moderate defect, showing a reduction of about 50%. The strain containing the E485G mutation possesses an oxygen consumption rate similar to that of the wild type strain, suggesting that the observed defect in oxidative growth may not be related to a reduction in respiratory ability.

4.3 MOLECULAR AND BIOCHEMICAL INVESTIGATIONS ON *ACO2* YEAST STRAINS

The previous paragraph demonstrates that all mutations are associated with several degrees of mitochondrial impairment. These analyses lead to the identification of two groups, based on the severity of the defect, highlighting 4 severe mutations and 3 mild thermosensitive mutations. This section of the thesis is aimed to understand the mechanisms underlying the different degrees of mitochondrial deficit, to better clarify the pathogenetic mechanism associated with these mutations in patients. The defects observed in mitochondrial activity, respiration and oxidative growth could be due to reduced steady state levels of mutated ACO2 protein. To evaluate this hypothesis, the aconitase protein levels in wild type and mutant strains were investigated through western blot. The null, wild type and mutant strains were inoculated in YP medium supplemented with 0.5% glucose and grown at 28 and 37°C for 18 hours. The cells were harvested to perform TCA protein extraction, subsequently loaded on polyacrylamide gel and transferred to a nitrocellulose membrane which was hybridized with the primary antibody anti-ACO2 and anti-Por1. The results of this analysis are shown in figure 4.6.

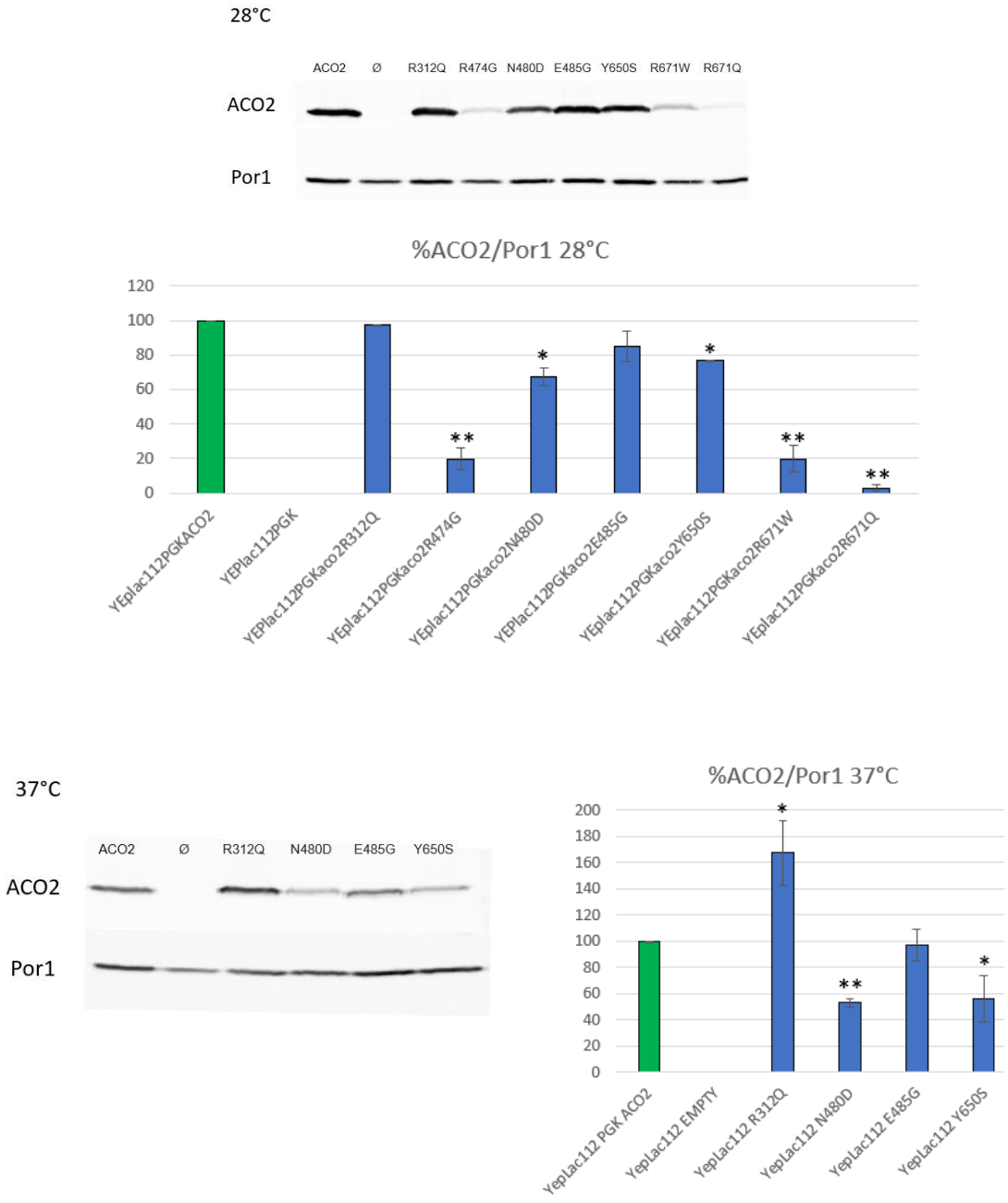

Figure 4.6: Western blot performed at 28 and 37 °C on *ACO2* wild type, null and mutant strains, and related quantification graphs using Por1 as housekeeping to quantify the ACO2 content. Values are represented as the mean of at least three values ± SD. P values are obtained using one-way analysis of variance followed by Bonferroni's test, *P<0.05; **P<0.01

The western blot quantification analysis highlights at 28°C a strong reduction in the steady state levels of the ACO2 protein in strains carrying the severe mutations (R474G, R671W and R671Q), suggesting a correlation between oxidative defect and the low mutant protein content. The other severe mutation (N480D) at 28°C displays a significant reduction in aconitase levels, but not severe enough to explain the consistent defect seen in the previous analysis. In this case, the reduced content of the mutated protein carrying the N480D mutation seems to be just one of the contributing causes to the severe defect, assuming the existence of other mechanisms that contribute to the pathological phenotype. In fact, even if the protein is present, it may not be able to catalyze the reaction due to the mutation in the enzymatic pocket of ACO2. However, the level of the N480D mutated protein is lower compared to that of the mutants able to grow on media with non-fermentable carbon sources, hypothesizing the existence of a possible critical protein content threshold, below which oxidative growth is completely abolished. Regarding the Y650S mutation, a perfect parallelism between ACO2 stability and mitochondrial defect is observed; in fact, in both analyses, slight defects are detected at 28°C, which became more marked in heat-stress conditions at 37°C. Interestingly, the thermosensitive R312Q mutation leads to a significant increase in ACO2 levels at 37°C. In this case, this increased in mutated protein content could be due to an attempt to compensate the presence of a defective protein. Furthermore, it is possible to hypothesize that the observed thermosensitive defect could be related to deficient protein turnover mechanisms, in which the balance between produced and degraded proteins is affected. Mitochondrial aconitase is considered as a metastable polypeptide, since its heat sensitivity could be attributed to its complex structural composition, containing an iron/sulfur cluster as large prosthetic group (Wilkening et al 2018). The increase in ACO2 levels in the presence of the R312Q mutation could also be due to a stabilizing effect of this substitution on the Fe-S centers present in the protein. Also in this analysis, the strain containing the E485G mutation behaved in the same manner as the *ACO2* wild type strain both at 28 and 37°C, making it difficult to justify the pathological phenotype associated with this mutation. Since ACO2 is a pivotal protein in mitochondrial processes, its activity is strictly required both for the stability of mitochondrial DNA and for the Krebs cycle. The evaluation of the ability to convert the citrate into isocitrate is a fundamental step in the mutation validation process. For this purpose, an enzymatic assay was performed to quantify the catalytic ability of the mitochondrial aconitase in the wild type or mutated strains. Cells were inoculated in 0.5% glucose-supplemented YP medium and grown for 18 hours at 28 and 37°C. Subsequently, 10^9 cells (100 OD) were collected

to carry out mitochondrial protein extraction. The spectrophotometric assay was performed on mitochondrial extracts derived from wild type and mutant strains to evaluate the aconitase activity through a coupled assay, in which the aconitase activity is assessed based on the reduction of $NADP^+$ to NADPH, promoted by isocitrate dehydrogenase, the enzyme that catalyzes the reaction immediately downstream the aconitase reaction in Krebs cycle. In fact, the NADPH reduction can be followed spectrophotometrically as it presents a particular absorption spectrum in the reduced form, with a specific peak at 340 nm, absent in the oxidized forms. Therefore, the absorption at 340 nm is proportional to the aconitase enzymatic activity. The results of this analysis are shown in figure 4.7.

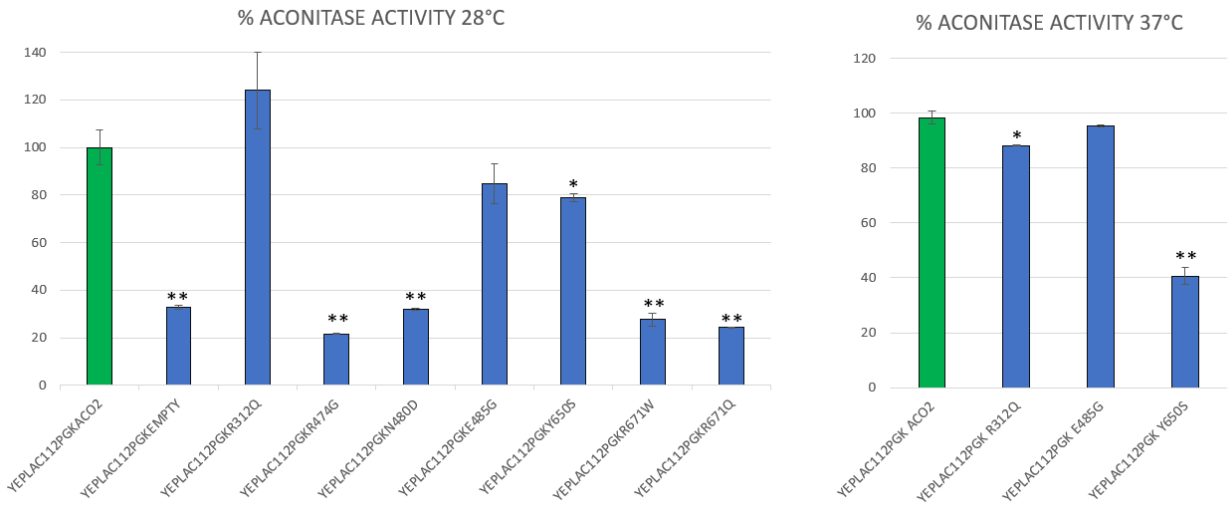

Figure 4.7: Enzymatic activity at 28 and 37°C of the W03-1B *aco1Δ* strain transformed with wild type and mutant alleles, and empty plasmid as a negative control. Values are represented as the mean of at least three values ± SD. p-values are obtained using one-way analysis of variance followed by Bonferroni's test, *P<0.05; **P<0.01.

This kind of analysis is more accurate than those carried out so far, since allows identifying the specific defect of the mutated enzyme and therefore highlighting small differences which could be lost in other analyses. An interesting detail to note, is the residual aconitase activity of about 30% in the *ACO1* deleted strain, probably due to the yeast cytoplasmic isoform *ACO2* which, even if with low affinity, could catalyze the citrate reduction. The results obtained show a positive correlation between the defects observed in OXPHOS metabolism and the activity of human aconitase in yeast

models. The mutations associated with a more severe phenotype possessed a behavior similar to the null mutant, leading to a total loss of function of the aconitase activity. The thermosensitive mutations R312Q and Y650S at 37°C show a slight and moderate enzymatic activity defect, respectively. It is necessary to note that the enzyme carrying the Y650S mutation in this analysis exhibited an enzymatic defect even at the physiological temperature of 28°C, probably for the greater sensitivity of this analysis. However, regarding the E485G mutation, it is not possible to establish a correlation between the observed oxidative defect and the activity of the mutated protein, since the latter is comparable to that of the wild type strain. The information obtained in this analysis allows hypothesizing that HON phenotype in *ACO2*-related patients is correlated with a defect, with several degrees of severity, of the mitochondrial aconitase activity for all the mutations studied, except for E485G in which the etiology is still uncertain. For almost all the analyzed mutations it is possible to establish a correlation between the enzymatic activity of the mutated protein and its steady state level, analyzed by western blot. The only exception concerns the severe mutation N480D, which exhibit an almost total abatement of the aconitase activity, but significant retention of the ACO2 content, approximately 50%. In this case, the mutation may not destabilize the structure of the protein but decrease the ability to convert the citrate into the isocitrate, maybe due to a loss of the interaction with the substrate. The analyses carried out so far allow explaining, partially in some cases, the pathological mechanism of the mutations studied in *ACO2*. Another important role of ACO2 in the mitochondrion is connected to its mtDNA stabilizing function, through the binding of the single-strand DNA during the mitochondrial replication. For these reasons, *ACO2* mutations could have effects on both the catalytic activity and the stability of mtDNA. To evaluate this hypothesis, a protocol for the relative quantification of mtDNA, using real-time PCR, was developed. The underlying idea in this experiment is that while in a haploid yeast strain the genes encoded by the nucleus are present in a single copy, those encoded by mtDNA are strictly dependent on its copy number, which varies greatly depending on the condition. Based on this consideration, the mutant, null and wild type strains were subjected to a total DNA extraction protocol, followed by a real-time PCR reaction, detecting the presence of the nuclear-encoded gene *ACT1* as a reference and the mitochondrial gene *COX1*, using the specific primer pairs qACT1-Fw / qACT1-Rv and qCOX1-Fw / qCOX1-Rv. Comparing the *COX1*/*ACT1* ratio in the various strains analyzed, it is possible to obtain the relative quantification of mtDNA. The experimental growth condition for the DNA extraction was finely tuned, depending on the strains ability to use non-fermentable carbon sources. In fact, the proficient respiratory strains, containing the mild

mutations, were pre-inoculated in a medium supplemented with 2% ethanol. This growth condition is necessary to counter-select the growth of *petite* colonies, since the presence of repeated sequences in *rho*$^{-}$ clones could alter the results. On the other hand, the respiratory deficient strains, containing severe mutations, were pre-inoculated in a medium containing glucose 2%, to allow their growth. All strains were then inoculated in the same condition, medium supplemented with 0.5% glucose, and incubated for 18 hours. At the end of the growth, total DNA extraction was carried out, and the results of the mtDNA quantification are shown in figure 4.8.

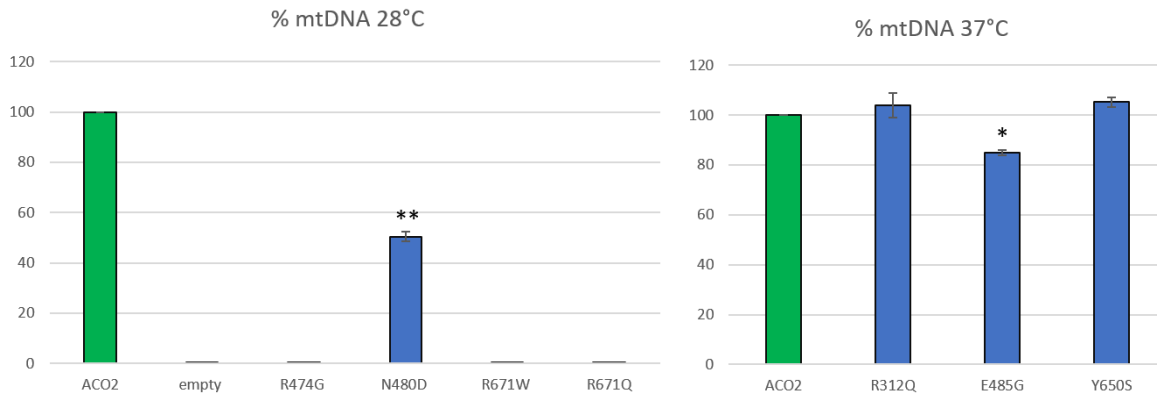

Figure 4.8: mtDNA content in wild type, mutated and deleted strains at 28 and 37°C. Values are represented as the mean of at least three values ± SD. P values are obtained using one-way analysis of variance followed by Bonferroni's test, *P<0.05; **P<0.01

The results obtained show that at 28°C the strains carrying severe mutations, except N480D, presented a total loss of the mitochondrial gene *COX1*, assuming a total loss of mtDNA. Interestingly, the N480D severe mutation is associated with partial maintenance of mtDNA. Combining the various findings obtained in this thesis, the N480D mutation is that with a severe phenotype that presents partial retention of the protein in the western blot analysis. Therefore, the stabilizing function may be not associated with the ability to convert citrate into isocitrate, since the enzymatic activity is almost abolished in this mutant, but seems probably to correlate with the amount of protein present in mitochondria and its ability to bind the DNA. Another interesting finding emerged in this analysis. The E485G thermosensitive mutation, associated only with a small defect in oxidative growth, exhibits a small but significant decrease in mtDNA levels at 37°C which could be

the cause of the pathological phenotype in the patient. The other mild mutations analyzed, on the other hand, does not show defects related to the stability of mtDNA, assuming that catalytic defects in patients, carrying these mutations, are the major cause of the disease. The yeast strain containing the R312Q mutation shows no defects in mtDNA stability, hypothesizing that other factors, such as the enzyme deficiency, are the main cause of the pathological phenotype in patient.

4.4 INHERITANCE ANALYSIS IN *ACO2* MUTANT YEAST STRAINS

Mutations identified in the *ACO2* gene, like those of *SDHA*, are heterozygous and therefore allegedly dominant in patients. The effect of the simultaneous presence, in *ACO1* null yeast strain, of the wild type gene in combination with the mutated allele (*ACO2*/*aco2**) was evaluated. To analyze the inheritance of these mutations in yeast, heteroallelic strains were constructed using the following method. Starting from the plasmid YepLac112*PGKACO2*, used for the haploid mutant preparations, the ORF of *ACO2* and the *PGK* promoter were subcloned into YepLac181 multicopy vector (*LEU2* marker) using the restriction enzymes *Hind*III and *Sac*I. To avoid the irreversible loss of mtDNA due to the absence of aconitase, the plasmid thus constructed (YepLac181*PGKACO2*) was used to transform the previously prepared W303-1B *aco1*Δ strains containing the pFL38*ACO1* and YepLac112*PGKACO2** (wild type and mutant alleles) or YepLac112*PGK* plasmids. Strains transiently containing 3 plasmids were then subjected to plasmid shuffling on a medium supplemented with 5-FOA to induce loss of pFL38*ACO1*. After two cycles of plasmid loss, the following strains were selected on SC without tryptophan (YEpLac112 plasmid selection) and Leucine (YEpLac181 plasmid selection).

W303-1B *aco1Δ* YepLac181*PGK ACO2*

YEplac112*PGKACO2*
YEplac112*PGK*
YEPlac112*PGKACO2*^{R312Q}
YEplac112*PGKACO2*^{R474G}
YEplac112*PGKACO2*^{N480D}
YEPlac112*PGKACO2*^{E485G}
YEplac112*PGKACO2*^{Y650S}
YEplac112*PGKACO2*^{R671W}
YEPlac112*PGKACO2*^{R671Q}

To investigate the inheritance of these alleles in yeast, the oxidative growth of the above-mentioned strains was evaluated on non-fermentable carbon sources at 28 and 37°C. The results of this analysis are shown in figure 4.9.

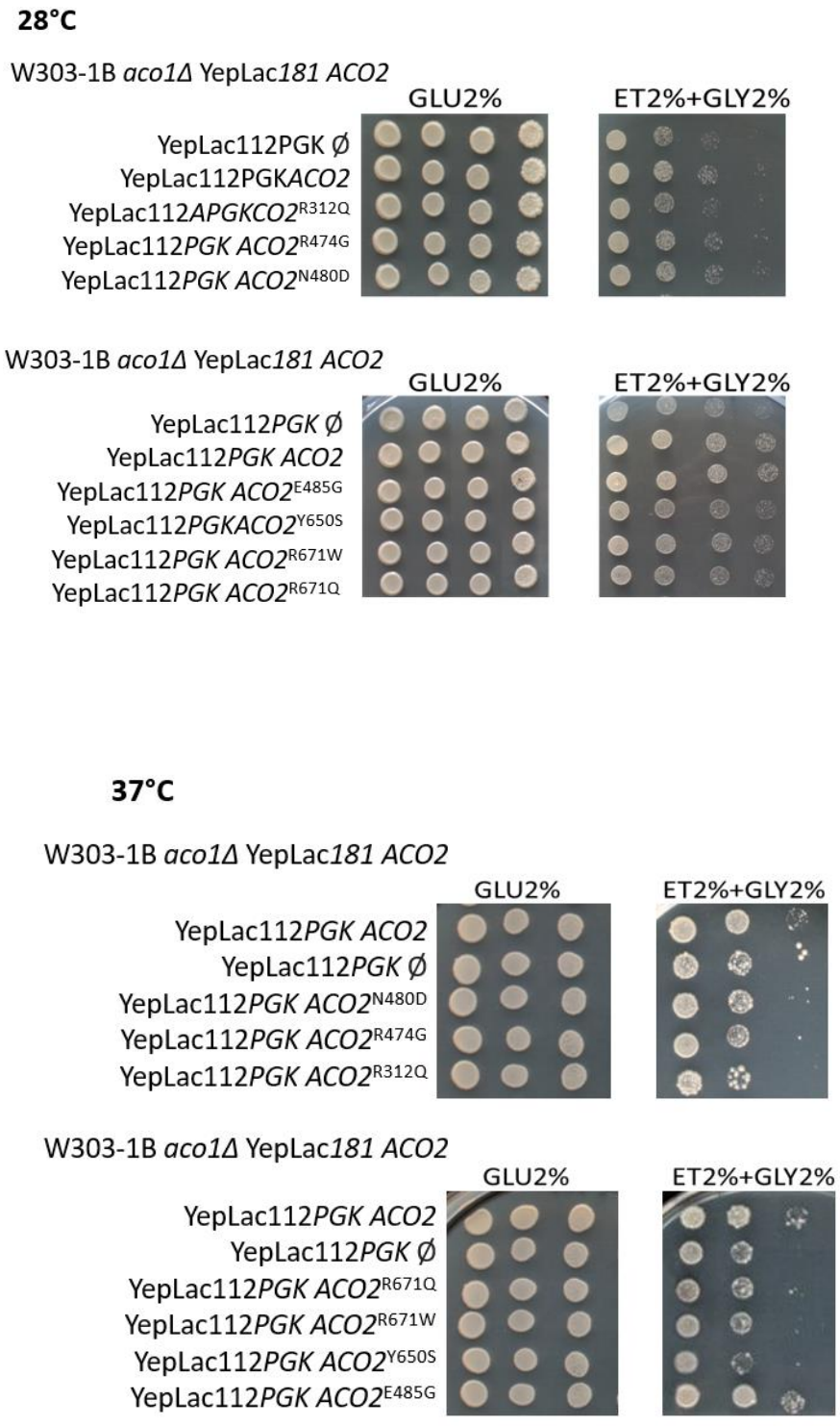

Figure 4.9: Oxidative growth of diploid strains containing wild type and mutated *ACO2* alleles at 28 and 37°C on non-fermentable carbon sources

From the analysis of the oxidative growth of heteroallelic strains, it is difficult to draw clear conclusions, even if it allows making hypotheses that can be confirmed with other analyses. Analyzing the behavior of these mutants on medium added with 2% glycerol and ethanol, a temperature-dependent effect is identified, with defects that became more severe with the increase of the temperature. Comparing the growth of the strain containing two copies of *ACO2* (homoallelic) with that containing only one gene (hemiallelic), a difference in growth is observed, hypothesizing a haploinsufficiency mechanism in which a single copy of *ACO2* is not able to restore the wild type growth phenotype at the maximum level. Since the *ACO2* gene is under the control of a strong promoter (PGK) in a plasmid multicopy context, identification of haploinsufficiency may appear uncommon. However, it has also been shown in this thesis that a high amount of protein is required to have a good degree of complementation, guaranteed by the expression system used. Analyzing the growth of heteroallelic strains carrying the R474G, N480D, R671W and R671Q mutations, an intermediate growth phenotype between the hemiallelic and homoallelic strains at 28°C was observed, that became more similar to the strain with only one copy of *ACO2* at 37°C, hypothesizing a possible dominance mechanism caused by haploinsufficiency. On the contrary, the R312Q and Y650S mutations exhibit a growth similar to the hemiallelic strain at 28°C, while at 37°C a negative effect of the mutant allele against the wild type is highlighted, hypothesizing a pathogenetic mechanism based on the negative dominant effect of these mutations. Regarding the E485G mutation, no growth differences are shown both at 28 and 37°C compared to the wild type homoallelic strain, assuming a recessive inheritance mechanism in yeast. However, a qualitative test such as the spot assay must be confirmed with other analyses, to better clarify the inheritance associated with these mutations. Since the mitochondrial aconitase acts indirectly in respiration, participating in the Krebs cycle and stabilization of mtDNA, analyses on the respiratory rate of these mutants were performed. To evaluate this hypothesis, the oxygen consumption rate analyses, which allow a quantification of the defects of the OXPHOS metabolism, were performed in heteroallelic strains. The experimental conditions replied those used for the assessment of the respiratory activity in haploid strains. The results obtained are shown in figure 4.10.

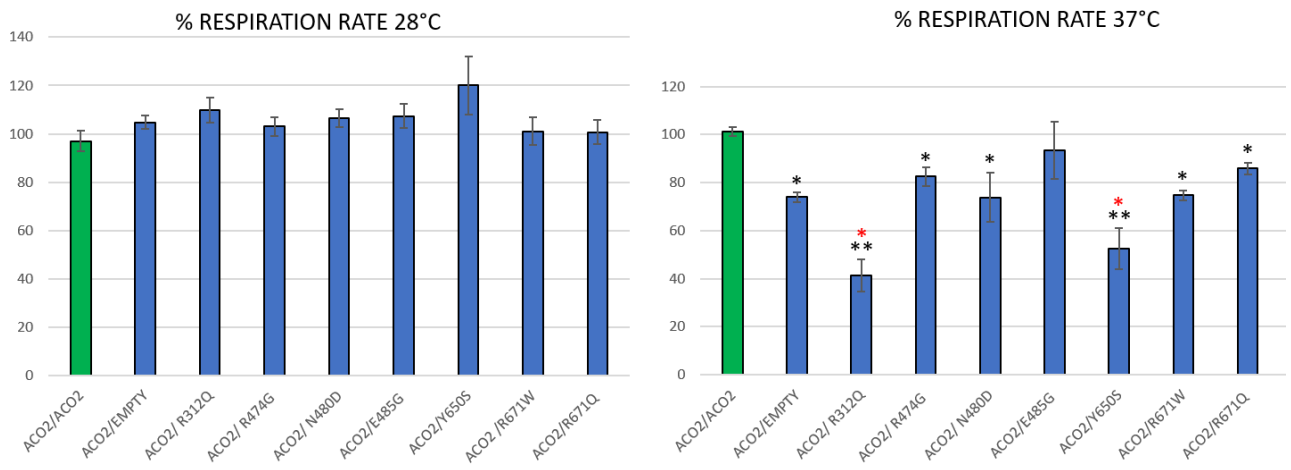

Figure 4.10 Figure 4.8: Oxygen consumption of *ACO2* heteroallelic strains at 28 and 37°C. The green bar indicates the wild type strain (positive control). Values are represented as the mean of at least three values ± SD. P values are obtained using one-way analysis of variance followed by Bonferroni's test. Black asterisks indicate the comparison with the homoallelic strain (*ACO2*/*ACO2*), while the red asterisks indicate the comparison with the hemiallelic strain (*ACO2* / empty), *P<0.05; **P<0.01

The analysis of this data at 28°C showed that the mutation does not influence the respiratory rate, since all the mutant strains exhibit similar respiration rate values compared to the homoallelic strain. Thus, the haploinsufficiency effect seen in oxidative growth is not detected in this analysis, indicating that this condition is not useful to evaluate the inheritance mechanisms in these strains. The same analysis was repeated at 37°C, to evaluate alleged thermosensitive defects. In fact, in this heat-stress condition, a different respiratory rate between the hemiallelic and homoallelic strains is observed, and therefore phenotypes associated with haploinsufficiency can be detected. Looking at the mutant phenotypes, good parallelism is highlighted concerning the hypotheses made in the previous analysis. The respiratory rate at 37°C of the mutant strains containing the R312Q and Y650S mutations showed a dominant profile attributable to a negative dominance mechanism, since the respiratory activity of these strains is significantly lower compared to that of the hemiallelic strain. The mutations R474G, N480D, R671W and R671Q, on the other hand, show similar behavior to the hemiallelic strain with a significant decrease in oxygen consumption rate compared to the homoallelic strain, confirming the haploinsufficiency. The E485G mutation presents a respiratory rate comparable to that of the homoallelic strain, obtaining a further confirmation of the recessivity

in yeast. To evaluate whether the decreased oxygen consumption rate is associated with a deficiency in the enzymatic aconitase activity in the heteroallelic strains, the enzymatic ability of the mutated aconitase to convert citrate into isocitrate was analyzed. Experimentally, the strains were inoculated in a selective medium, to maintain the plasmids, supplemented with 0,5% glucose and cells were grown for 18 hours at 28 and 37°C. Subsequently, the protocol of mitochondrial proteins extraction through mechanical break was carried out, to obtain the extracts used to evaluate the aconitase activity in the mutant heteroallelic strains. The results are shown in figure 4.11.

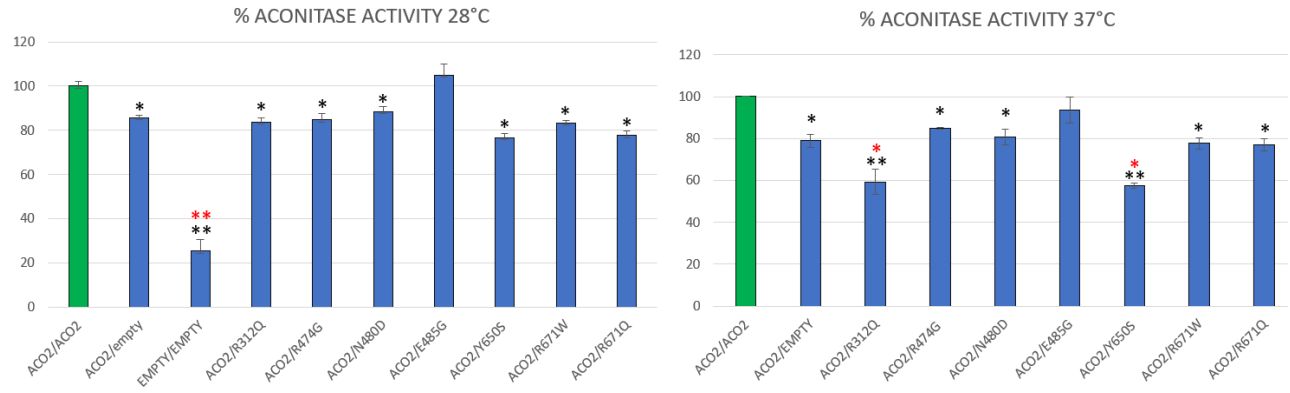

Figure 4.11: Enzymatic activity at 28 and 37°C of the *ACO2* heteroallelic strains. The green bar indicates the wild type strain (positive control). Values are represented as the mean of at least three values ± SD. P values are obtained using one-way analysis of variance followed by Bonferroni's test. Black asterisks indicate the comparison with the homoallelic strain (*ACO2/ACO2*), while the red asterisks indicate the comparison with the hemiallelic strain (*ACO2*/ empty), *P<0.05; **P<0.01

This analysis provided more accurate details compared to that of the respiratory rate and oxidative growth. In this more accurate analysis, also at 28°C, the phenotypes described above are confirmed. In fact, this analysis allows identifying the primary effect of the mutation directly in the enzyme function, without the interference of other factors which could mask the phenotype. The enzymatic activities of wild type and mutated proteins analysis lead to a further confirmation of the results obtained above. These experiments, performed at 28 and 37°C, confirm the dominance of all mutations, except R485G. At 37 °C the simultaneous presence of the thermosensitive R312Q or Y650S mutations in combination with the wild type *ACO2* allele lead to a minor aconitase activity compared to the hemiallelic strain, associating the dominance seen in patients with a dominance

negative mechanism. However, these mutations at 28 °C show a mild mild defect, probably masked by the temperature. The other mutations, except E485G, in combination with the wild type allele, lead to a defect in enzyme activity similar to that of the hemiallelic strain at both 28 and 37 °C, associating the presence of these mutations in patients, with a mechanism of haploinsufficiency. The mutation E485G shows recessive heredity in the yeast model, behaving like the homoallelic strain, contrasting the patient outcome. The discrepancy observed between human and yeast data, as described for the L367P mutation in *SDH1*, could be caused by the presence of another undetected mutation. However, the intrinsic factor of the *ACO2* yeast model, must be also considered. In fact, the heteroallelic strains were engineered to simultaneously overexpress the wild type and mutated *ACO2* copy, a condition that could mask the effect of mild mutations, such as E485G. On the other hand, since there is no concordance between the dominance in the patient and the yeast phenotype, this substitution may not be the direct cause of the disease in human. Except for the discrepancy identified for the E485G variant, yeast once again proved to be an excellent model for the validation of mutations associated with OXPHOS defects, and for the identification of genetic-molecular mechanisms underlying the disease in patients.

4.5 DISCUSSION

This part of the thesis concerns the study of seven mutations identified in the *ACO2* gene, encoding the mitochondrial aconitase, using the *S. cerevisiae* model. Adopting a heterologous complementation approach, due to the ability of the human *ACO2* gene to complement the absence of the *ACO1* ortholog, the yeast models were constructed by inserting the pathological allele identified in the patients in a *ACO1* deleted strain. This allowed the evaluation of several defects associated with mitochondrial activity, as shown in figure 4.12, which could lead to the pathological phenotype in patients.

MUTATION	OXIDATIVE GROWTH	RESPIRATION	ACO2 STABILITY	ACO2 ACTIVITY	INHERITANCE	INHERITANCE MECCHANISM
R312Q	DECREASED	DECREASED	INCREASED	DECREASED	DOMINANT	NEGATIVE DOMINANCE
R474G	STRONG DECREASE	STRONG DECREASE	STRONG DECREASE	STRONG DECREASE	DOMINANT	HAPLOINSUFFICIENCY
N480D	STRONG DECREASE	STRONG DECREASE	DECREASED	STRONG DECREASE	DOMINANT	HAPLOINSUFFICIENCY
E485G	DECRESEAD	NO DEFECT	NO DEFECT	NO DEFECT	RECESSIVE?	----------
Y650S	DECRESEAD	DECREASED	DECREASED	DECREASED	DOMINANT	NEGATIVE DOMINANCE
R671W	STRONG DECREASE	STRONG DECREASE	STRONG DECREASE	STRONG DECREASE	DOMINANT	HAPLOINSUFFICIENCY
R671Q	STRONG DECREASE	STRONG DECREASE	STRONG DECREASE	STRONG DECREASE	DOMINANT	HAPLOINSUFFICIENCY

4.12: Schematic representation of the results obtained in *ACO2* mutant strains

To validate the pathological effect of the mutations, defects associated with OXPHOS metabolism were evaluated, analyzing oxidative growth on non-fermentable carbon sources and respiratory activities. The analysis carried out shows perfect parallelism in the behavior of the mutants in the two different processes evaluated. In fact, the analyses allow dividing the mutations into two subclasses, based on the observed phenotype. Of the seven mutations studied, four are associated with a severe phenotype (R474G, N480D, R671W and R671Q), since a total inability to use non-fermentable carbon sources and consistent respiratory defects are observed, and three mutations (R312Q, E485G and Y650S), associated with a thermosensitive moderate mitochondrial deficit. Aconitase is a key enzyme of the Krebs cycle, a process underlying the mitochondrial energy mechanisms. Therefore, the impairment of this enzyme could lead to the block of the cycle, reducing both the intermediates and the molecules used as substrates for oxidative phosphorylation,

explaining the negative effect also on respiration. Subsequent molecular analyzes, using enzymatic assays designed to specifically evaluate the aconitic activity, clarified that the various phenotypes observed among the seven mutations in analyses are due to a different catalytic capacity of the mutated enzyme. The severe mutations show an almost total loss of function of the aconitase enzyme, while mild mutations are associated with thermosensitive moderate enzymatic defects. For all mutations, it is possible to observe a cause-effect relationship between a respiratory defect and enzymatic deficit, except for the E485G mutation that presented a behavior similar to the control. Modeling analysis highlights that the mutations characterized by a severe phenotype lie in the enzymatic pocket of the enzyme and some of these (arginine 474 and 671) interact directly with the citrate, the substrate of the aconitase reaction, explaining the drastic reduction of the enzymatic activity. On the contrary, the mild mutations all clustered in surface residues, with probable structural function, compatible with the observed thermosensitive phenotype. Since aconitase also is pivotal for the maintenance of mtDNA, the quantity of mtDNA in the various strains containing the mutations was evaluated through real-time PCR. This analysis demonstrated that total loss of mtDNA is observed in all severe mutations, except N480D. In the presence of the N480D mutation, a residual mtDNA stability is maintained, assuming a stabilization mechanism independent of the enzymatic capacity. In fact, the severe mutations with a high degree of mtDNA instability also presented an almost total reduction of the Aco2 protein levels present in the mitochondrion, while the partial maintenance of mtDNA in the strain carrying the N480D mutation is associated with a non-total loss of the mutant protein, which although catalytically inactive leads to a partial stabilizing effect. Furthermore, this analysis allows correlating the slight defect in the oxidative growth of the strain bearing the E485G mutation with a small but significant reduction in the mtDNA stability. The mutations under analysis were detected in patients in a heterozygous, therefore dominant, condition. Yeast allowed the investigation of the mechanisms associated with the inheritance of these mutations, through the evaluation of defects in oxidative phosphorylation and enzymatic assays in heteroallelic strains, carrying the wild type *ACO2* allele in compound with the mutated allele. These analyses confirmed the dominance of all mutations except E485G, which is associated with a recessive inheritance in yeast. In particular, the R312Q and Y650S mutations showed a negative dominance, in which the mutated allele negatively affected the wild type allele function. The underlying mechanism of inheritance in the other dominant mutations is haploinsufficiency. Regarding the E485G mutation, no concordance between yeast and humans is observed, since the mutation is dominant in humans and seems to be recessive in yeast. This

difference could be explained by the presence of a second undetected mutation that could contribute to the patient pathological phenotype. However, it could also be due to the simultaneous overexpression of the wild type and mutated alleles which could mask the effect of a mild mutation such as E485G. Despite this, the constructed models allowed obtaining useful information on the dominance mechanisms associated with all the other mutations, proving to be a powerful tool not only for the validation of mutations but also for the identification of the pathogenetic mechanisms associated with them.

CHAPTER 5: CONCLUSIONS

This thesis concerned the study of new variants identified in patients with HON diseases, exploiting the model organism *S. cerevisiae*. The results obtained allow associating, to each mutation identified, a series of phenotypic defects that could be the cause of the disease in humans. All variants in the *SDHA*, *MECR*, *MTFMT* and *ACO2* genes modeled in yeast are associated with defects in OXPHOS metabolism, thus confirming mitochondrial dysfunctionality. Furthermore, the molecular analysis highlighted the mechanisms underlying the pathology. Using *in vitro* enzymatic assays, the pathological phenotype observed in *SDHA* and *ACO2* patients, is clearly associated with the protein enzyme deficiency for most mutations. For the mutations identified in the *MECR* and *MTFMT* genes, on the other hand, yeast was used to evaluate secondary defects due to alterations in these proteins. Specifically, the main effect associated with the *MECR* mutation was due to the defective production of lipoic acid with a consequent negative effect on the lipoylated enzymes that take part in the Krebs cycle. As concern *MTFMT*, this thesis set up the conditions for the validation of the pathological effect of mutations in this gene. From the analysis carried out, it was possible to associate the patient phenotype with a defect in the mitochondrial protein synthesis. The dominance of the mutations in the *SDHA* and *ACO2* genes, in most cases, was in agreement with the yeast models results (except for the L367P and E485G mutations), confirming the great ability of this organism to mimic the patient pathological context. It was possible to establish the mechanism underlying the inheritance of the disease, that yeast has demonstrated to be associated with negative dominance or haploinsufficiency. Considering these results, most mutations are validated as the specific cause of the disease in patients. Another relevant result described in this thesis was the possible therapeutic approach proposed for the patient with the recessive mutation in *MECR* gene through the administration of lipoic acid, in order to decrease the higth oxidative stress level associated to the R258W mutation.

CHAPTER 6:

MATERIAL AND METHODS

6.1 STRAINS USED

All *S. cerevisiae* strains used in this work are listed below:

STRAIN	GENOTYPE	REFERENCE
W303-1B	*Matα, ade2-1, leu2-3, ura3-1, trp1-1, his3-11, can1-100*	(Thomas and Rothstein 1989)
BY4741 *sdh1Δ*	*Mata his3Δ1 leu2Δ0 met15Δ0 ura3Δ0 sdh1::kanMX4*	Euroscarf collection; (Brachmann et al. 1998)
BY4741 *etr1Δ*	*Mata his3Δ1 leu2Δ0 met15Δ0 ura3Δ0 sdh1::kanMX4*	Euroscarf collection; (Brachmann et al. 1998)
BY4741 *fmt1Δ*	*Mata his3Δ1 leu2Δ0 met15Δ0 ura3Δ0 sdh1::kanMX4*	Euroscarf collection; (Brachmann et al. 1998)
BY4741 *aco1Δ*	*Mata his3Δ1 leu2Δ0 met15Δ0 ura3Δ0 aco1::kanMX4*	Euroscarf collection; (Brachmann et al. 1998)
W303-1B *sdh1Δ*	*Matα, ade2-1, leu2-3, ura3-1, trp1-1, his3-11, sdh1::kanMX4*	This work
W303-1B *sdh1Δ* pFL38 $SDH1^{L367P}$	*Matα, ade2-1, leu2-3, ura3-1, trp1-1, his3-11, sdh1::kanMX4*	This work
W303-1B *sdh1Δ* pFL38 $SDH1^{R444C}$	*Matα, ade2-1, leu2-3, ura3-1, trp1-1, his3-11, sdh1::kanMX4*	This work
W303-1B *sdh1Δ* pFL38 $SDH1^{R593Q}$	*Matα, ade2-1, leu2-3, ura3-1, trp1-1, his3-11, sdh1::kanMX4*	This work
W303-1B *fmt1Δ*	*Matα, ade2-1, leu2-3, ura3-1, trp1-1, his3-11, fmt1::kanMX4*	This work
W303-1B *fmt1Δ pFL38 FMT1*	*Matα, ade2-1, leu2-3, ura3-1, trp1-1, his3-11, fmt1::kanMX4*	This work
W303-1B *fmt1Δ* pFl39*TET*off *MTFMT*	*Matα, ade2-1, leu2-3, ura3-1, trp1-1, his3-11, fmt1::kanMX4*	This work

W303-1B *fmt1Δ* pFl39*TET*off *MTFMTT*^{173I}	*Matα, ade2-1, leu2-3, ura3-1, trp1-1, his3-11, fmt1::kanMX4*	This work
W303-1B *fmt1Δ* YepLac112*TET*off *MTFMT*	*Matα, ade2-1, leu2-3, ura3-1, trp1-1, his3-11, fmt1::kanMX4*	This work
W303-1B *etr1Δ*	*Matα, ade2-1, leu2-3, ura3-1, trp1-1, his3-11, etr1::kanMX4*	This work
W303-1B *etr1Δ* pFL38 *ETR1*	*Matα, ade2-1, leu2-3, ura3-1, trp1-1, his3-11, etr1::kanMX4*	This work
W303-1B *etr1Δ* pFL39*TET*off *MECR*	*Matα, ade2-1, leu2-3, ura3-1, trp1-1, his3-11, etr1::kanMX4*	This work
W303-1B *etr1Δ* YepLac112*TET*off *MECR*	*Matα, ade2-1, leu2-3, ura3-1, trp1-1, his3-11, etr1::kanMX4*	This work
W303-1B *etr1Δ* YepLac112*TET*off *MECR*^{R258W}	*Matα, ade2-1, leu2-3, ura3-1, trp1-1, his3-11, etr1::kanMX4*	This work
W303-1B *aco1Δ pFL*38 *ACO1*	*Matα, ade2-1, leu2-3, ura3-1, trp1-1, his3-11, aco1::kanMX4*	This work
W303-1B *aco1Δ* YepLac112*TET*off *ACO2*	*Matα, ade2-1, leu2-3, ura3-1, trp1-1, his3-11, aco1::kanMX4*	This work
W303-1B *aco1Δ* YepLac112*PGK ACO2*	*Matα, ade2-1, leu2-3, ura3-1, trp1-1, his3-11, aco1::kanMX4*	This work
W303-1B *aco1Δ* YepLac112*PGK ACO2*^{R312Q}	*Matα, ade2-1, leu2-3, ura3-1, trp1-1, his3-11, aco1::kanMX4*	This work
W303-1B *aco1Δ* YepLac112*PGK ACO2*^{R474G}	*Matα, ade2-1, leu2-3, ura3-1, trp1-1, his3-11, aco1::kanMX4*	This work
W303-1B *aco1Δ* YepLac112*PGK ACO2*^{N480D}	*Matα, ade2-1, leu2-3, ura3-1, trp1-1, his3-11, aco1::kanMX4*	This work
W303-1B *aco1Δ* YepLac112*PGK ACO2*^{E485G}	*Matα, ade2-1, leu2-3, ura3-1, trp1-1, his3-11, aco1::kanMX4*	This work
W303-1B *aco1Δ* YepLac112*PGK ACO2*^{Y650S}	*Matα, ade2-1, leu2-3, ura3-1, trp1-1, his3-11, aco1::kanMX4*	This work
W303-1B *aco1Δ* YepLac112*PGK ACO2*^{R671W}	*Matα, ade2-1, leu2-3, ura3-1, trp1-1, his3-11, aco1::kanMX4*	This work
W303-1B *aco1Δ* YepLac112*PGK ACO2*^{R671Q}	*Matα, ade2-1, leu2-3, ura3-1, trp1-1, his3-11, aco1::kanMX4*	This work

W303-1B *aco1Δ* YepLac181*PGK ACO2*	*Matα, ade2-1, leu2-3, ura3-1, trp1-1, his3-11, aco1::kanMX4*	This work
W303-1B YepLac*195 SDH1*	*Matα, ade2-1, leu2-3, ura3-1, trp1-1, his3-11, can1-100*	This work
W303-1B YepLac*195 SDH1*^{L367P}	*Matα, ade2-1, leu2-3, ura3-1, trp1-1, his3-11, can1-100*	This work
W303-1B YepLac*195 SDH1*^{R444C}	*Matα, ade2-1, leu2-3, ura3-1, trp1-1, his3-11, can1-100*	This work
W303-1B YepLac*195 SDH1*^{R593N}	*Matα, ade2-1, leu2-3, ura3-1, trp1-1, his3-11, can1-100*	This work
W303-14A	*Mata ade2-1 leu2-3 ura3-1 trp1-1 his3-11 can1-100*	Our laboratory
W303-14A sdh1*Δ*	*Mata, ade2-1, leu2-3, ura3-1, trp1-1, his3-11, sdh1::kanMX4*	This work
W303-14A sdh1*Δ* pFL39*SDH*1	*Mata, ade2-1, leu2-3, ura3-1, trp1-1, his3-11, sdh1::kanMX4*	This work
W303-1B *aco1Δ* YepLac181*PGK ACO2 /* YepLac112*PGK ACO2*	*Matα, ade2-1, leu2-3, ura3-1, trp1-1, his3-11, aco1::kanMX4*	This work
W303-1B *aco1Δ* YepLac181*PGK ACO2 /* YepLac112*PGK*	*Matα, ade2-1, leu2-3, ura3-1, trp1-1, his3-11, aco1::kanMX4*	This work
W303-1B *aco1Δ* YepLac181*PGK ACO2 /* YepLac112*PGK ACO2*^{R312Q}	*Matα, ade2-1, leu2-3, ura3-1, trp1-1, his3-11, aco1::kanMX4*	This work
W303-1B *aco1Δ* YepLac181*PGK ACO2 /* YepLac112*PGK ACO2*^{R474G}	*Matα, ade2-1, leu2-3, ura3-1, trp1-1, his3-11, aco1::kanMX4*	This work
W303-1B *aco1Δ* YepLac181*PGK ACO2 /* YepLac112*PGK ACO2*^{N480D}	*Matα, ade2-1, leu2-3, ura3-1, trp1-1, his3-11, aco1::kanMX4*	This work
W303-1B *aco1Δ* YepLac181*PGK ACO2 /* YepLac112*PGK ACO2*^{E485G}	*Matα, ade2-1, leu2-3, ura3-1, trp1-1, his3-11, aco1::kanMX4*	This work
W303-1B *aco1Δ* YepLac181*PGK ACO2 /* YepLac112*PGK ACO2*^{Y650S}	*Matα, ade2-1, leu2-3, ura3-1, trp1-1, his3-11, aco1::kanMX4*	This work
W303-1B *aco1Δ* YepLac181*PGK ACO2 /* YepLac112*PGK ACO2*^{R671W}	*Matα, ade2-1, leu2-3, ura3-1, trp1-1, his3-11, aco1::kanMX4*	This work
W303-1B *aco1Δ* YepLac181*PGK ACO2 /* YepLac112*PGK ACO2*^{R671Q}	*Matα, ade2-1, leu2-3, ura3-1, trp1-1, his3-11, aco1::kanMX4*	This work

W303-14B *sdh1Δ pFL39 SDH1* x W303-1B *sdh1Δ pFL38 SDH1* (2n)	*Mata/Matα, ade2-1/ade2-1, leu2- 3/leu2-3, ura3-1/ura3-1, trp1- 1/trp1-1, his3-11/his3-11, can1- 100/can1-100 sdh1::KanMX4/sdh1::KanMX4*	This work
W303-14B *sdh1Δ pFL39 SDH1* x W303-1B *sdh1Δ pFL38* (2n)	*Mata/Matα, ade2-1/ade2-1, leu2- 3/leu2-3, ura3-1/ura3-1, trp1- 1/trp1-1, his3-11/his3-11, can1- 100/can1-100 sdh1::KanMX4/sdh1::KanMX4*	This work
W303-14B *sdh1Δ pFL39 SDH1* x W303-1B *sdh1Δ pFL38 SDH1L^{367P}*(2n)	*Mata/Matα, ade2-1/ade2-1, leu2- 3/leu2-3, ura3-1/ura3-1, trp1- 1/trp1-1, his3-11/his3-11, can1- 100/can1-100 sdh1::KanMX4/sdh1::KanMX4*	This work
W303-14B *sdh1Δ pFL39 SDH1* x W303-1B *sdh1Δ pFL38 SDH1^{R444C}*(2n)	*Mata/Matα, ade2-1/ade2-1, leu2- 3/leu2-3, ura3-1/ura3-1, trp1- 1/trp1-1, his3-11/his3-11 ,can1- 100/can1-100 sdh1::KanMX4/sdh1::KanMX4*	This work
W303-14B *sdh1Δ pFL39 SDH1* x W303-1B *sdh1Δ pFL38 SDH1^{R593N}* (2n)	*Mata/Matα, ade2-1/ade2-1, leu2- 3/leu2-3, ura3-1/ura3-1, trp1- 1/trp1-1, his3-11/his3-11, can1- 100/can1-100 sdh1::KanMX4/sdh1::KanMX4*	This work

The bacteria strain used in this work is listed below**:**

STRAIN	GENOTYPE
DH10B	*F-mcrA Δ(mrr-hsdRMS-mcrBC) φ80d DlacZ ΔM15 ΔlacX74 deoR recA1 endA1 araD139 Δ(ara, leu)7697 galU galKλ-rpsL hupG*

6.2 Plasmids

PLASMID	MARKER	TYPE	REFERENCE	FIGURE
pFL39	*TRP1*	CENTROMERIC	(Bonneaud et al. 1991)	6.1(A)
pFL39*TEToff*	*TRP1*	CENTROMERIC	(Nolli et al. 2015)	6.1(A) *
pFL38	*URA3*	CENTROMERIC	(Bonneaud et al. 1991)	6.1(B)
YepLac112*PGK*	*TRP1*	EPISOMAL	(Cappuccio et al. 2021)	6.1(C) *
YepLac112*TET*off	*TRP1*	EPISOMAL	(Nolli et al. 2015)	6.1(C) *
YepLac181*PGK*	*LEU3*	EPISOMAL	Our laboratory	6.1(D) *
YepLac195*PGK*	*URA3*	EPISOMAL	(Gietz and Sugino 1988)	6.1(E) *

* no maps are available for these plasmids, the figure shows the vector backbone used for the insertion of the *PGK* or *TET*off promoter.

The plasmids containing the *PGK* and *TEToff* promoters were previously prepared in our laboratory, subcloning the promoters from the pFL61 and PCM189 plasmids respectively plasmids. Specifically, *PGK* promote subcloning was performed by digestion with *Bgl*II and *Bam*HI, while the *TET*off promoter was subcloned exploiting the *Hind*III and *Eco*RI restriction sites.

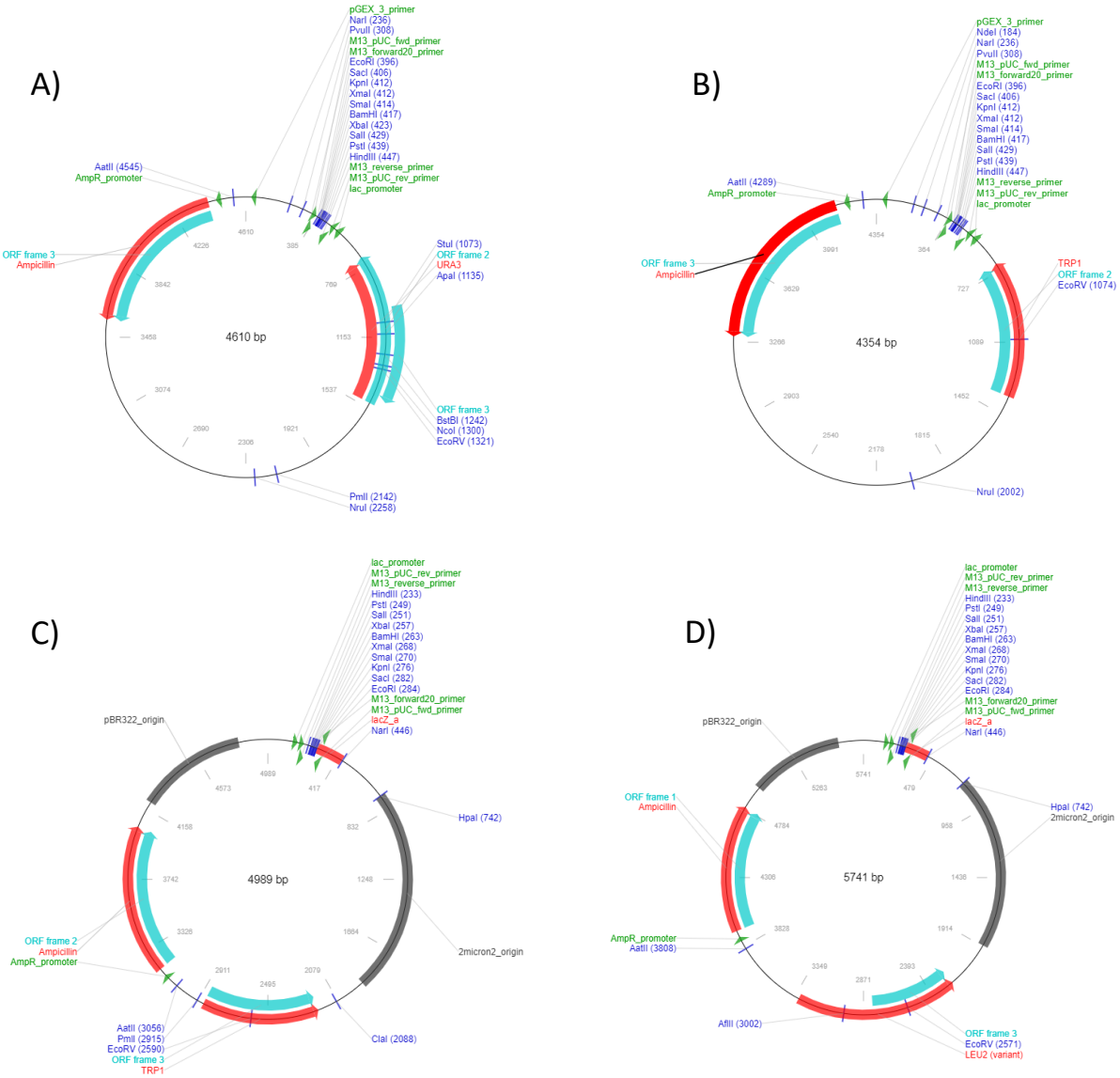

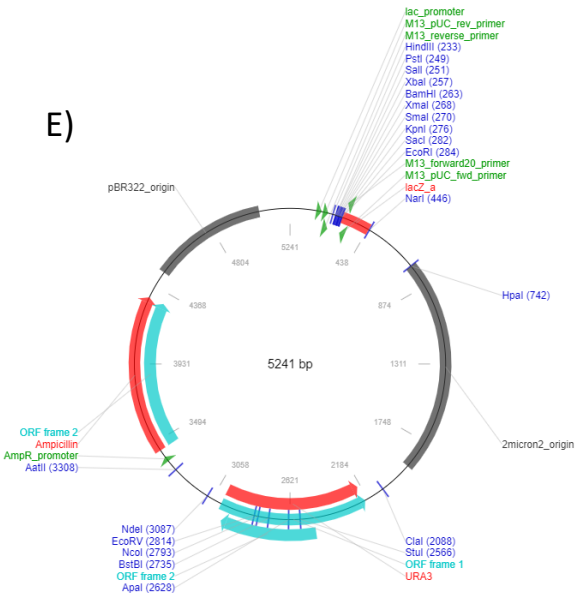

Figure 6.1: A) pFL38; B) pFL39; The plasmids (C)YepLac112; D) YepLac181; E) YepLac195) were used as templates for subcloning the *PGK* and *TET*off promoters

6.3 MEDIUM AND GROWTH CONDITION

List and composition of media used for yeast growth:

- YP (1% peptone, 0.5% yeast extract)
- YPA (2% peptone, 1% yeast extract, 75mg/ml adenine)
- SD (1.9 g/l YNB w/o aminoacids w/o NH4SO4ForMedium™, 5 g/l NH4SO4).

  Minimum media was enriched with drop-out powder (Kaiser et al. 1994) to obtain SC medium.
- 5-FOA SD: YNB with 1 g/l 5-Fluoroorotic Acid (ForMedium™), 50 mg/l

  uracil with amino acids necessary to complement the auxotrophies

  (Boeke, LaCroute, and Fink 1984)).

Singles amino acids, if it is necessary, could be omitted from complete drop-out to maintain the plasmids selective pressure. For the solidification 2% agar (ForMedium™) was added. Fermentable or non-fermentable carbon sources were added at a final concentration of 2%, if not specified differently. The sources used were Glucose (D), Galactose (Gal) Ethanol (E), Glycerol (G), Lactate (L).

S. cerevisiae was cultured at 28˚C and 120 rpm constant shaking in liquid media. To induce heat stress, cultures were incubated at 37˚C in thermostat.

E. coli LB media used :1% bacto tryptone , 0.5% yeast extract Formedium™, 0.5% NaCl, pH 7.2-7.5. 2% Agar and 100 µg/ml ampicillin (Formedium™) were added if necessary. To allow α-complementation selection, 80µl 2% of 5-bromo-4-chloro-3-indolyl-b-Dgalactopyranoside (Xgal) (dissolved in dimethilformamide) and 40µl 23.8 mg/ml isopropyl-betaD-thiogalactopyranoside (IPTG) were added. Cultures were incubated at 37˚C under shaking.

6.4 POLYMERASE CHAIN REACTION (PCR)

Manufacturer indications were followed to perform PCR reactions. Two types of DNA polymerase were utilized, GoTaq® DNA polymerase (Promega) for analytical purposes, and KOD Hot Start HiFi DNA polymerase (Novagen®) for preparative PCR, a more accurate enzyme used to introduce site-specific mutations or for the gene amplification in the cloning process. All the reactions were performed using "Applied Biosystem 2720 Thermal Cycler".

6.4.1 Overlap PCR

The overlap PCR technique was used to construct the *SDH1* mutant strains (Ho et al., 1989). The first part of the protocol consists in amplifying two contiguous portions of the *SDH1* gene, with an overlap zone, in which the mutation to introduce lies. The reactions were performed using the plasmid pFL38*SDH1* as a template, with the following pairs of primer:

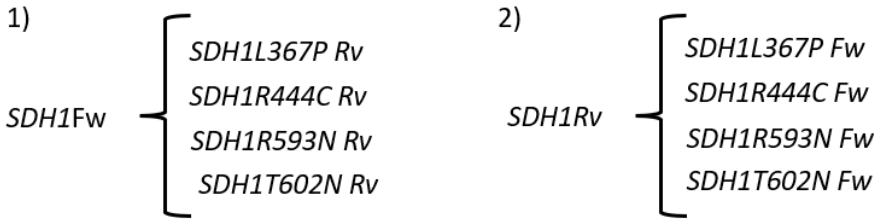

The subsequent reaction leads to the formation of the complete fragment bearing the mutation of interest. In fact, a mixture of the amplicons produced during the first two reactions, corresponding to the specific mutations, was used as a template. The first 10 reaction cycles were performed without primers, to allow the 3'OH ends recognition by polymerase, synthesizing the missing part of the *SDH1* gene. At the end of the 10th cycle, the external primers SDH1Fw and SDH1Rv were added to each reaction to amplify the *SDH1* fragment carrying the mutation. The amplification conditions of the extension phase (10 cycles without primers) and of the subsequent elongation phase (after adding the external primers) were reported below.

Extension phase

- 2' at 95°C

10 cycles:

- 20'' at 95°C
- 30'' at 60°C
- 1'10''/Kb at 70°C

Elongation phase

25 cycles:

- 20'' at 95°C
- 18'' at 54°C
- 1'10''/Kb at 70°C
- 3' at 70°C
- ∞ at 10°C

6.4.2 Quick change PCR

This site-specific mutagenesis technique was used for the introduction of mutations in the *ACO2*, *MTFMT* and *MECR* genes. DNA used as a template normally was a vector containing the gene of interest, isolated from a methylating microorganism (dam+); the two primers utilized in this reaction are oligonucleotides, containing the substitution to introduce in the wild type gene, complementary to the vector region: these primers, once annealed to the template, were extended by KOD DNA polymerase, until the amplification of the entire plasmid was done. Annealing and extension of the mutagenic primers lead to the obtaining of a large amount of mutant plasmid. The PCR reaction details are reported below:

- 2’ at 95°C
- 18 cycles:
    - 30’’ at 95°C
    - 50’’ at annealing temperature
    - 45’’/Kb at 68°C
- 5’ at 68°C
- ∞ at 10°C

At the end of the reaction, three types of plasmids were present:

- Parental plasmids: containing both parental strands (without mutation)
- Mixed plasmids: consisting of a newly synthesized strand (containing the mutation) and a wild type parental strand
- Mutated plasmids: containing the mutation on both strands.

In order to obtain only the latter, it was necessary to carry out digestion using the enzyme *Dpn*I. This enzyme recognized the 5'-Gm^{6}ATC-3' sequence and was able to digest methylated and hemi-methylated DNA. Since the template of the reaction was derived from a methylating *E. coli* (dam+) and the amplification reaction was carried out *in vitro*, without enzymes able to methylate the DNA, after the *DpnI* treatment only the mutated plasmid should be obtained. After digestion, the mix containing the plasmid of interest was precipitated overnight through sodium acetate and ethanol at -20 °C. Subsequently the mix, after wash steps with ethanol, was utilized to transform *E. coli,* which allows amplifying the mutant plasmid of interest.

6.4.3 Real-time PCR

The real time PCR protocol was used for mtDNA quantification in *ACO2* mutant strains. The template of the reaction was the total DNA, extracted through a commercial high-efficiency kit (VWR International) of the wild type and mutant strains standardized at the concentration of 5ng/μl. This method involved the specific amplification of the nuclear gene *ACT1* and the mitochondrial *COX1* gene using the primers reported in table 5.1. The volumes used for each reaction were shown below:

REAGENT	VOLUME
Platinum® SYBR® Green	7,5 µl
Primer forward 3 µM	0,6 µl
Primer revers 3µM	0,6 µl
Template 5ng/µl	3 µl
H_2O	3,3 µl

The Real Time instrument used was the QuantStudio 3 with its QuantStudio 3 Design and Analysis Software 1.0.1. The amplification phases were shown below

1 cycle:

- 2’ at 50°C
- 6‘ at 95°C

40 cycles:

- 15’’ at 95°C
- 1’ at 60°C

1 cycle:

- 15’’ at 95°C
- 15’’ at 60°C

For each strain the mtDNA content was calculated using the comparative quantification method - ΔΔCt. After the amplification reaction, the Ct value corresponding to the number of cycles needed to reach a fluorescence threshold was recorded, which was used for the subsequent comparison between the various samples. To determine the difference in mtDNA content the following method was used:

ΔCt:

· ΔCt (wild type) = Ct(COX1) – Ct(ACT1)

· ΔCt (mutant) = Ct (COX1)– Ct(ACT1)

ΔΔCt = ΔCt (mutant) – ΔCt (wild type)

Fold change= $2^{-\Delta\Delta Ct}$

6.5 PRIMERS

PRIMER NAME	SEQUENCE 5'-3'	USE
SDH1DFW	CAGGCATCCTCGACTCTAAC	*SDH1* DELETION
SDH1DRV	GCCATATGACTTTCTCCTGC	*SDH1* DELETION
SDH1FW	CCGGAGCTCCCAACCCTTTTACTATCTCTCG	*SDH1* CLONING
SDH1RV	CCCGTCGACGCACCCTTGTACAGCAATTCG	*SDH1* CLONING
SDH1L367PFW	CCATCTACCTCCGGAAGTTCCTAAGGAAAGATTGCCAGGTATC	*SDH1* MUTAGENESIS
SDH1L367PRV	GATACCTGGCAATCTTTCCTTAGGAACTTCCGGAGGTAGATGG	*SDH1* MUTAGENESIS
SDH1R444CFW	GTTTCTGTCCATGGTGCCAACTGCCTAGGTGCCAATTCCTTGTTG	*SDH1* MUTAGENESIS
SDH1R444CRV	CAACAAGGAATTGGCACCTAGGCAGTTGGCACCATGGACAGAAAC	*SDH1* MUTAGENESIS
SDH1R593QFW	CAAGAGAGGATTATCCAAATCAAGATGACGAACATTGGATGAAGC	*SDH1* MUTAGENESIS
SDH1R593QRV	GCTTCATCCAATGTTCGTCATCTTGATTTGGATAATCCTCTCTTG	*SDH1* MUTAGENESIS
SDH1T602NFW	CGAACATTGGATGAAGCATAACTTATCCTGGCAAAAGGACG	*SDH1* MUTAGENESIS
SDH1T602NRV	CGTCCTTTTGCCAGGATAAGTTATGCTTCATCCAATGTTCG	*SDH1* MUTAGENESIS
ETR1DFw	CCTTAAAAGAGTGGTTCTCC	*ETR1* DELETION
ETR1DRv	CTCCTACAAAGATAGCACTGG	*ETR1* DELETION
FMT1DFw	CCTGCTATTATGGAGAGGAG	*FMT1* DELETION
FMT1DRv	CACTCTGTTATGAACTACAAGC	*FMT1* DELETION
ETR1CBamFw	GGCCGGGATCCGATAGATTAAGAGAGAAGGCTCG	*ETR1* CLONING
ETR1CPstRv	GCGCACTGCAGCCATTCTCAGGAAAAATTGC	*ETR1* CLONING
FMT1CBamFw	GGCCCGGATCCCATGCTCAGCCCATAGAACG	*FMT1* CLONING
FMT1CPstRv	GCGCCCTGCAGCACTCTGTTATGAACTACAAGC	*FMT1* CLONING
MTFMTCNOTFW	CATGTAGCGGCCGCATGAGGGTGTTGGTGCG	*MTFMT* CLONING
MTFMTCNOTRV	CATCAAGCGGCCGCCTTCTTCCTAACTACTCAATGC	*MTFMT* CLONING
MECRCNOTFW	CATGTAGCGGCCGCACACAATGTGGGTCTGCAGTACCCTG	*MECR* CLONING
MECRCNOTRV	CATGAAGCGGCCGCGGATGATCACATGGTGAGAATCTGC	*MECR* CLONING
MECRR258WFw	GGACATGCCCCAGCCATGGCTTGCTCTCAACTGTGTTGGTG	*MECR* MUTAGENESIS
MECRR258WRv	CACCAACACAGTTGAGAGCAAGCCATGGCTGGGGCATGTCC	*MECR* MUTAGENESIS
MTFMTT173IFw	GGAGACACAGTTACTGGAGTGATCATTATGCAAATTAGACC	*MTFMT* MUTAGENESIS
MTFMTT173IRv	GGTCTAATTTGCATAATGATCACTCCAGTAACTGTGTCTCC	*MTFMT* MUTAGENESIS
ACO1FwBamHI	GCGCGGATCCGAAATCGGCAAAGGTCCTGAC	*ACO1* CLONING

ACO1RvHindIII	GCGCAAGCTTTTGACTTCTCCAGCCGAACG	*ACO1* CLONING
hACO2NotIFw	CCTGTTAACATCGATAGCGGCCGCAC	*ACO2* CLONING
hACO2NotIRv	GCCCTAGCGGCCGCGAATTCACTAGTGATTG	*ACO2* CLONING
hACO2R312QFw	GTACCTGAGCAAGACCGGGCAGGAAGACATTGCCAATCTAGCTG	*ACO2* MUTAGENESIS
hACO2R312QRv	CAGCTAGATTGGCAATGTCTTCCTGCCCGGTCTTGCTCAGGTAC	*ACO2* MUTAGENESIS
hACO2N480DFw	CAACAGGAACTTCACGGGTCGCGACGACGCAAACCCCGAG	*ACO2* MUTAGENESIS
hACO2N480DRv	CTCGGGGTTTGCGTCGTCGCGACCCGTGAAGTTCCTGTTG	*ACO2* MUTAGENESIS
hACO2E485GFw	GCAACGACGCAAACCCCGGGACCCATGCCTTTGTCACGTCC	*ACO2* MUTAGENESIS
hACO2E485GRv	GGACGTGACAAAGGCATGGGTCCCGGGGTTTGCGTCGTTGC	*ACO2* MUTAGENESIS
hACO2R474GFw	CAATCGTCACCTCGTACAACGGGAACTTCACGGGCCGCAAC	*ACO2* MUTAGENESIS
hACO2R474GRv	GTTGCGGCCCGTGAAGTTCCCGTTGTACGAGGTGACGATTG	*ACO2* MUTAGENESIS
hACO2Y650SFw	CCTGACACTGCCCGGTACTCCAAGAAACATGGCATCAGGTGG	*ACO2* MUTAGENESIS
hACO2Y650SRv	CCACCTGATGCCATGTTTCTTGGAGTACCGGGCAGTGTCAGG	*ACO2* MUTAGENESIS
hACO2R671WFw	GAACTACGGCGAGGGCTCAAGCTGGGAGCATGCAGCTCTGG	*ACO2* MUTAGENESIS
hACO2R671WRv	CCAGAGCTGCATGCTCCCAGCTTGAGCCCTCGCCGTAGTTC	*ACO2* MUTAGENESIS
hACO2R671QFw	GAACTACGGCGAGGGCTCAAGCCAGGAGCATGCAGCTCTGG	*ACO2* MUTAGENESIS
hACO2R671QRv	CCAGAGCTGCATGCTCCTGGCTTGAGCCCTCGCCGTAGTTC	*ACO2* MUTAGENESIS
qCOX1-Fw	CTACAGATACAGCATTTCCAAGA	mtDNA CONTENT
qCOX1-Rw	GTGCCTGAATAGATGATAATGGT	mtDNA CONTENT
qACT1-Fw	GTATGTGTAAAGCCGGTTTTG	mtDNA CONTENT
qACT1-Rw	CATGATACCTTGGTGTCTTGG	mtDNA CONTENT

6.6 *S. cerevisiae* TRANSFORMATION

Yeast transformation was performed following the short protocol t described in (Daniel Gietz and Woods 2002). To reach greater efficiency, the long LiAc/SS carrier DNA/PEG method was used This protocol was exploited for gene disruption, regenerating the cells in two ml of YPAD for 2h, before plating them on medium added with 200 µg/ml G418-sulphate.

6.7 ANALYSES IN WHOLE CELL

6.7.1 Spot assay

Spot assay is a classical comparative phenotypic analysis used to test the oxidative growth of different strains in different conditions. 10-fold serial dilutions were prepared starting from $1x10^7$ cells/ml culture, performed three times to the final $1x10^4$ cells/ml suspsension. From each dilution,

5 µl were spotted on agar plates and then incubated for several days at 28°C, the yeast growth physiological temperature, or 37°C to induce a heat-stress.

6.7.2. Oxygen consumption rate

To measure the respiratory activity, strains were pre-grown in a medium supplemented with 2% glucose. Cells were inoculated at the optimized concentration, depending on the strains type, in a medium supplemented with 0.5% glucose to induce oxidative metabolism after fermentation and grown for 18 h. The evaluation of oxygen consumption rate was performed on whole cells at 30°C using a Clark-type oxygen electrode (Oxygraph System Hansatech Instruments England) after the total exhaustion of glucose by adding in the oxigraph chamber 50 µl of concentrated cells, 850 µl of air-saturated respiration buffer (0,1M phthalate-KOH, pH 5,0) and 100 µl 5% glucose. Oxygen consumption rate was expressed as nmol O_2 consumed in one minute for mg of dry cells (nmolO_2/min mg).

6.7.3 Plasmid shuffling

The plasmid shuffling technique was exploited to construct the strains for the validation of *ACO2* gene, to avoid irreversible loss of mitochondrial DNA. Plasmid shuffling was used to promote the loss of plasmids pFL38, containing the *URA3* selection marker. In fact, in the presence of the gene product of the *URA3* gene, 5-FOA was converted into a toxic product that do not permit growth, allowing to counter-select all the cells that possessed a plasmid with *URA3* marker. Experimentally, the cells were cultured in a uracil-supplemented medium, to allow the loss plasmid harboring *URA3* gene. Subsequently, the cells were replica-plated twice on medium containing 5-FOA, allowing the growth only of cells that lost the plasmid (*URA3* marker). After this counterselection phase, cells were recovered in a selective medium for the maintenance of the plasmid of interest, thus ensuring that the strains were unable to grow on medium without uracil.

6.7.4 H_2O_2 sensitivity

Assessment of oxidative stress through H_2O_2 treatment was performed on *MECR* yeast strains. The cells were pre-inoculated in a medium supplemented with 2% glucose for 24h, subsequently were exposed to different concentrations of H_2O_2 for different times (1, 2 and 3 hours). At the end of the treatment, the cells were washed to avoid residual effects of H_2O_2. Different amounts of cells were plated depending on the stimulus administered (1000, 500, 100 cells) and after incubation at 28°C for several days, the unit forming colonies (CFU) were counted to calculate the survival rate. The same protocol was slightly modified for the evaluation of the effects of lipoic acid on oxidative stress. In this case, the cells were pre-cultured for 24h in medium added with 2% glucose and subsequently inoculated in the same medium supplemented with lipoic acid at the different concentrations tested (40 / 4 / 0.4 µg/ml) and incubated at 28°C for 18h. The cells were washed twice with sterile water, to avoid contamination of lipoic acid. Once collected, 10^7cells/ml were inoculated in a medium supplemented with 2% glucose and H_2O_2 at different concentrations and different time intervals. The survival rate was assessed as previously described**.**

6.8 QUANTIFICATION OF PROTEINS WITH BRADFORD METHOD

Protein concentration was determined with the colorimetric Bradford assay (Bradford 1976). The "BioRad Protein Assay" commercial kit was utilized following the manufacturer's instructions. For each quantification, 200 µl of Bradford reagent (an acidified solution of Coomassie G-250 dye) were added to 800 µl of protein solution (or water as reference). After 15' of incubation at room temperature the absorbance was measured at Cary spectrophotometer with λ = 595nm

6.9 ANALYSIS IN MITOCHONDRIA

6.9.1 Preparation of a mitochondrial enriched fraction (Soto et al. 2009)

Cells were pre-inoculated on a medium supplemented with 2% glucose for 24h, then they were inoculated in the same medium containing 0.5% glucose and grown until an OD/ml = 1.5-2 was reached. The following protocol was used:

1. Harvest 100 OD of cells
2. Centrifuge at 4000-5000 rpm for 5 min
3. Wash the pellet in 25 ml of H_2O and centrifugate at 4000-5000 rpm for 3 min
4. Resuspend pellet in 1 ml of H_2O and transfer cells in eppendorf tubes. Spin at 7000 rpm for 30 sec and discard the supernatant.
5. Resuspend pellet in 400µl of sorbitol 0.6M and DTT 5mM and incubate the samples at RT for 10'
6. Centrifuge at 7000 rpm for 30 sec and discard the supernatant
7. Resuspend pellet in 400 µl of sorbitol 1.2M and Tris-HCl 10mM pH 7.5 and zymolyase 6 mg/ml
8. Incubate at 29°C for 10-40 min, until 80-90% of the cells have been converted to spheroplasts.
9. Work on ice. Centrifuge at 5400 g for 8 min at 4°C and discard the supernatant
10. Wash pellet twice with 1 ml of STE solution (sorbitol 0.6M, Tris-HCl 20mM pH 7.5, EDTA 1mM). Centrifuge at 5400 g for 5 min at 4°C.
11. Resuspend the pellet in 100-200 µl STE solution
12. Freeze at -80°C and defrost at RT three times (10 min freeze + 10 min defrost)
13. Determine protein concentration as described in paragraph 5.8

6.9.2 Succinate Dehydrogenase (SQDR) activity

This assay was used to measure the rate of reduction of an artificial electron acceptor the dichlorophenolindophenol (DCPIP), by succinate dehydrogenase complex (Kim and Beattie 1973). Mitochondria were prepared as described in section 5.9.1.

The following reagents are needed:

REAGENT	VOLUME
KH_2PO_4 10mm EDTA 0,5M	780µl
MITOCHONDRIAL EXTRACT	10µl
KCN 80 mM	4,8µl
ATP 50 mM	6,4µl
SUCCINATE 1M	16µl
DCPIP 20 mM	12,8µl
dUQ_2	3,2µl

The specificity of the SDH reaction was evaluated by inserting 10 µl of malonate, the specific inhibitor of the reaction. The extracts were standardized at the final concentration of 4 mg/ml and SDH activity was recorded at 600 nm. SQDR activity was calculated with ε of 22 and the following formula (ΔOD*ε/min mg).

6.9.3 Cytochrome c oxidase (COX) activity (Wharton and Tzagoloff 1967)

Using this assay, the rate of cytochrome c oxidation by complex IV was measured in the *MTFMT* yeast model. Mitochondria were prepared as described in section 5.9.1.
Solutions needed:
- 20mM K-phosphate pH 7.5
- 1% cytochrome c in 20mM K-phosphate pH 7.5
- KFeCN3

Before initiating the reaction, cytochrome C must be reduced using DTT (Dithiothreitol). The color of the solution change when the cytochrome is reduced. Mitochondrial extracts were aliquoted at the final concentration of 2 mg/ml, COX activity was recorded at 550 nm. Specific Activity: COX activity was calculated with ε of 18.5 and the following formula [2.3log (A1/A2)/(ε*min*mg)]*ΔOD.

6.9.4 Aconitase activity (Brown et al. 1998)

Cells were pre-inoculated on medium supplemented with 2% glucose, and after 24h of growth cells were inoculated in the same medium supplemented with 0.5% glucose until an OD/ml = 1-2 was reached. Cell extracts were prepared by resuspending cells in Cell lysis buffer (50 mM Tris HCl pH 8, 50mM KCl, 2mM Sodium Citrate, 10% glycerol, 7mM ß-mercaptoethanol and 1mM PMSF) using the proportion of 1 gr of cells in 2.5 ml of cell lysis buffer, and subsequently subjected to mechanical breakage with glass beads. Cell debris and unbroken cells were separated using low speed centrifugation (2000 x g for 5 min at 4°C), and supernatant was retained. Total protein concentration was determined as described in paragraph 5.8. Aconitase activity was evaluated by the aconitase-isocitrate dehydrogenase coupled assay, in which the NADPH production was monitored at 340 nm, where the oxidized form presented a characteristic peak. Solutions used:

- 240µ REACTION MIX (1M Tris HCl pH 8, 10mM $MgCl_2$, 10mM NADP+ and 0.32U ICDH)
- 16µl of 50mM Sodium citrate
- 48µl whole-cell extract
- H_2O to 800µl

The aconitase activity was recorded on standardized 3 mg/ml whole-cell extract and the specific activity was calculated with ε of 6.22 and the following formula (ΔOD*ε/min mg).

6.10 Western blot

6.10.1 TCA protein extraction

Cells were pre-inoculated for 24h on medium supplemented with 2% glucose and then were inoculated in medium added with 0.5% glucose for 18h. The TCA extraction protocol is reported below:

1. centrifugate the culture 5’ 5000 rpm

2. Harvest the equivalent of 10 OD of cells through centrifugation 1’ 6000-8000 rpm.

3. Wash the pellet with water and resuspend the cells with 75 µl of Rodel mix (NaOH 1.85 M, β-mercaptoethanol 7.5%, PMSF 0.1 M)

4. Add 500 µl of water

5. Add 575 µl of TCA 50%

6. Incubate on ice for 30 minutes. Centrifuge 10’ at 15000 rpm 4°C.

7. Wash the pellet with 1 ml of 0.5M Tris-base without resuspending, spin the tube and remove the supernatant

8. Wash pellet with 1 ml of water without resuspending, spin the tube and remove the supernatant9.
9.Resuspend in 1X Lammli Buffer (Tris-HCl pH 6.8 33.5 mM, 5% glycerol, 5% β-mercaptoethanol, 2% SDS, Bromophenol blue) (150 µl for 10 OD)

10. Add 1-5 µl of Tris-base 0.5M if the color is yellow, until become blu

6.10.2 Protein separation with SDS-page

Protein separation with SDS-page was performed following the Laemmli protocol (Laemmli 1970). Running gels were prepared at 12% polyacrylamide, stacking gels at 6%. Gels were prepared using the following reagents

SOLUTION	RUNNING GEL 12% (TWO GELS)	STACKING GEL 6% (TWO GELS)
Tris HCL 1M pH 8.8	1.876 ml	-
Tris HCL 1M pH 6.8	-	750 µl
Poliacrilamide-bis (37.5-1)	4.5 ml	900 µl
SDS 20%	150 µl	60 µl

APS 10%	50 µl	30 µl
TEMED	12,5 µl	9 µl
H_2O	8,4 ml	4,26 ml

Running Buffer 5X (1L): 15 g Tris-Base, 72 g glycine, H_2O to final volume. Running buffer was used at the final concentration 1X and added with 0.5% SDS. Running was performed for 1h 30'-2h at 100 Volts.

6.10.3 Western Blotting and Ig-detection

The gels containing the separated proteins were transferred to nitrocellulose membranes through electro-blot for 1hr 40' at 2.5-3mA/cm2 in PerfectBlue™ Semi-Dry ElectroBlotter (PeqLab). Transfer buffer, containing 200mM glycine, 25 mM Tris, 20% methanol, was used. After semi-dry protein transfer, membranes were incubated 1hr at room temperature with 5% non-fat dry milk prepared in washing buffer, containing TBS (TBS 10X: TRI-HCL 0,2 M, NaCl 1,37 M pH 7,6) 1%, tween 0.1%, and then incubated o/n with appropriate primary antibody (mono or polyclonal, 5% non-fat dry milk prepared in washing buffer) at 4°C. After the incubation with the antibody, the membranes were washed with 10' 3 times with washing buffer (TBS 1%, tween 0.1%,). The secondary antibodies were prepared in 5% non-fat dry milk dissolved in washing buffer (containing only TBS 1X, without tween). The membranes were incubated 2h at room temperature in dark boxes. To remove the excess of antibody, the membranes were washed three times with washing buffer containing TBS 1x tween 0,05%. Detection of the protein of interest was performed by ChemiDoc MP Imaging, able to detect the fluorophore conjugated with the secondary antibody, using the specific channel of fluorescence. List of primary and secondary antibodies used was reported below.

PRIMARY ANTIBODIES	SECONDARY ANTIBODIES
ANTI-MECR 1: 2000	ANTI-RABBIT 1: 7500
ANTI-MTFMT 1:2000	ANTI-RABBIT 1: 7500
ANTI-Cox2 1:3000	ANTI-MOUSE 1:5000
ANTI-Lipoic Acid 1:2000	ANTI-RABBIT 1: 7500

ANTI-SDHA 1:1000	ANTI-RABBIT 1:7500
ANTI-Por1 1:10000	ANTI MOUSE 1:10000
ANTI-SDHB 1:2000	ANTI-RABBIT 1:7500
ANTI-ACO2 1:2000	ANTI-RABBIT 1:7500

The bands quantification was performed using the ImageLab software (BioRad).

6.11 MITOCHONDRIAL PROTEIN SYNTHESIS

The ability to synthesize mitochondrial proteins in *MTFMT* strains was evaluated using the following protocol. Strains were pre-inoculated in SC-TRP medium supplemented with 2% glucose for 24h, and subsequently the strains were inoculated in the same medium supplemented with 2% galactose and 0.2%glucose. The cells were grown until OD_{600}=0,6-2.

1. Harvest the cell cultures, centrifuge 1' at RT 5000 rpm and discard the supernatant

2. Wash the pellet twice with 1ml of phosphate buffer (400 mM phosphate, 2% galactose), to completely remove the methionine.

3. Resuspend the cells in 1 ml of phosphate buffer and transfer the equivalent of 1.2 OD in a new eppendorf, adding 500 µl water

4. Incubate 3' the cells at 28°C with 10 µl of cycloheximide (8 mg/ml in water)

5. Add 2-5 µl of mix ^{35}S-L-methionine and ^{35}S-L-cysteine purchased by Perkin Elmer (EasyTagTM EXPRE^{35}S^{35}S Protein. Mix Stabilized aqueous solution Shipped ambient. >1000Ci(37.0TBq)/mmo)) and incubate 10' at 28°C

6. Centrifuge 1' 13000 rpm end discard the supernatant

7. Resuspend pellet with 75 µl of Rodel mix (NaOH 1.85 M, β-mercaptoethanol 7.5%, PMSF 0.1 M)

8. Add 500 µl of water and then 575 µl of TCA 50%

9. Chill on ice 30’

10. Centrifuge 10’ 13000 rpm 4°C and discard the supernatant

11. Add 1 ml of Tris-base 0.5 M without resuspending and centrifuge 5’ 13000 rpm 4°C

12. Wash the pellet with 1 ml of water without resuspending, centrifuge 2’ 13000 rpm 4°C

13. Resuspend the pellet in 23 µl of loading buffer (2% SDS; 10%Glycerol; 60 mM Tris-HCl pH 6,8; 2,5% β-mercaptoethanol; bromophenol blue)

The samples were loaded on the polyacrylamide gels (Paragraph 5.9.2). Run was performed at a maximum of 40 mA until the blue reach the bottom. Semidry transfer into nitrocellulose membrane for 90’ at 200mA was then performed. The membranes containing the radioactive mitochondrial proteins were used to impress the autoradiography films.

CHAPTER 7:

REFERENCES

Achilli, Alessandro, Luisa Iommarini, Anna Olivieri, Maria Pala, Baharak Hooshiar Kashani, Pascal Reynier, Chiara La Morgia, et al. 2012. 'Rare Primary Mitochondrial DNA Mutations and Probable Synergistic Variants in Leber's Hereditary Optic Neuropathy'. *PloS One* 7 (8): e42242. https://doi.org/10.1371/journal.pone.0042242.

Ackrell, Brian A.C. 2000. 'Progress in Understanding Structure-Function Relationships in Respiratory Chain Complex II'. *FEBS Letters* 466 (1): 1–5. https://doi.org/10.1016/S0014-5793(99)01749-4.

Aghajanian, Suren, and D. Margaret Worrall. 2002. 'Identification and Characterization of the Gene Encoding the Human Phosphopantetheine Adenylyltransferase and Dephospho-CoA Kinase Bifunctional Enzyme (CoA Synthase)'. *The Biochemical Journal* 365 (Pt 1): 13–18. https://doi.org/10.1042/BJ20020569.

Alston, Charlotte L., James E. Davison, Francesca Meloni, Francois H. van der Westhuizen, Langping He, Hue-Tran Hornig-Do, Andrew C. Peet, et al. 2012. 'Recessive Germline SDHA and SDHB Mutations Causing Leukodystrophy and Isolated Mitochondrial Complex II Deficiency'. *Journal of Medical Genetics* 49 (9): 569–77. https://doi.org/10.1136/jmedgenet-2012-101146.

Amar, Laurence, Karel Pacak, Olivier Steichen, Scott A. Akker, Simon J. B. Aylwin, Eric Baudin, Alexandre Buffet, et al. 2021. 'International Consensus on Initial Screening and Follow-up of Asymptomatic SDHx Mutation Carriers'. *Nature Reviews. Endocrinology* 17 (7): 435–44. https://doi.org/10.1038/s41574-021-00492-3.

Anderson, S., A. T. Bankier, B. G. Barrell, M. H. L. de Bruijn, A. R. Coulson, J. Drouin, I. C. Eperon, et al. 1981. 'Sequence and Organization of the Human Mitochondrial Genome'. *Nature* 290 (5806): 457–65. https://doi.org/10.1038/290457a0.

Artymiuk, Peter J., and Jeffrey Green. 2006. 'The Double Life of Aconitase'. *Structure* 14 (1): 2–4. https://doi.org/10.1016/j.str.2005.12.001.

Astuti, D., F. Latif, A. Dallol, P. L. Dahia, F. Douglas, E. George, F. Sköldberg, E. S. Husebye, C. Eng, and E. R. Maher. 2001. 'Gene Mutations in the Succinate Dehydrogenase Subunit SDHB Cause Susceptibility to Familial Pheochromocytoma and to Familial Paraganglioma'. *American Journal of Human Genetics* 69 (1): 49–54. https://doi.org/10.1086/321282.

Atorino, Luigia, Laura Silvestri, Mirko Koppen, Laura Cassina, Andrea Ballabio, Roberto Marconi, Thomas Langer, and Giorgio Casari. 2003. 'Loss of M-AAA Protease in Mitochondria Causes Complex I Deficiency and Increased Sensitivity to Oxidative Stress in Hereditary Spastic Paraplegia'. *The Journal of Cell Biology* 163 (4): 777–87. https://doi.org/10.1083/jcb.200304112.

Bannon, Amber E., Jason Kent, Isaac Forquer, Ajia Town, Lillian R. Klug, Kelly McCann, Carol Beadling, et al. 2017. 'Biochemical, Molecular, and Clinical Characterization of Succinate Dehydrogenase Subunit A Variants of Unknown Significance'. *Clinical Cancer Research* 23 (21): 6733–43. https://doi.org/10.1158/1078-0432.CCR-17-1397.

Barbet, Fabienne, Sylvie Gerber, Sélim Hakiki, Isabelle Perrault, Sylvain Hanein, Dominique Ducroq, Gaëlle Tanguy, et al. 2003. 'A First Locus for Isolated Autosomal Recessive Optic Atrophy (ROA1) Maps to Chromosome 8q'. *European Journal of Human Genetics: EJHG* 11 (12): 966–71. https://doi.org/10.1038/sj.ejhg.5201070.

Barrientos, Antoni, Karine Gouget, Darryl Horn, Ileana C. Soto, and Flavia Fontanesi. 2009. 'Suppression Mechanisms of COX Assembly Defects in Yeast and Human: Insights into the COX Assembly Process'. *Biochimica et Biophysica Acta (BBA) - Molecular Cell Research* 1793 (1): 97–107. https://doi.org/10.1016/j.bbamcr.2008.05.003.

Baruffini, Enrico, Rita Horvath, Cristina Dallabona, Birgit Czermin, Eleonora Lamantea, Laurence Bindoff, Federica Invernizzi, Iliana Ferrero, Massimo Zeviani, and Tiziana Lodi. 2011. 'Predicting the Contribution of Novel POLG Mutations to Human Disease through Analysis in Yeast Model'. *Mitochondrion* 11 (1): 182–90. https://doi.org/10.1016/j.mito.2010.09.007.

Baruffini, Enrico, Tiziana Lodi, Cristina Dallabona, Andrea Puglisi, Massimo Zeviani, and Iliana Ferrero. 2006. 'Genetic and Chemical Rescue of the Saccharomyces Cerevisiae Phenotype Induced by Mitochondrial DNA Polymerase Mutations Associated with Progressive External Ophthalmoplegia in Humans'. *Human Molecular Genetics* 15 (19): 2846–55. https://doi.org/10.1093/hmg/ddl219.

Baruffini, Enrico, Fausta Serafini, Iliana Ferrero, and Tiziana Lodi. 2012. 'Overexpression of DNA Polymerase Zeta Reduces the Mitochondrial Mutability Caused by Pathological Mutations in DNA Polymerase Gamma in Yeast'. Edited by Janine Santos. *PLoS ONE* 7 (3): e34322. https://doi.org/10.1371/journal.pone.0034322.

Bassett, D. E., M. A. Basrai, C. Connelly, K. M. Hyland, K. Kitagawa, M. L. Mayer, D. M. Morrow, et al. 1996. 'Exploiting the Complete Yeast Genome Sequence'. *Current Opinion in Genetics & Development* 6 (6): 763–66. https://doi.org/10.1016/s0959-437x(96)80033-5.

Basu, Urmimala, Alicia M. Bostwick, Kalyan Das, Kristin E. Dittenhafer-Reed, and Smita S. Patel. 2020. 'Structure, Mechanism, and Regulation of Mitochondrial DNA Transcription Initiation'. *Journal of Biological Chemistry* 295 (52): 18406–25. https://doi.org/10.1074/jbc.REV120.011202.

Baysal, B. E., R. E. Ferrell, J. E. Willett-Brozick, E. C. Lawrence, D. Myssiorek, A. Bosch, A. van der Mey, et al. 2000. 'Mutations in SDHD, a Mitochondrial Complex II Gene, in Hereditary Paraganglioma'. *Science (New York, N.Y.)* 287 (5454): 848–51. https://doi.org/10.1126/science.287.5454.848.

Bereiter-Hahn, J., and M. Vöth. 1994. 'Dynamics of Mitochondria in Living Cells: Shape Changes, Dislocations, Fusion, and Fission of Mitochondria: DYNAMICS OF MITOCHONDRIA'. *Microscopy Research and Technique* 27 (3): 198–219. https://doi.org/10.1002/jemt.1070270303.

Berk, Arnold J., and David A. Clayton. 1974. 'Mechanism of Mitochondrial DNA Replication in Mouse L-Cells: Asynchronous Replication of Strands, Segregation of Circular Daughter Molecules, Aspects of Topology and Turnover of an Initiation Sequence'. *Journal of Molecular Biology* 86 (4): 801–24. https://doi.org/10.1016/0022-2836(74)90355-6.

Birch-Machin, M. A., R. W. Taylor, B. Cochran, B. A. Ackrell, and D. M. Turnbull. 2000. 'Late-Onset Optic Atrophy, Ataxia, and Myopathy Associated with a Mutation of a Complex II Gene'. *Annals of Neurology* 48 (3): 330–35.

Blattner, F. R., G. Plunkett, C. A. Bloch, N. T. Perna, V. Burland, M. Riley, J. Collado-Vides, et al. 1997. 'The Complete Genome Sequence of Escherichia Coli K-12'. *Science (New York, N.Y.)* 277 (5331): 1453–62. https://doi.org/10.1126/science.277.5331.1453.

Boeke, J. D., F. LaCroute, and G. R. Fink. 1984. 'A Positive Selection for Mutants Lacking Orotidine-5'-Phosphate Decarboxylase Activity in Yeast: 5-Fluoro-Orotic Acid Resistance'. *Molecular & General Genetics: MGG* 197 (2): 345–46. https://doi.org/10.1007/BF00330984.

Bonekamp, Nina A., and Nils-Göran Larsson. 2018. 'SnapShot: Mitochondrial Nucleoid'. *Cell* 172 (1–2): 388-388.e1. https://doi.org/10.1016/j.cell.2017.12.039.

Bonneaud, N., O. Ozier-Kalogeropoulos, G. Y. Li, M. Labouesse, L. Minvielle-Sebastia, and F. Lacroute. 1991. 'A Family of Low and High Copy Replicative, Integrative and Single-Stranded S. Cerevisiae/E. Coli Shuttle Vectors'. *Yeast (Chichester, England)* 7 (6): 609–15. https://doi.org/10.1002/yea.320070609.

Botstein, David. 1991. 'Why Yeast?' *Hospital Practice* 26 (10): 157–64. https://doi.org/10.1080/21548331.1991.11705312.

Boubekeur, Samira, Odile Bunoust, Nadine Camougrand, Michel Castroviejo, Michel Rigoulet, and Bernard Guérin. 1999. 'A Mitochondrial Pyruvate Dehydrogenase Bypass in the YeastSaccharomyces Cerevisiae'. *Journal of Biological Chemistry* 274 (30): 21044–48. https://doi.org/10.1074/jbc.274.30.21044.

Brachmann, C. B., A. Davies, G. J. Cost, E. Caputo, J. Li, P. Hieter, and J. D. Boeke. 1998. 'Designer Deletion Strains Derived from Saccharomyces Cerevisiae S288C: A Useful Set of Strains and Plasmids for PCR-Mediated Gene Disruption and Other Applications'. *Yeast (Chichester, England)* 14 (2): 115–32. https://doi.org/10.1002/(SICI)1097-0061(19980130)14:2<115::AID-YEA204>3.0.CO;2-2.

Bradford, M. M. 1976. 'A Rapid and Sensitive Method for the Quantitation of Microgram Quantities of Protein Utilizing the Principle of Protein-Dye Binding'. *Analytical Biochemistry* 72 (May): 248–54. https://doi.org/10.1006/abio.1976.9999.

Brown, N. M., S. A. Anderson, D. W. Steffen, T. B. Carpenter, M. C. Kennedy, W. E. Walden, and R. S. Eisenstein. 1998. 'Novel Role of Phosphorylation in Fe-S Cluster Stability Revealed by Phosphomimetic Mutations at Ser-138 of Iron Regulatory Protein 1'. *Proceedings of the National Academy of Sciences of the United States of America* 95 (26): 15235–40. https://doi.org/10.1073/pnas.95.26.15235.

Burger, Gertraud, Michael W. Gray, and B. Franz Lang. 2003. 'Mitochondrial Genomes: Anything Goes'. *Trends in Genetics: TIG* 19 (12): 709–16. https://doi.org/10.1016/j.tig.2003.10.012.

Burnichon, Nelly, Jean-Jacques Brière, Rossella Libé, Laure Vescovo, Julie Rivière, Frédérique Tissier, Elodie Jouanno, et al. 2010. 'SDHA Is a Tumor Suppressor Gene Causing Paraganglioma'. *Human Molecular Genetics* 19 (15): 3011–20. https://doi.org/10.1093/hmg/ddq206.

Calvo, Sarah E., and Vamsi K. Mootha. 2010. 'The Mitochondrial Proteome and Human Disease'. *Annual Review of Genomics and Human Genetics* 11 (1): 25–44. https://doi.org/10.1146/annurev-genom-082509-141720.

Cappuccio, Gerarda, Camilla Ceccatelli Berti, Enrico Baruffini, Jennifer Sullivan, Vandana Shashi, Tamison Jewett, Tara Stamper, et al. 2021. 'Bi-allelic *KARS1* Pathogenic Variants Affecting Functions of Cytosolic and Mitochondrial Isoforms Are Associated with a Progressive and Multisystem Disease'. *Human Mutation* 42 (6): 745–61. https://doi.org/10.1002/humu.24210.

Carelli, Valerio, Fred N. Ross-Cisneros, and Alfredo A. Sadun. 2004. 'Mitochondrial Dysfunction as a Cause of Optic Neuropathies'. *Progress in Retinal and Eye Research* 23 (1): 53–89. https://doi.org/10.1016/j.preteyeres.2003.10.003.

Castellani, Christina A., Ryan J. Longchamps, Jason A. Sumpter, Charles E. Newcomb, John A. Lane, Megan L. Grove, Jan Bressler, et al. 2020. 'Mitochondrial DNA Copy Number Can Influence Mortality and Cardiovascular Disease via Methylation of Nuclear DNA CpGs'. *Genome Medicine* 12 (1): 84. https://doi.org/10.1186/s13073-020-00778-7.

Ceccatelli Berti, Camilla, Cristina Dallabona, Mirca Lazzaretti, Sabrina Dusi, Elena Tosi, Valeria Tiranti, and Paola Goffrini. 2015. 'Modeling Human Coenzyme A Synthase Mutation in Yeast Reveals Altered Mitochondrial Function, Lipid Content and Iron Metabolism'. *Microbial Cell (Graz, Austria)* 2 (4): 126–35. https://doi.org/10.15698/mic2015.04.196.

Ceccatelli Berti, Camilla, Giulia di Punzio, Cristina Dallabona, Enrico Baruffini, Paola Goffrini, Tiziana Lodi, and Claudia Donnini. 2021. 'The Power of Yeast in Modelling Human Nuclear Mutations Associated with Mitochondrial Diseases'. *Genes* 12 (2): 300. https://doi.org/10.3390/genes12020300.

Cecchini, Gary, Imke Schröder, Robert P Gunsalus, and Elena Maklashina. 2002. 'Succinate Dehydrogenase and Fumarate Reductase from Escherichia Coli'. *Biochimica et Biophysica Acta (BBA) - Bioenergetics* 1553 (1–2): 140–57. https://doi.org/10.1016/S0005-2728(01)00238-9.

Chakraborty, Arka, Sébastien Lyonnais, Federica Battistini, Adam Hospital, Giorgio Medici, Rafel Prohens, Modesto Orozco, Josep Vilardell, and Maria Solà. 2017. 'DNA Structure Directs Positioning of the Mitochondrial Genome Packaging Protein Abf2p'. *Nucleic Acids Research* 45 (2): 951–67. https://doi.org/10.1093/nar/gkw1147.

Charif, Majida, Agathe Roubertie, Sara Salime, Sonia Mamouni, Cyril Goizet, Christian P. Hamel, and Guy Lenaers. 2015. 'A Novel Mutation of AFG3L2 Might Cause Dominant Optic Atrophy in Patients with Mild Intellectual Disability'. *Frontiers in Genetics* 6 (October). https://doi.org/10.3389/fgene.2015.00311.

Chen, Binbin, Jee Loon Foo, Hua Ling, and Matthew Wook Chang. 2020. 'Mechanism-Driven Metabolic Engineering for Bio-Based Production of Free R-Lipoic Acid in Saccharomyces Cerevisiae Mitochondria'. *Frontiers in Bioengineering and Biotechnology* 8 (August): 965. https://doi.org/10.3389/fbioe.2020.00965.

Chen, Peng, Qiu-Gang Ma, Cheng Ji, Jian-Yun Zhang, Li-Hong Zhao, Yong Zhang, and Yong-Ze Jie. 2011. 'Dietary Lipoic Acid Influences Antioxidant Capability and Oxidative Status of Broilers'. *International Journal of Molecular Sciences* 12 (12): 8476–88. https://doi.org/10.3390/ijms12128476.

Chen, X. J., X. Wang, and R. A. Butow. 2007. 'Yeast Aconitase Binds and Provides Metabolically Coupled Protection to Mitochondrial DNA'. *Proceedings of the National Academy of Sciences* 104 (34): 13738–43. https://doi.org/10.1073/pnas.0703078104.

Chen, Xin Jie, Xiaowen Wang, Brett A. Kaufman, and Ronald A. Butow. 2005. 'Aconitase Couples Metabolic Regulation to Mitochondrial DNA Maintenance'. *Science (New York, N.Y.)* 307 (5710): 714–17. https://doi.org/10.1126/science.1106391.

Chen, Zhi-Jun, Regina Pudas, Satyan Sharma, Oliver S. Smart, André H. Juffer, J. Kalervo Hiltunen, Rik K. Wierenga, and Antti M. Haapalainen. 2008. 'Structural Enzymological Studies of 2-Enoyl Thioester Reductase of the Human Mitochondrial FAS II Pathway: New Insights into Its Substrate Recognition Properties'. *Journal of Molecular Biology* 379 (4): 830–44. https://doi.org/10.1016/j.jmb.2008.04.041.

Chien, M.C., W.T. Huang, P.W. Wang, C.W. Liou, T.K. Lin, C.J. Hsieh, and S.W. Weng. 2012. 'Role of Mitochondrial DNA Variants and Copy Number in Diabetic Atherogenesis'. *Genetics and Molecular Research* 11 (3): 3339–48. https://doi.org/10.4238/2012.September.17.4.

Chinnery, P. F., and G. Hudson. 2013. 'Mitochondrial Genetics'. *British Medical Bulletin* 106 (1): 135–59. https://doi.org/10.1093/bmb/ldt017.

Chinnery, Patrick F. 2003. 'Searching for Nuclear-Mitochondrial Genes'. *Trends in Genetics: TIG* 19 (2): 60–62. https://doi.org/10.1016/s0168-9525(02)00030-6.

Claypool, Steven. 2013. 'The Power of Yeast to Model Diseases of the Powerhouse of the Cell'. *Frontiers in Bioscience* 18 (1): 241. https://doi.org/10.2741/4098.

Colby, Geoffrey, Yoshihide Ishii, and Alexander Tzagoloff. 1998. 'Suppression Ofsdh1 Mutations by TheSDH1b Gene OfSaccharomyces Cerevisiae'. *Yeast* 14 (11): 1001–6. https://doi.org/10.1002/(SICI)1097-0061(199808)14:11<1001::AID-YEA304>3.0.CO;2-K.

Contamine, Véronique, and Marguerite Picard. 2000. 'Maintenance and Integrity of the Mitochondrial Genome: A Plethora of Nuclear Genes in the Budding Yeast'. *Microbiology and Molecular Biology Reviews* 64 (2): 281–315. https://doi.org/10.1128/MMBR.64.2.281-315.2000.

Costanzo, M. C., M. E. Crawford, J. E. Hirschman, J. E. Kranz, P. Olsen, L. S. Robertson, M. S. Skrzypek, et al. 2001. 'YPD, PombePD and WormPD: Model Organism Volumes of the BioKnowledge Library, an Integrated Resource for Protein Information'. *Nucleic Acids Research* 29 (1): 75–79. https://doi.org/10.1093/nar/29.1.75.

Courage, Carolina, Christopher B. Jackson, Dagmar Hahn, Liliya Euro, Jean-Marc Nuoffer, Sabina Gallati, and André Schaller. 2017. '*SDHA* Mutation with Dominant Transmission Results in Complex II Deficiency with Ocular, Cardiac, and Neurologic Involvement'. *American Journal of Medical Genetics Part A* 173 (1): 225–30. https://doi.org/10.1002/ajmg.a.37986.

Cruciat, C. M., K. Hell, H. Fölsch, W. Neupert, and R. A. Stuart. 1999. 'Bcs1p, an AAA-Family Member, Is a Chaperone for the Assembly of the Cytochrome Bc(1) Complex'. *The EMBO Journal* 18 (19): 5226–33. https://doi.org/10.1093/emboj/18.19.5226.

Daniel Gietz, R., and Robin A. Woods. 2002. 'Transformation of Yeast by Lithium Acetate/Single-Stranded Carrier DNA/Polyethylene Glycol Method'. In *Methods in Enzymology*, 350:87–96. Elsevier. https://doi.org/10.1016/S0076-6879(02)50957-5.

D'Erchia, Anna Maria, Anna Atlante, Gemma Gadaleta, Giulio Pavesi, Matteo Chiara, Caterina De Virgilio, Caterina Manzari, et al. 2015. 'Tissue-Specific MtDNA Abundance from Exome Data and Its Correlation with Mitochondrial Transcription, Mass and Respiratory Activity'. *Mitochondrion* 20 (January): 13–21. https://doi.org/10.1016/j.mito.2014.10.005.

Di Meo, Ivano, Chiara Cavestro, Silvia Pedretti, Tingting Fu, Simona Ligorio, Antonello Manocchio, Lucrezia Lavermicocca, et al. 2020. 'Neuronal Ablation of CoA Synthase Causes Motor Deficits, Iron Dyshomeostasis, and Mitochondrial Dysfunctions in a CoPAN Mouse Model'. *International Journal of Molecular Sciences* 21 (24): E9707. https://doi.org/10.3390/ijms21249707.

Dimmer, Kai Stefan, Stefan Fritz, Florian Fuchs, Marlies Messerschmitt, Nadja Weinbach, Walter Neupert, and Benedikt Westermann. 2002. 'Genetic Basis of Mitochondrial Function and Morphology in *Saccharomyces Cerevisiae*'. Edited by Randy W. Schekman. *Molecular Biology of the Cell* 13 (3): 847–53. https://doi.org/10.1091/mbc.01-12-0588.

Dusi, Sabrina, Lorella Valletta, Tobias B. Haack, Yugo Tsuchiya, Paola Venco, Sebastiano Pasqualato, Paola Goffrini, et al. 2014. 'Exome Sequence Reveals Mutations in CoA Synthase as a Cause of Neurodegeneration with Brain Iron Accumulation'. *The American Journal of Human Genetics* 94 (1): 11–22. https://doi.org/10.1016/j.ajhg.2013.11.008.

Dziembowski, Andrzej, Jan Piwowarski, Rafal Hoser, Michal Minczuk, Aleksandra Dmochowska, Michel Siep, Hans van der Spek, Les Grivell, and Piotr P. Stepien. 2003. 'The Yeast Mitochondrial Degradosome'. *Journal of Biological Chemistry* 278 (3): 1603–11. https://doi.org/10.1074/jbc.M208287200.

Elliott, Hannah R., David C. Samuels, James A. Eden, Caroline L. Relton, and Patrick F. Chinnery. 2008. 'Pathogenic Mitochondrial DNA Mutations Are Common in the General Population'. *The American Journal of Human Genetics* 83 (2): 254–60. https://doi.org/10.1016/j.ajhg.2008.07.004.

Ellis, Timothy P, Melissa S Schonauer, and Carol L Dieckmann. 2005. '*CBT1* Interacts Genetically With *CBP1* and the Mitochondrially Encoded Cytochrome *b* Gene and Is Required to Stabilize the Mature Cytochrome *b* MRNA of *Saccharomyces Cerevisiae*'. *Genetics* 171 (3): 949–57. https://doi.org/10.1534/genetics.104.036467.

Euro, Liliya, Gregory A. Farnum, Eino Palin, Anu Suomalainen, and Laurie S. Kaguni. 2011. 'Clustering of Alpers Disease Mutations and Catalytic Defects in Biochemical Variants Reveal New Features of Molecular Mechanism of the Human Mitochondrial Replicase, Pol γ'. *Nucleic Acids Research* 39 (21): 9072–84. https://doi.org/10.1093/nar/gkr618.

Falkenberg, Maria. 2018. 'Mitochondrial DNA Replication in Mammalian Cells: Overview of the Pathway'. Edited by Caterina Garone and Michal Minczuk. *Essays in Biochemistry* 62 (3): 287–96. https://doi.org/10.1042/EBC20170100.

Fernandez-Vizarra, Erika, Marianna Bugiani, Paola Goffrini, Franco Carrara, Laura Farina, Elena Procopio, Alice Donati, Graziella Uziel, Iliana Ferrero, and Massimo Zeviani. 2007. 'Impaired Complex III Assembly Associated with BCS1L Gene Mutations in Isolated Mitochondrial Encephalopathy'. *Human Molecular Genetics* 16 (10): 1241–52. https://doi.org/10.1093/hmg/ddm072.

Figuccia, Sonia, Andrea Degiorgi, Camilla Ceccatelli Berti, Enrico Baruffini, Cristina Dallabona, and Paola Goffrini. 2021. 'Mitochondrial Aminoacyl-TRNA Synthetase and Disease: The Yeast Contribution for Functional Analysis of Novel Variants'. *International Journal of Molecular Sciences* 22 (9): 4524. https://doi.org/10.3390/ijms22094524.

Fontanesi, F. 2004. 'Mutations in AAC2, Equivalent to Human AdPEO-Associated ANT1 Mutations, Lead to Defective Oxidative Phosphorylation in Saccharomyces Cerevisiae and Affect Mitochondrial DNA Stability'. *Human Molecular Genetics* 13 (9): 923–34. https://doi.org/10.1093/hmg/ddh108.

Forkink, Marleen, Farhan Basit, José Teixeira, Herman G. Swarts, Werner J.H. Koopman, and Peter H.G.M. Willems. 2015. 'Complex I and Complex III Inhibition Specifically Increase Cytosolic Hydrogen Peroxide Levels without Inducing Oxidative Stress in HEK293 Cells'. *Redox Biology* 6 (December): 607–16. https://doi.org/10.1016/j.redox.2015.09.003.

Foury, Françoise, Tiziana Roganti, Nicolas Lecrenier, and Bénédicte Purnelle. 1998. 'The Complete Sequence of the Mitochondrial Genome of *Saccharomyces Cerevisiae*'. *FEBS Letters* 440 (3): 325–31. https://doi.org/10.1016/S0014-5793(98)01467-7.

Franco, Leticia Veloso Ribeiro, Bruno S. Moda, Maria A. K. M. Soares, and Mario H. Barros. 2019. 'Msc6p Is Required for Mitochondrial Translation Initiation in the Absence of Formylated Met- TRNA ^{fMet}'. *The FEBS Journal* 286 (7): 1407–19. https://doi.org/10.1111/febs.14785.

Frazier, Ann E., David R. Thorburn, and Alison G. Compton. 2019. 'Mitochondrial Energy Generation Disorders: Genes, Mechanisms, and Clues to Pathology'. *Journal of Biological Chemistry* 294 (14): 5386–95. https://doi.org/10.1074/jbc.R117.809194.

Fusté, Javier Miralles, Sjoerd Wanrooij, Elisabeth Jemt, Caroline E. Granycome, Tricia J. Cluett, Yonghong Shi, Neli Atanassova, Ian J. Holt, Claes M. Gustafsson, and Maria Falkenberg. 2010. 'Mitochondrial RNA Polymerase Is Needed for Activation of the Origin of Light-Strand DNA Replication'. *Molecular Cell* 37 (1): 67–78. https://doi.org/10.1016/j.molcel.2009.12.021.

Garrido, Nuria, Lorena Griparic, Eija Jokitalo, Jorma Wartiovaara, Alexander M. van der Bliek, and Johannes N. Spelbrink. 2003. 'Composition and Dynamics of Human Mitochondrial Nucleoids'. Edited by Thomas D. Fox. *Molecular Biology of the Cell* 14 (4): 1583–96. https://doi.org/10.1091/mbc.e02-07-0399.

Ghezzi, Daniele, Paola Goffrini, Graziella Uziel, Rita Horvath, Thomas Klopstock, Hanns Lochmüller, Pio D'Adamo, et al. 2009. 'SDHAF1, Encoding a LYR Complex-II Specific Assembly Factor, Is Mutated in SDH-Defective Infantile Leukoencephalopathy'. *Nature Genetics* 41 (6): 654–56. https://doi.org/10.1038/ng.378.

Gietz, R. D., and A. Sugino. 1988. 'New Yeast-Escherichia Coli Shuttle Vectors Constructed with in Vitro Mutagenized Yeast Genes Lacking Six-Base Pair Restriction Sites'. *Gene* 74 (2): 527–34. https://doi.org/10.1016/0378-1119(88)90185-0.

Giglione, C., A. Serero, M. Pierre, B. Boisson, and T. Meinnel. 2000. 'Identification of Eukaryotic Peptide Deformylases Reveals Universality of N-Terminal Protein Processing Mechanisms'. *The EMBO Journal* 19 (21): 5916–29. https://doi.org/10.1093/emboj/19.21.5916.

Gilea, Alexandru Ionut, Camilla Ceccatelli Berti, Martina Magistrati, Giulia di Punzio, Paola Goffrini, Enrico Baruffini, and Cristina Dallabona. 2021. 'Saccharomyces Cerevisiae as a Tool for Studying Mutations in Nuclear Genes Involved in Diseases Caused by Mitochondrial DNA Instability'. *Genes* 12 (12): 1866. https://doi.org/10.3390/genes12121866.

Gill, Anthony J. 2018. 'Succinate Dehydrogenase (SDH)-Deficient Neoplasia'. *Histopathology* 72 (1): 106–16. https://doi.org/10.1111/his.13277.

Goffeau, A., B. G. Barrell, H. Bussey, R. W. Davis, B. Dujon, H. Feldmann, F. Galibert, et al. 1996. 'Life with 6000 Genes'. *Science (New York, N.Y.)* 274 (5287): 546, 563–67. https://doi.org/10.1126/science.274.5287.546.

Gomkale, Ridhima, Andreas Linden, Piotr Neumann, Alexander Benjamin Schendzielorz, Stefan Stoldt, Olexandr Dybkov, Markus Kilisch, et al. 2021. 'Mapping Protein Interactions in the Active TOM-TIM23 Supercomplex'. *Nature Communications* 12 (1): 5715. https://doi.org/10.1038/s41467-021-26016-1.

Graziewicz, Maria A., Matthew J. Longley, and William C. Copeland. 2006. 'DNA Polymerase γ in Mitochondrial DNA Replication and Repair'. *Chemical Reviews* 106 (2): 383–405. https://doi.org/10.1021/cr040463d.

Green, Douglas R., and John C. Reed. 1998. 'Mitochondria and Apoptosis'. *Science* 281 (5381): 1309–12. https://doi.org/10.1126/science.281.5381.1309.

Gualerzi, C. O., and C. L. Pon. 1990. 'Initiation of MRNA Translation in Prokaryotes'. *Biochemistry* 29 (25): 5881–89. https://doi.org/10.1021/bi00477a001.

Gueguen, V., D. Macherel, M. Jaquinod, R. Douce, and J. Bourguignon. 2000. 'Fatty Acid and Lipoic Acid Biosynthesis in Higher Plant Mitochondria'. *The Journal of Biological Chemistry* 275 (7): 5016–25. https://doi.org/10.1074/jbc.275.7.5016.

Haack, Tobias B., Matteo Gorza, Katharina Danhauser, Johannes A. Mayr, Birgit Haberberger, Thomas Wieland, Laura Kremer, et al. 2014. 'Phenotypic Spectrum of Eleven Patients and Five Novel MTFMT Mutations Identified by Exome Sequencing and Candidate Gene Screening'. *Molecular Genetics and Metabolism* 111 (3): 342–52. https://doi.org/10.1016/j.ymgme.2013.12.010.

Hanein, Sylvain, Isabelle Perrault, Olivier Roche, Sylvie Gerber, Noman Khadom, Marlene Rio, Nathalie Boddaert, et al. 2009. 'TMEM126A, Encoding a Mitochondrial Protein, Is Mutated in Autosomal-Recessive Nonsyndromic Optic Atrophy'. *American Journal of Human Genetics* 84 (4): 493–98. https://doi.org/10.1016/j.ajhg.2009.03.003.

Hao, Huai-Xiang, Oleh Khalimonchuk, Margit Schraders, Noah Dephoure, Jean-Pierre Bayley, Henricus Kunst, Peter Devilee, et al. 2009. '*SDH5* , a Gene Required for Flavination of Succinate Dehydrogenase, Is Mutated in Paraganglioma'. *Science* 325 (5944): 1139–42. https://doi.org/10.1126/science.1175689.

Harbauer, Angelika B., René P. Zahedi, Albert Sickmann, Nikolaus Pfanner, and Chris Meisinger. 2014. 'The Protein Import Machinery of Mitochondria—A Regulatory Hub in Metabolism, Stress, and Disease'. *Cell Metabolism* 19 (3): 357–72. https://doi.org/10.1016/j.cmet.2014.01.010.

Harington, A., C. J. Herbert, B. Tung, G. S. Getz, and P. P. Slonimski. 1993. 'Identification of a New Nuclear Gene (CEM1) Encoding a Protein Homologous to a Beta-Keto-Acyl Synthase Which Is Essential for Mitochondrial Respiration in Saccharomyces Cerevisiae'. *Molecular Microbiology* 9 (3): 545–55. https://doi.org/10.1111/j.1365-2958.1993.tb01715.x.

Hatanaka, Takashi, Yukiyo Takemoto, Mitsuru Hashimoto, Eiji Majima, Yasuo Shinohara, and Hiroshi Terada. 2001. 'Significant Expression of Functional Human Type 1 Mitochondrial ADP/ATP Carrier in Yeast Mitochondria.' *Biological and Pharmaceutical Bulletin* 24 (6): 595–99. https://doi.org/10.1248/bpb.24.595.

He, Yong-Han, Xiang Lu, Huan Wu, Wang-Wei Cai, Li-Qin Yang, Liang-You Xu, Hong-Peng Sun, and Qing-Peng Kong. 2014. 'Mitochondrial DNA Content Contributes to Healthy Aging in Chinese: A Study from Nonagenarians and Centenarians'. *Neurobiology of Aging* 35 (7): 1779.e1-1779.e4. https://doi.org/10.1016/j.neurobiolaging.2014.01.015.

Heimer, Gali, Juha M. Kerätär, Lisa G. Riley, Shanti Balasubramaniam, Eran Eyal, Laura P. Pietikäinen, J. Kalervo Hiltunen, et al. 2016. 'MECR Mutations Cause Childhood-Onset Dystonia and Optic Atrophy, a Mitochondrial Fatty Acid Synthesis Disorder'. *American Journal of Human Genetics* 99 (6): 1229–44. https://doi.org/10.1016/j.ajhg.2016.09.021.

Hermann, Greg J., and Janet M. Shaw. 1998. 'MITOCHONDRIAL DYNAMICS IN YEAST'. *Annual Review of Cell and Developmental Biology* 14 (1): 265–303. https://doi.org/10.1146/annurev.cellbio.14.1.265.

Hermes, Fatemah A., and John E. Cronan. 2013. 'The Role of the *Saccharomyces Cerevisiae* Lipoate Protein Ligase Homologue, Lip3, in Lipoic Acid Synthesis: Role of Lip3 in Lipoate Synthesis'. *Yeast*, August, n/a-n/a. https://doi.org/10.1002/yea.2979.

Herst, Patries M., Matthew R. Rowe, Georgia M. Carson, and Michael V. Berridge. 2017. 'Functional Mitochondria in Health and Disease'. *Frontiers in Endocrinology* 8 (November): 296. https://doi.org/10.3389/fendo.2017.00296.

Hillen, Hauke S., Yaroslav I. Morozov, Azadeh Sarfallah, Dmitry Temiakov, and Patrick Cramer. 2017. 'Structural Basis of Mitochondrial Transcription Initiation'. *Cell* 171 (5): 1072-1081.e10. https://doi.org/10.1016/j.cell.2017.10.036.

Hiltunen, J. Kalervo, Zhijun Chen, Antti M. Haapalainen, Rik K. Wierenga, and Alexander J. Kastaniotis. 2010. 'Mitochondrial Fatty Acid Synthesis – An Adopted Set of Enzymes Making a Pathway of Major Importance for the Cellular Metabolism'. *Progress in Lipid Research* 49 (1): 27–45. https://doi.org/10.1016/j.plipres.2009.08.001.

Hiltunen, J. Kalervo, Melissa S. Schonauer, Kaija J. Autio, Telsa M. Mittelmeier, Alexander J. Kastaniotis, and Carol L. Dieckmann. 2009. 'Mitochondrial Fatty Acid Synthesis Type II: More than Just Fatty Acids'. *The Journal of Biological Chemistry* 284 (14): 9011–15. https://doi.org/10.1074/jbc.R800068200.

Hinttala, Reetta, Florin Sasarman, Tamiko Nishimura, Hana Antonicka, Catherine Brunel-Guitton, Jeremy Schwartzentruber, Somayyeh Fahiminiya, et al. 2015. 'An N-Terminal Formyl Methionine on COX 1 Is Required for the Assembly of Cytochrome c Oxidase'. *Human Molecular Genetics* 24 (14): 4103–13. https://doi.org/10.1093/hmg/ddv149.

Hoja, Ursula, Sandra Marthol, Jörg Hofmann, Sabine Stegner, Rainer Schulz, Sandra Meier, Eva Greiner, and Eckhart Schweizer. 2004. 'HFA1 Encoding an Organelle-Specific Acetyl-CoA Carboxylase Controls Mitochondrial Fatty Acid Synthesis in Saccharomyces Cerevisiae'. *The Journal of Biological Chemistry* 279 (21): 21779–86. https://doi.org/10.1074/jbc.M401071200.

Holt, Ian J., Jiuya He, Chih-Chieh Mao, Jerome D. Boyd-Kirkup, Peter Martinsson, Hiroshi Sembongi, Aurelio Reyes, and Johannes N. Spelbrink. 2007. 'Mammalian Mitochondrial Nucleoids: Organizing an Independently Minded Genome'. *Mitochondrion* 7 (5): 311–21. https://doi.org/10.1016/j.mito.2007.06.004.

Horvath, Susanne E., and Günther Daum. 2013. 'Lipids of Mitochondria'. *Progress in Lipid Research* 52 (4): 590–614. https://doi.org/10.1016/j.plipres.2013.07.002.

Hudson, Gavin, Valerio Carelli, Liesbeth Spruijt, Mike Gerards, Catherine Mowbray, Alessandro Achilli, Angela Pyle, et al. 2007. 'Clinical Expression of Leber Hereditary Optic Neuropathy Is Affected by the Mitochondrial DNA–Haplogroup Background'. *The American Journal of Human Genetics* 81 (2): 228–33. https://doi.org/10.1086/519394.

Hughes, T. R., M. J. Marton, A. R. Jones, C. J. Roberts, R. Stoughton, C. D. Armour, H. A. Bennett, et al. 2000. 'Functional Discovery via a Compendium of Expression Profiles'. *Cell* 102 (1): 109–26. https://doi.org/10.1016/s0092-8674(00)00015-5.

Ikon, Nikita, and Robert O. Ryan. 2017. 'Cardiolipin and Mitochondrial Cristae Organization'. *Biochimica et Biophysica Acta (BBA) - Biomembranes* 1859 (6): 1156–63. https://doi.org/10.1016/j.bbamem.2017.03.013.

Johnston, M. 2000. 'The Yeast Genome: On the Road to the Golden Age'. *Current Opinion in Genetics & Development* 10 (6): 617–23. https://doi.org/10.1016/s0959-437x(00)00145-3.

Joubert, Frédéric, and Nicolas Puff. 2021. 'Mitochondrial Cristae Architecture and Functions: Lessons from Minimal Model Systems'. *Membranes* 11 (7): 465. https://doi.org/10.3390/membranes11070465.

Kastaniotis, Alexander J., Kaija J. Autio, Raija T. Sormunen, and J. Kalervo Hiltunen. 2004. 'Htd2p/Yhr067p Is a Yeast 3-Hydroxyacyl-ACP Dehydratase Essential for Mitochondrial Function and Morphology'. *Molecular Microbiology* 53 (5): 1407–21. https://doi.org/10.1111/j.1365-2958.2004.04191.x.

Kaushik, Virendar K., Michael Kavana, Jessica M. Volz, Stephen C. Weldon, Susan Hanrahan, Jian Xu, Shari L. Caplan, and Brian K. Hubbard. 2009. 'Characterization of Recombinant Human Acetyl-CoA Carboxylase-2 Steady-State Kinetics'. *Biochimica Et Biophysica Acta* 1794 (6): 961–67. https://doi.org/10.1016/j.bbapap.2009.02.004.

Kearsey, S. E. 1993. 'Identification of a Saccharomyces Cerevisiae Gene Closely Related to FAS3 (Acetyl-CoA Carboxylase)'. *DNA Sequence: The Journal of DNA Sequencing and Mapping* 4 (1): 69–70. https://doi.org/10.3109/10425179309015625.

Khurana, Vikram, and Susan Lindquist. 2010. 'Modelling Neurodegeneration in Saccharomyces Cerevisiae: Why Cook with Baker's Yeast?' *Nature Reviews. Neuroscience* 11 (6): 436–49. https://doi.org/10.1038/nrn2809.

Kim, I. C., and D. S. Beattie. 1973. 'Formation of the Yeast Mitochondrial Membrane. 1. Effects of Inhibitors of Protein Synthesis on the Kinetics of Enzyme Appearance during Glucose Derepression'. *European Journal of Biochemistry* 36 (2): 509–18. https://doi.org/10.1111/j.1432-1033.1973.tb02937.x.

Kollberg, Gittan, Már Tulinius, Atle Melberg, Niklas Darin, Oluf Andersen, Daniel Holmgren, Anders Oldfors, and Elisabeth Holme. 2009. 'Clinical Manifestation and a New ISCU Mutation in Iron-Sulphur Cluster Deficiency Myopathy'. *Brain: A Journal of Neurology* 132 (Pt 8): 2170–79. https://doi.org/10.1093/brain/awp152.

Kozak, M. 1983. 'Comparison of Initiation of Protein Synthesis in Procaryotes, Eucaryotes, and Organelles'. *Microbiological Reviews* 47 (1): 1–45. https://doi.org/10.1128/mr.47.1.1-45.1983.

Kukat, C., C. A. Wurm, H. Spahr, M. Falkenberg, N.-G. Larsson, and S. Jakobs. 2011. 'Super-Resolution Microscopy Reveals That Mammalian Mitochondrial Nucleoids Have a Uniform Size and Frequently

Contain a Single Copy of MtDNA'. *Proceedings of the National Academy of Sciences* 108 (33): 13534–39. https://doi.org/10.1073/pnas.1109263108.

Kumar, A., and M. Snyder. 2001. 'Emerging Technologies in Yeast Genomics'. *Nature Reviews. Genetics* 2 (4): 302–12. https://doi.org/10.1038/35066084.

Kunkel, T A, and A Soni. 1988. 'Exonucleolytic Proofreading Enhances the Fidelity of DNA Synthesis by Chick Embryo DNA Polymerase-Gamma.' *Journal of Biological Chemistry* 263 (9): 4450–59. https://doi.org/10.1016/S0021-9258(18)68947-1.

Kunkel, Thomas A., and Dale W. Mosbaugh. 1989. 'Exonucleolytic Proofreading by a Mammalian DNA Polymerase .Gamma.' *Biochemistry* 28 (3): 988–95. https://doi.org/10.1021/bi00429a011.

Kuzmenko, Anton, Gemma C. Atkinson, Sergey Levitskii, Nikolay Zenkin, Tanel Tenson, Vasili Hauryliuk, and Piotr Kamenski. 2014. 'Mitochondrial Translation Initiation Machinery: Conservation and Diversification'. *Biochimie* 100 (May): 132–40. https://doi.org/10.1016/j.biochi.2013.07.024.

Laemmli, U. K. 1970. 'Cleavage of Structural Proteins during the Assembly of the Head of Bacteriophage T4'. *Nature* 227 (5259): 680–85. https://doi.org/10.1038/227680a0.

Land, John M., John A. Morgan-Hughes, Iain Hargreaves, and Simon J. R. Heales. 2004. 'Mitochondrial Disease: A Historical, Biochemical, and London Perspective'. *Neurochemical Research* 29 (3): 483–91. https://doi.org/10.1023/B:NERE.0000014819.53972.b0.

Lane, Nick, and William Martin. 2010. 'The Energetics of Genome Complexity'. *Nature* 467 (7318): 929–34. https://doi.org/10.1038/nature09486.

Larsson, Nils-Gran, Mar H. Tulinius, Elisabeth Holme, and Anders Oldfors. 1995. 'Pathogenetic Aspects of the A8344G Mutation of Mitochondrial DNA Associated with MERRF Syndrome and Multiple Symmetric Lipomas'. *Muscle & Nerve* 18 (S14): S102–6. https://doi.org/10.1002/mus.880181421.

Laurent, Jon M., Riddhiman K. Garge, Ashley I. Teufel, Claus O. Wilke, Aashiq H. Kachroo, and Edward M. Marcotte. 2020. 'Humanization of Yeast Genes with Multiple Human Orthologs Reveals Functional Divergence between Paralogs'. Edited by Andreas Hejnol. *PLOS Biology* 18 (5): e3000627. https://doi.org/10.1371/journal.pbio.3000627.

Lee, Young-Sam, W. Dexter Kennedy, and Y. Whitney Yin. 2009. 'Structural Insight into Processive Human Mitochondrial DNA Synthesis and Disease-Related Polymerase Mutations'. *Cell* 139 (2): 312–24. https://doi.org/10.1016/j.cell.2009.07.050.

Legati, Andrea, Aurelio Reyes, Camilla Ceccatelli Berti, Oliver Stehling, Silvia Marchet, Costanza Lamperti, Alberto Ferrari, et al. 2017. 'A Novel de Novo Dominant Mutation in *ISCU* Associated with Mitochondrial Myopathy'. *Journal of Medical Genetics* 54 (12): 815–24. https://doi.org/10.1136/jmedgenet-2017-104822.

Lenaz, Giorgio. 1998. 'Role of Mitochondria in Oxidative Stress and Ageing'. *Biochimica et Biophysica Acta (BBA) - Bioenergetics* 1366 (1–2): 53–67. https://doi.org/10.1016/S0005-2728(98)00120-0.

Lenaz, Giorgio, and Maria Luisa Genova. 2010. 'Structure and Organization of Mitochondrial Respiratory Complexes: A New Understanding of an Old Subject'. *Antioxidants & Redox Signaling* 12 (8): 961–1008. https://doi.org/10.1089/ars.2009.2704.

Leonard, Jv, and Ahv Schapira. 2000. 'Mitochondrial Respiratory Chain Disorders II: Neurodegenerative Disorders and Nuclear Gene Defects'. *The Lancet* 355 (9201): 389–94. https://doi.org/10.1016/S0140-6736(99)05226-5.

Li, Yan, William B. Holmes, Dean R. Appling, and Uttam L. RajBhandary. 2000. 'Initiation of Protein Synthesis in *Saccharomyces Cerevisiae* Mitochondria without Formylation of the Initiator TRNA'. *Journal of Bacteriology* 182 (10): 2886–92. https://doi.org/10.1128/JB.182.10.2886-2892.2000.

Lodi, Tiziana, Claudio Bove, Flavia Fontanesi, Anna Maria Viola, and Iliana Ferrero. 2006. 'Mutation D104G in ANT1 Gene: Complementation Study in Saccharomyces Cerevisiae as a Model System'. *Biochemical and Biophysical Research Communications* 341 (3): 810–15. https://doi.org/10.1016/j.bbrc.2006.01.034.

Lodi, Tiziana, Cristina Dallabona, Cecilia Nolli, Paola Goffrini, Claudia Donnini, and Enrico Baruffini. 2015. 'DNA Polymerase Î³ and Disease: What We Have Learned from Yeast'. *Frontiers in Genetics* 6 (March). https://doi.org/10.3389/fgene.2015.00106.

Longley, M. J., R. Prasad, D. K. Srivastava, S. H. Wilson, and W. C. Copeland. 1998. 'Identification of 5'-Deoxyribose Phosphate Lyase Activity in Human DNA Polymerase and Its Role in Mitochondrial Base Excision Repair in Vitro'. *Proceedings of the National Academy of Sciences* 95 (21): 12244–48. https://doi.org/10.1073/pnas.95.21.12244.

Lonlay, P. de, I. Valnot, A. Barrientos, M. Gorbatyuk, A. Tzagoloff, J. W. Taanman, E. Benayoun, et al. 2001. 'A Mutant Mitochondrial Respiratory Chain Assembly Protein Causes Complex III Deficiency in Patients with Tubulopathy, Encephalopathy and Liver Failure'. *Nature Genetics* 29 (1): 57–60. https://doi.org/10.1038/ng706.

Magri, Stefania, Valentina Fracasso, Massimo Plumari, Enrico Alfei, Daniele Ghezzi, Cinzia Gellera, Paola Rusmini, et al. 2018. 'Concurrent AFG3L2 and SPG7 Mutations Associated with Syndromic Parkinsonism and Optic Atrophy with Aberrant OPA1 Processing and Mitochondrial Network Fragmentation'. *Human Mutation* 39 (12): 2060–71. https://doi.org/10.1002/humu.23658.

Mai, Nicole, Zofia M. A. Chrzanowska-Lightowlers, and Robert N. Lightowlers. 2017. 'The Process of Mammalian Mitochondrial Protein Synthesis'. *Cell and Tissue Research* 367 (1): 5–20. https://doi.org/10.1007/s00441-016-2456-0.

Mao, Yinhe, and Changbin Chen. 2019. 'The Hap Complex in Yeasts: Structure, Assembly Mode, and Gene Regulation'. *Frontiers in Microbiology* 10 (July): 1645. https://doi.org/10.3389/fmicb.2019.01645.

Martínez-Reyes, Inmaculada, and Navdeep S. Chandel. 2020. 'Mitochondrial TCA Cycle Metabolites Control Physiology and Disease'. *Nature Communications* 11 (1): 102. https://doi.org/10.1038/s41467-019-13668-3.

Martzen, M. R., S. M. McCraith, S. L. Spinelli, F. M. Torres, S. Fields, E. J. Grayhack, and E. M. Phizicky. 1999. 'A Biochemical Genomics Approach for Identifying Genes by the Activity of Their Products'. *Science (New York, N.Y.)* 286 (5442): 1153–55. https://doi.org/10.1126/science.286.5442.1153.

Marvin, Marcus E., Peter H. Williams, and Annette M. Cashmore. 2001. 'The Isolation and Characterisation of a Saccharomyces Cerevisiae Gene (LIP2) Involved in the Attachment of Lipoic Acid Groups to Mitochondrial Enzymes'. *FEMS Microbiology Letters* 199 (1): 131–36. https://doi.org/10.1111/j.1574-6968.2001.tb10663.x.

Matus-Ortega, M. G., C. A. Cárdenas-Monroy, O. Flores-Herrera, G. Mendoza-Hernández, M. Miranda, B. González-Pedrajo, H. Vázquez-Meza, and J. P. Pardo. 2015. 'New Complexes Containing the Internal Alternative NADH Dehydrogenase (Ndi1) in Mitochondria of *Saccharomyces Cerevisiae*: Mitochondrial Complexes Containing the Alternative NADH Dehydrogenase'. *Yeast* 32 (10): 629–41. https://doi.org/10.1002/yea.3086.

McCarthy, Alun D., and D.Grahame Hardie. 1984. 'Fatty Acid Synthase — an Example of Protein Evolution by Gene Fusion'. *Trends in Biochemical Sciences* 9 (2): 60–63. https://doi.org/10.1016/0968-0004(84)90184-1.

McCommis, Kyle S., and Brian N. Finck. 2015. 'Mitochondrial Pyruvate Transport: A Historical Perspective and Future Research Directions'. *Biochemical Journal* 466 (3): 443–54. https://doi.org/10.1042/BJ20141171.

McKenzie, Matthew, Danae Liolitsa, and Michael G. Hanna. 2004. 'Mitochondrial Disease: Mutations and Mechanisms'. *Neurochemical Research* 29 (3): 589–600. https://doi.org/10.1023/B:NERE.0000014829.42364.dd.

Metodiev, Metodi Dimitrov, Sylvie Gerber, Laurence Hubert, Agnès Delahodde, Dominique Chretien, Xavier Gérard, Patrizia Amati-Bonneau, et al. 2014. 'Mutations in the Tricarboxylic Acid Cycle Enzyme, Aconitase 2, Cause Either Isolated or Syndromic Optic Neuropathy with Encephalopathy and Cerebellar Atrophy'. *Journal of Medical Genetics* 51 (12): 834–38. https://doi.org/10.1136/jmedgenet-2014-102532.

Miinalainen, Ilkka J., Zhi-Jun Chen, Juha M. Torkko, Päivi L. Pirilä, Raija T. Sormunen, Ulrich Bergmann, Yong-Mei Qin, and J. Kalervo Hiltunen. 2003. 'Characterization of 2-Enoyl Thioester Reductase from Mammals. An Ortholog of YBR026p/MRF1'p of the Yeast Mitochondrial Fatty Acid Synthesis Type II'. *The Journal of Biological Chemistry* 278 (22): 20154–61. https://doi.org/10.1074/jbc.M302851200.

Minczuk, Michal, Jiuya He, Anna M. Duch, Thijs J. Ettema, Aleksander Chlebowski, Karol Dzionek, Leo G. J. Nijtmans, Martijn A. Huynen, and Ian J. Holt. 2011. 'TEFM (C17orf42) Is Necessary for Transcription of Human MtDNA'. *Nucleic Acids Research* 39 (10): 4284–99. https://doi.org/10.1093/nar/gkq1224.

Miralles Fusté, Javier, Yonghong Shi, Sjoerd Wanrooij, Xuefeng Zhu, Elisabeth Jemt, Örjan Persson, Nasim Sabouri, Claes M. Gustafsson, and Maria Falkenberg. 2014. 'In Vivo Occupancy of Mitochondrial Single-Stranded DNA Binding Protein Supports the Strand Displacement Mode of DNA Replication'. Edited by Nils-Göran Larsson. *PLoS Genetics* 10 (12): e1004832. https://doi.org/10.1371/journal.pgen.1004832.

Moosavi, Behrooz, Xiao-lei Zhu, Wen-Chao Yang, and Guang-Fu Yang. 2020. 'Molecular Pathogenesis of Tumorigenesis Caused by Succinate Dehydrogenase Defect'. *European Journal of Cell Biology* 99 (1): 151057. https://doi.org/10.1016/j.ejcb.2019.151057.

Morales, M J, Y L Dang, Y C Lou, P Sulo, and N C Martin. 1992. 'A 105-KDa Protein Is Required for Yeast Mitochondrial RNase P Activity.' *Proceedings of the National Academy of Sciences* 89 (20): 9875–79. https://doi.org/10.1073/pnas.89.20.9875.

Mörl, Mario, and Anita Marchfelder. 2001. 'The Final Cut: The Importance of TRNA 3'-processing'. *EMBO Reports* 2 (1): 17–20. https://doi.org/10.1093/embo-reports/kve006.

Na, Un, Wendou Yu, James Cox, Daniel K. Bricker, Knut Brockmann, Jared Rutter, Carl S. Thummel, and Dennis R. Winge. 2014. 'The LYR Factors SDHAF1 and SDHAF3 Mediate Maturation of the Iron-Sulfur Subunit of Succinate Dehydrogenase'. *Cell Metabolism* 20 (2): 253–66. https://doi.org/10.1016/j.cmet.2014.05.014.

Nagai, S., N. Yanagishima, and H. Nagai. 1961. 'Advances in the Study of Respiration-Deficient (RD) Mutation in Yeast and Other Microorganisms'. *Bacteriological Reviews* 25 (December): 404–26. https://doi.org/10.1128/br.25.4.404-426.1961.

Nagarajan, Lakshmanan, and Reginald K. Storms. 1997. 'Molecular Characterization of GCV3, the Saccharomyces Cerevisiae Gene Coding for the Glycine Cleavage System Hydrogen Carrier Protein'. *Journal of Biological Chemistry* 272 (7): 4444–50. https://doi.org/10.1074/jbc.272.7.4444.

Narahari, Janaki, Rong Ma, Man Wang, and William E. Walden. 2000. 'The Aconitase Function of Iron Regulatory Protein 1'. *Journal of Biological Chemistry* 275 (21): 16227–34. https://doi.org/10.1074/jbc.M910450199.

Nasca, Alessia, Teresa Rizza, Mara Doimo, Andrea Legati, Andrea Ciolfi, Daria Diodato, Cristina Calderan, et al. 2017. 'Not Only Dominant, Not Only Optic Atrophy: Expanding the Clinical Spectrum Associated with OPA1 Mutations'. *Orphanet Journal of Rare Diseases* 12 (1): 89. https://doi.org/10.1186/s13023-017-0641-1.

Neeve, Vivienne C. M., Angela Pyle, Veronika Boczonadi, Aurora Gomez-Duran, Helen Griffin, Mauro Santibanez-Koref, Ulrike Gaiser, et al. 2013. 'Clinical and Functional Characterisation of the Combined Respiratory Chain Defect in Two Sisters Due to Autosomal Recessive Mutations in MTFMT'. *Mitochondrion* 13 (6): 743–48. https://doi.org/10.1016/j.mito.2013.03.002.

Neumann, Marie Anne-Catherine, Dajana Grossmann, Simone Schimpf-Linzenbold, Dana Dayan, Katarina Stingl, Reut Ben-Menachem, Ophry Pines, et al. 2020. 'Haploinsufficiency Due to a Novel ACO2

Deletion Causes Mitochondrial Dysfunction in Fibroblasts from a Patient with Dominant Optic Nerve Atrophy'. *Scientific Reports* 10 (1): 16736. https://doi.org/10.1038/s41598-020-73557-4.

Neupert, Walter, and Johannes M. Herrmann. 2007. 'Translocation of Proteins into Mitochondria'. *Annual Review of Biochemistry* 76 (1): 723–49. https://doi.org/10.1146/annurev.biochem.76.052705.163409.

Ng, Yi Shiau, and Doug M. Turnbull. 2016. 'Mitochondrial Disease: Genetics and Management'. *Journal of Neurology* 263 (1): 179–91. https://doi.org/10.1007/s00415-015-7884-3.

Ni, Min, Ashley Solmonson, Chunxiao Pan, Chendong Yang, Dan Li, Ashley Notzon, Ling Cai, et al. 2019. 'Functional Assessment of Lipoyltransferase-1 Deficiency in Cells, Mice, and Humans'. *Cell Reports* 27 (5): 1376-1386.e6. https://doi.org/10.1016/j.celrep.2019.04.005.

Nissanka, Nadee, and Carlos T Moraes. 2020. 'Mitochondrial DNA Heteroplasmy in Disease and Targeted Nuclease-based Therapeutic Approaches'. *EMBO Reports* 21 (3). https://doi.org/10.15252/embr.201949612.

Nolli, Cecilia, Paola Goffrini, Mirca Lazzaretti, Claudia Zanna, Rita Vitale, Tiziana Lodi, and Enrico Baruffini. 2015. 'Validation of a MGM1/OPA1 Chimeric Gene for Functional Analysis in Yeast of Mutations Associated with Dominant Optic Atrophy'. *Mitochondrion* 25 (November): 38–48. https://doi.org/10.1016/j.mito.2015.10.002.

Nowinski, Sara M., Jonathan G. Van Vranken, Katja K. Dove, and Jared Rutter. 2018. 'Impact of Mitochondrial Fatty Acid Synthesis on Mitochondrial Biogenesis'. *Current Biology* 28 (20): R1212–19. https://doi.org/10.1016/j.cub.2018.08.022.

Ochoa, Severo. 2006. 'Enzymic Mechanisms in the Citric Acid Cycle'. In *Advances in Enzymology - and Related Areas of Molecular Biology*, edited by F. F. Nord, 183–270. Hoboken, NJ, USA: John Wiley & Sons, Inc. https://doi.org/10.1002/9780470122600.ch5.

Olsson, A., L. Lind, L.-E. Thornell, and M. Holmberg. 2008. 'Myopathy with Lactic Acidosis Is Linked to Chromosome 12q23.3-24.11 and Caused by an Intron Mutation in the ISCU Gene Resulting in a Splicing Defect'. *Human Molecular Genetics* 17 (11): 1666–72. https://doi.org/10.1093/hmg/ddn057.

Palmieri, Luigi, Simona Alberio, Isabella Pisano, Tiziana Lodi, Mija Meznaric-Petrusa, Janez Zidar, Antonella Santoro, et al. 2005. 'Complete Loss-of-Function of the Heart/Muscle-Specific Adenine Nucleotide Translocator Is Associated with Mitochondrial Myopathy and Cardiomyopathy'. *Human Molecular Genetics* 14 (20): 3079–88. https://doi.org/10.1093/hmg/ddi341.

Parfait, B., D. Chretien, A. Rötig, C. Marsac, A. Munnich, and P. Rustin. 2000. 'Compound Heterozygous Mutations in the Flavoprotein Gene of the Respiratory Chain Complex II in a Patient with Leigh Syndrome'. *Human Genetics* 106 (2): 236–43. https://doi.org/10.1007/s004390051033.

Perham, R. N. 2000. 'Swinging Arms and Swinging Domains in Multifunctional Enzymes: Catalytic Machines for Multistep Reactions'. *Annual Review of Biochemistry* 69: 961–1004. https://doi.org/10.1146/annurev.biochem.69.1.961.

Pinz, Kevin G., and Daniel F. Bogenhagen. 2006. 'The Influence of the DNA Polymerase γ Accessory Subunit on Base Excision Repair by the Catalytic Subunit'. *DNA Repair* 5 (1): 121–28. https://doi.org/10.1016/j.dnarep.2005.08.014.

Piper, M, S Hong, T Eising, P Sealey, and I Dawes. 2002. 'Regulation of the Yeast Glycine Cleavage Genes Is Responsive to the Availability of Multiple Nutrients'. *FEMS Yeast Research* 2 (1): 59–71. https://doi.org/10.1016/S1567-1356(01)00061-7.

Repetto, B, and A Tzagoloff. 1991. 'In Vivo Assembly of Yeast Mitochondrial Alpha-Ketoglutarate Dehydrogenase Complex'. *Molecular and Cellular Biology* 11 (8): 3931–39. https://doi.org/10.1128/mcb.11.8.3931-3939.1991.

Resnick, M. A., and B. S. Cox. 2000. 'Yeast as an Honorary Mammal'. *Mutation Research* 451 (1–2): 1–11. https://doi.org/10.1016/s0027-5107(00)00036-1.

Reynier, P., P. Amati-Bonneau, C. Verny, A. Olichon, G. Simard, A. Guichet, C. Bonnemains, et al. 2004. 'OPA3 Gene Mutations Responsible for Autosomal Dominant Optic Atrophy and Cataract'. *Journal of Medical Genetics* 41 (9): e110. https://doi.org/10.1136/jmg.2003.016576.

Reznik, Ed, Martin L Miller, Yasin Şenbabaoğlu, Nadeem Riaz, Judy Sarungbam, Satish K Tickoo, Hikmat A Al-Ahmadie, et al. 2016. 'Mitochondrial DNA Copy Number Variation across Human Cancers'. *ELife* 5 (February): e10769. https://doi.org/10.7554/eLife.10769.

Rinaldi, Teresa, Cristina Dallabona, Ileana Ferrero, Laura Frontali, and Monique Bolotin-Fukuhara. 2010. 'Mitochondrial Diseases and the Role of the Yeast Models'. *FEMS Yeast Research* 10 (8): 1006–22. https://doi.org/10.1111/j.1567-1364.2010.00685.x.

Robberson, D. L., H. Kasamatsu, and J. Vinograd. 1972. 'Replication of Mitochondrial DNA. Circular Replicative Intermediates in Mouse L Cells'. *Proceedings of the National Academy of Sciences* 69 (3): 737–41. https://doi.org/10.1073/pnas.69.3.737.

Robbins, A H, and C D Stout. 1989. 'Structure of Activated Aconitase: Formation of the [4Fe-4S] Cluster in the Crystal.' *Proceedings of the National Academy of Sciences* 86 (10): 3639–43. https://doi.org/10.1073/pnas.86.10.3639.

Ropp, Philip A., and William C. Copeland. 1996. 'Cloning and Characterization of the Human Mitochondrial DNA Polymerase, DNA Polymerase γ'. *Genomics* 36 (3): 449–58. https://doi.org/10.1006/geno.1996.0490.

Rossum, Harmen M. van, Barbara U. Kozak, Matthijs S. Niemeijer, Hendrik J. Duine, Marijke A. H. Luttik, Viktor M. Boer, Peter Kötter, Jean-Marc G. Daran, Antonius J. A. van Maris, and Jack T. Pronk. 2016.

'Alternative Reactions at the Interface of Glycolysis and Citric Acid Cycle in *Saccharomyces Cerevisiae*'. Edited by Jens Nielsen. *FEMS Yeast Research* 16 (3): fow017. https://doi.org/10.1093/femsyr/fow017.

Rubio-Cosials, Anna, and Maria Solà. 2013. 'U-Turn DNA Bending by Human Mitochondrial Transcription Factor A'. *Current Opinion in Structural Biology* 23 (1): 116–24. https://doi.org/10.1016/j.sbi.2012.12.004.

Rupani, Dhwani N., and Gregory J. Connell. 2016. 'Transferrin Receptor MRNA Interactions Contributing to Iron Homeostasis'. *RNA* 22 (8): 1271–82. https://doi.org/10.1261/rna.056184.116.

Ryan, Michael T., and Nicholas J. Hoogenraad. 2007. 'Mitochondrial-Nuclear Communications'. *Annual Review of Biochemistry* 76 (1): 701–22. https://doi.org/10.1146/annurev.biochem.76.052305.091720.

Sadun, A. A. 2002. 'Mitochondrial Optic Neuropathies'. *Journal of Neurology, Neurosurgery, and Psychiatry* 72 (4): 423–25. https://doi.org/10.1136/jnnp.72.4.423.

Sadun, Alfredo A, Valerio Carelli, Solange R Salomao, Adriana Berezovsky, Peter A Quiros, Federico Sadun, Anna-Maria DeNegri, et al. 2003. 'Extensive Investigation of a Large Brazilian Pedigree of 11778/Haplogroup J Leber Hereditary Optic Neuropathy'. *American Journal of Ophthalmology* 136 (2): 231–38. https://doi.org/10.1016/S0002-9394(03)00099-0.

Sáez-Vásquez, Julio, and Olivier Gadal. 2010. 'Genome Organization and Function: A View from Yeast and Arabidopsis'. *Molecular Plant* 3 (4): 678–90. https://doi.org/10.1093/mp/ssq034.

Schieber, Michael, and Navdeep S. Chandel. 2014. 'ROS Function in Redox Signaling and Oxidative Stress'. *Current Biology* 24 (10): R453–62. https://doi.org/10.1016/j.cub.2014.03.034.

Schneider, R., B. Brors, F. Bürger, S. Camrath, and H. Weiss. 1997. 'Two Genes of the Putative Mitochondrial Fatty Acid Synthase in the Genome of Saccharomyces Cerevisiae'. *Current Genetics* 32 (6): 384–88. https://doi.org/10.1007/s002940050292.

Schon, Eric A., Eduardo Bonilla, and Salvatore DiMauro. 1997. '[No Title Found]'. *Journal of Bioenergetics and Biomembranes* 29 (2): 131–49. https://doi.org/10.1023/A:1022685929755.

Schonauer, Melissa S., Alexander J. Kastaniotis, J. Kalervo Hiltunen, and Carol L. Dieckmann. 2008. 'Intersection of RNA Processing and the Type II Fatty Acid Synthesis Pathway in Yeast Mitochondria'. *Molecular and Cellular Biology* 28 (21): 6646–57. https://doi.org/10.1128/MCB.01162-08.

Schonauer, Melissa S., Alexander J. Kastaniotis, V. A. Samuli Kursu, J. Kalervo Hiltunen, and Carol L. Dieckmann. 2009. 'Lipoic Acid Synthesis and Attachment in Yeast Mitochondria'. *Journal of Biological Chemistry* 284 (35): 23234–42. https://doi.org/10.1074/jbc.M109.015594.

Schwartz, W. 1973. 'Lynn Margulis, Origin of Eukaryotic Cells. Evidence and Research Implications for a Theory of the Origin and Evolution of Microbial, Plant, and Animal Cells on the Precambrian Earth. XXII u. 349 S., 89 Abb., 49 Tab. New Haven-London 1970: Yale University'. *Zeitschrift Für Allgemeine Mikrobiologie* 13 (2): 186–186. https://doi.org/10.1002/jobm.19730130220.

Schwimmer, Christine, Linnka Lefebvre-Legendre, Malgorzata Rak, Anne Devin, Piotr P. Slonimski, Jean-Paul di Rago, and Michel Rigoulet. 2005. 'Increasing Mitochondrial Substrate-Level Phosphorylation Can Rescue Respiratory Growth of an ATP Synthase-Deficient Yeast'. *Journal of Biological Chemistry* 280 (35): 30751–59. https://doi.org/10.1074/jbc.M501831200.

Shankar, Suma P., John H. Fingert, Valerio Carelli, Maria L. Valentino, Terri M. King, Stephen P. Daiger, Solange R. Salomao, et al. 2008. 'Evidence for a Novel X-Linked Modifier Locus for Leber Hereditary Optic Neuropathy'. *Ophthalmic Genetics* 29 (1): 17–24. https://doi.org/10.1080/13816810701867607.

Sharkia, Rajech, Klaas J. Wierenga, Amit Kessel, Abdussalam Azem, Enrico Bertini, Rosalba Carrozzo, Alessandra Torraco, et al. 2019. 'Clinical, Radiological, and Genetic Characteristics of 16 Patients with *ACO2* Gene Defects: Delineation of an Emerging Neurometabolic Syndrome'. *Journal of Inherited Metabolic Disease* 42 (2): 264–75. https://doi.org/10.1002/jimd.12022.

Sharma, Pankaj, Elena Maklashina, Gary Cecchini, and T. M. Iverson. 2018. 'Crystal Structure of an Assembly Intermediate of Respiratory Complex II'. *Nature Communications* 9 (1): 274. https://doi.org/10.1038/s41467-017-02713-8.

Shay, Kate Petersen, Régis F. Moreau, Eric J. Smith, Anthony R. Smith, and Tory M. Hagen. 2009. 'Alpha-Lipoic Acid as a Dietary Supplement: Molecular Mechanisms and Therapeutic Potential'. *Biochimica et Biophysica Acta (BBA) - General Subjects* 1790 (10): 1149–60. https://doi.org/10.1016/j.bbagen.2009.07.026.

Sickmann, Albert, Jörg Reinders, Yvonne Wagner, Cornelia Joppich, René Zahedi, Helmut E. Meyer, Birgit Schönfisch, et al. 2003. 'The Proteome of Saccharomyces Cerevisiae Mitochondria'. *Proceedings of the National Academy of Sciences of the United States of America* 100 (23): 13207–12. https://doi.org/10.1073/pnas.2135385100.

Sinclair, D. A., and I. W. Dawes. 1995. 'Genetics of the Synthesis of Serine from Glycine and the Utilization of Glycine as Sole Nitrogen Source by Saccharomyces Cerevisiae'. *Genetics* 140 (4): 1213–22. https://doi.org/10.1093/genetics/140.4.1213.

Soto, Ileana C., Flavia Fontanesi, Melvys Valledor, Darryl Horn, Rajiv Singh, and Antoni Barrientos. 2009. 'Synthesis of Cytochrome c Oxidase Subunit 1 Is Translationally Downregulated in the Absence of Functional F1F0-ATP Synthase'. *Biochimica et Biophysica Acta (BBA) - Molecular Cell Research* 1793 (11): 1776–86. https://doi.org/10.1016/j.bbamcr.2009.09.002.

Spencer, Angela C., and Linda L. Spremulli. 2004. 'Interaction of Mitochondrial Initiation Factor 2 with Mitochondrial FMet-TRNA'. *Nucleic Acids Research* 32 (18): 5464–70. https://doi.org/10.1093/nar/gkh886.

Spiegel, Ronen, Ophry Pines, Asaf Ta-Shma, Efrat Burak, Avraham Shaag, Jonatan Halvardson, Shimon Edvardson, et al. 2012. 'Infantile Cerebellar-Retinal Degeneration Associated with a Mutation in Mitochondrial Aconitase, ACO2'. *The American Journal of Human Genetics* 90 (3): 518–23. https://doi.org/10.1016/j.ajhg.2012.01.009.

Spinazzola, A., F. Invernizzi, F. Carrara, E. Lamantea, A. Donati, M. Dirocco, I. Giordano, et al. 2009. 'Clinical and Molecular Features of Mitochondrial DNA Depletion Syndromes'. *Journal of Inherited Metabolic Disease* 32 (2): 143–58. https://doi.org/10.1007/s10545-008-1038-z.

Stribinskis, V. 2001. 'Rpm2p: Separate Domains Promote TRNA and Rpm1r Maturation in Saccharomyces Cerevisiae Mitochondria'. *Nucleic Acids Research* 29 (17): 3631–37. https://doi.org/10.1093/nar/29.17.3631.

Sulo, P., and N. C. Martin. 1993. 'Isolation and Characterization of LIP5. A Lipoate Biosynthetic Locus of Saccharomyces Cerevisiae'. *The Journal of Biological Chemistry* 268 (23): 17634–39.

Sun, Fei, Xia Huo, Yujia Zhai, Aojin Wang, Jianxing Xu, Dan Su, Mark Bartlam, and Zihe Rao. 2005. 'Crystal Structure of Mitochondrial Respiratory Membrane Protein Complex II'. *Cell* 121 (7): 1043–57. https://doi.org/10.1016/j.cell.2005.05.025.

Takeuchi, N., M. Kawakami, A. Omori, T. Ueda, L. L. Spremulli, and K. Watanabe. 1998. 'Mammalian Mitochondrial Methionyl-TRNA Transformylase from Bovine Liver. Purification, Characterization, and Gene Structure'. *The Journal of Biological Chemistry* 273 (24): 15085–90. https://doi.org/10.1074/jbc.273.24.15085.

Taylor, Robert W., and Doug M. Turnbull. 2005. 'Mitochondrial DNA Mutations in Human Disease'. *Nature Reviews Genetics* 6 (5): 389–402. https://doi.org/10.1038/nrg1606.

Thomas, Barbara J., and Rodney Rothstein. 1989. 'Elevated Recombination Rates in Transcriptionally Active DNA'. *Cell* 56 (4): 619–30. https://doi.org/10.1016/0092-8674(89)90584-9.

Tucci, Arianna, Yo-Tsen Liu, Elisabeth Preza, Robert D. S. Pitceathly, Annapurna Chalasani, Vincent Plagnol, John M. Land, et al. 2014. 'Novel C12orf65 Mutations in Patients with Axonal Neuropathy and Optic Atrophy'. *Journal of Neurology, Neurosurgery, and Psychiatry* 85 (5): 486–92. https://doi.org/10.1136/jnnp-2013-306387.

Tucker, Elena J., Steven G. Hershman, Caroline Köhrer, Casey A. Belcher-Timme, Jinal Patel, Olga A. Goldberger, John Christodoulou, et al. 2011. 'Mutations in MTFMT Underlie a Human Disorder of Formylation Causing Impaired Mitochondrial Translation'. *Cell Metabolism* 14 (3): 428–34. https://doi.org/10.1016/j.cmet.2011.07.010.

Tuppen, Helen A. L., Janev Fehmi, Birgit Czermin, Paola Goffrini, Francesca Meloni, Iliana Ferrero, Langping He, et al. 2010. 'Long-Term Survival of Neonatal Mitochondrial Complex III Deficiency Associated with a Novel BCS1L Gene Mutation'. *Molecular Genetics and Metabolism* 100 (4): 345–48. https://doi.org/10.1016/j.ymgme.2010.04.010.

Tzagoloff, A., and C. L. Dieckmann. 1990. 'PET Genes of Saccharomyces Cerevisiae'. *Microbiological Reviews* 54 (3): 211–25. https://doi.org/10.1128/mr.54.3.211-225.1990.

Uetz, P., and R. E. Hughes. 2000. 'Systematic and Large-Scale Two-Hybrid Screens'. *Current Opinion in Microbiology* 3 (3): 303–8. https://doi.org/10.1016/s1369-5274(00)00094-1.

Van Vranken, Jonathan G, Mi-Young Jeong, Peng Wei, Yu-Chan Chen, Steven P Gygi, Dennis R Winge, and Jared Rutter. 2016. 'The Mitochondrial Acyl Carrier Protein (ACP) Coordinates Mitochondrial Fatty Acid Synthesis with Iron Sulfur Cluster Biogenesis'. *ELife* 5 (August): e17828. https://doi.org/10.7554/eLife.17828.

Vatrinet, Renaud, Giulia Leone, Monica De Luise, Giulia Girolimetti, Michele Vidone, Giuseppe Gasparre, and Anna Maria Porcelli. 2017. 'The α-Ketoglutarate Dehydrogenase Complex in Cancer Metabolic Plasticity'. *Cancer & Metabolism* 5 (1): 3. https://doi.org/10.1186/s40170-017-0165-0.

Venkatesan, Rajaram, Shiv K. Sah-Teli, Luqman O. Awoniyi, Guangyu Jiang, Piotr Prus, Alexander J. Kastaniotis, J. Kalervo Hiltunen, Rik K. Wierenga, and Zhijun Chen. 2014. 'Insights into Mitochondrial Fatty Acid Synthesis from the Structure of Heterotetrameric 3-Ketoacyl-ACP Reductase/3R-Hydroxyacyl-CoA Dehydrogenase'. *Nature Communications* 5 (1): 4805. https://doi.org/10.1038/ncomms5805.

Venter, J. C., M. D. Adams, E. W. Myers, P. W. Li, R. J. Mural, G. G. Sutton, H. O. Smith, et al. 2001. 'The Sequence of the Human Genome'. *Science (New York, N.Y.)* 291 (5507): 1304–51. https://doi.org/10.1126/science.1058040.

Vergani, L., R. Rossi, C. H. Brierley, M. Hanna, and I. J. Holt. 1999. 'Introduction of Heteroplasmic Mitochondrial DNA (MtDNA) from a Patient with NARP Into Two Human Cell Lines Is Associated Either With Selection and Maintenance of NARP Mutant MtDNA or Failure to Maintain MtDNA'. *Human Molecular Genetics* 8 (9): 1751–55. https://doi.org/10.1093/hmg/8.9.1751.

Vozáriková, Veronika, Nina Kunová, Jacob A. Bauer, Ján Frankovský, Veronika Kotrasová, Katarína Procházková, Vladimíra Džugasová, et al. 2020. 'Mitochondrial HMG-Box Containing Proteins: From Biochemical Properties to the Roles in Human Diseases'. *Biomolecules* 10 (8): 1193. https://doi.org/10.3390/biom10081193.

Wachnowsky, Christine, Amber L. Hendricks, Nathaniel A. Wesley, Connor Ferguson, Insiya Fidai, and J. A. Cowan. 2019. 'Understanding the Mechanism of [4Fe-4S] Cluster Assembly on Eukaryotic Mitochondrial and Cytosolic Aconitase'. *Inorganic Chemistry* 58 (20): 13686–95. https://doi.org/10.1021/acs.inorgchem.9b01278.

Walker, Scott C., and David R. Engelke. 2006. 'Ribonuclease P: The Evolution of an Ancient RNA Enzyme'. *Critical Reviews in Biochemistry and Molecular Biology* 41 (2): 77–102. https://doi.org/10.1080/10409230600602634.

Wallace, D. C., G. Singh, M. T. Lott, J. A. Hodge, T. G. Schurr, A. M. Lezza, L. J. Elsas, and E. K. Nikoskelainen. 1988. 'Mitochondrial DNA Mutation Associated with Leber's Hereditary Optic Neuropathy'. *Science (New York, N.Y.)* 242 (4884): 1427–30. https://doi.org/10.1126/science.3201231.

Wang, Fei, Deyu Zhang, Dejiu Zhang, Peifeng Li, and Yanyan Gao. 2021. 'Mitochondrial Protein Translation: Emerging Roles and Clinical Significance in Disease'. *Frontiers in Cell and Developmental Biology* 9 (July): 675465. https://doi.org/10.3389/fcell.2021.675465.

Wang, Jian, and Kostas Pantopoulos. 2011. 'Regulation of Cellular Iron Metabolism'. *Biochemical Journal* 434 (3): 365–81. https://doi.org/10.1042/BJ20101825.

Wang, Ying, Robyn Branicky, Alycia Noë, and Siegfried Hekimi. 2018. 'Superoxide Dismutases: Dual Roles in Controlling ROS Damage and Regulating ROS Signaling'. *Journal of Cell Biology* 217 (6): 1915–28. https://doi.org/10.1083/jcb.201708007.

Wanrooij, S., J. M. Fuste, G. Farge, Y. Shi, C. M. Gustafsson, and M. Falkenberg. 2008. 'Human Mitochondrial RNA Polymerase Primes Lagging-Strand DNA Synthesis in Vitro'. *Proceedings of the National Academy of Sciences* 105 (32): 11122–27. https://doi.org/10.1073/pnas.0805399105.

Warren, Graham, and William Wickner. 1996. 'Organelle Inheritance'. *Cell* 84 (3): 395–400. https://doi.org/10.1016/S0092-8674(00)81284-2.

Wernig, Florian, Sandra Born, Eckhard Boles, Martin Grininger, and Mislav Oreb. 2020. 'Fusing α and β Subunits of the Fungal Fatty Acid Synthase Leads to Improved Production of Fatty Acids'. *Scientific Reports* 10 (1): 9780. https://doi.org/10.1038/s41598-020-66629-y.

Wharton, David C., and Alexander Tzagoloff. 1967. '[45] Cytochrome Oxidase from Beef Heart Mitochondria'. In *Methods in Enzymology*, 10:245–50. Elsevier. https://doi.org/10.1016/0076-6879(67)10048-7.

Winzeler, E. A., D. D. Shoemaker, A. Astromoff, H. Liang, K. Anderson, B. Andre, R. Bangham, et al. 1999. 'Functional Characterization of the S. Cerevisiae Genome by Gene Deletion and Parallel Analysis'. *Science (New York, N.Y.)* 285 (5429): 901–6. https://doi.org/10.1126/science.285.5429.901.

Wong, Tai Wai, and David A. Clayton. 1985. 'In Vitro Replication of Human Mitochondrial DNA: Accurate Initiation at the Origin of Light-Strand Synthesis'. *Cell* 42 (3): 951–58. https://doi.org/10.1016/0092-8674(85)90291-0.

Yaffe, Michael P. 1999. 'Dynamic Mitochondria'. *Nature Cell Biology* 1 (6): E149–50. https://doi.org/10.1038/14101.

Yakubovskaya, Elena, Zhixin Chen, José A. Carrodeguas, Caroline Kisker, and Daniel F. Bogenhagen. 2006. 'Functional Human Mitochondrial DNA Polymerase γ Forms a Heterotrimer'. *Journal of Biological Chemistry* 281 (1): 374–82. https://doi.org/10.1074/jbc.M509730200.

Yang, Fan, Song Sun, Guihong Tan, Michael Costanzo, David E. Hill, Marc Vidal, Brenda J. Andrews, Charles Boone, and Frederick P. Roth. 2017. 'Identifying Pathogenicity of Human Variants via Paralog-Based Yeast Complementation'. *PLoS Genetics* 13 (5): e1006779. https://doi.org/10.1371/journal.pgen.1006779.

Yu, Seungyoon B., and Gulcin Pekkurnaz. 2018. 'Mechanisms Orchestrating Mitochondrial Dynamics for Energy Homeostasis'. *Journal of Molecular Biology* 430 (21): 3922–41. https://doi.org/10.1016/j.jmb.2018.07.027.

Yu-Wai-Man, Patrick, Philip G. Griffiths, and Patrick F. Chinnery. 2011. 'Mitochondrial Optic Neuropathies - Disease Mechanisms and Therapeutic Strategies'. *Progress in Retinal and Eye Research* 30 (2): 81–114. https://doi.org/10.1016/j.preteyeres.2010.11.002.

Zehavi, Yoav, Ann Saada, Haneen Jabaly-Habib, Moshe Dessau, Avraham Shaag, Orly Elpeleg, and Ronen Spiegel. 2021. 'A Novel de Novo Heterozygous Pathogenic Variant in the SDHA Gene Results in Childhood Onset Bilateral Optic Atrophy and Cognitive Impairment'. *Metabolic Brain Disease* 36 (4): 581–88. https://doi.org/10.1007/s11011-021-00671-1.

Zeviani, M. 2004. 'Mitochondrial Disorders'. *Brain* 127 (10): 2153–72. https://doi.org/10.1093/brain/awh259.

Zeviani, Massimo, and Valerio Carelli. 2007. 'Mitochondrial Disorders'. *Current Opinion in Neurology* 20 (5): 564–71. https://doi.org/10.1097/WCO.0b013e3282ef58cd.

Zhou, Zhi Dong, and Eng-King Tan. 2017. 'Iron Regulatory Protein (IRP)-Iron Responsive Element (IRE) Signaling Pathway in Human Neurodegenerative Diseases'. *Molecular Neurodegeneration* 12 (1): 75. https://doi.org/10.1186/s13024-017-0218-4.

Zhu, H., M. Bilgin, R. Bangham, D. Hall, A. Casamayor, P. Bertone, N. Lan, et al. 2001. 'Global Analysis of Protein Activities Using Proteome Chips'. *Science (New York, N.Y.)* 293 (5537): 2101–5. https://doi.org/10.1126/science.1062191.